



HAL
open science

TROLL 4.0: representing water and carbon fluxes, leaf phenology and intraspecific trait variation in a mixed-species individual-based forest dynamics model – Part 1: Model description

Isabelle Maréchaux, Fabian Jörg Fischer, Sylvain Schmitt, Jérôme Chave

► To cite this version:

Isabelle Maréchaux, Fabian Jörg Fischer, Sylvain Schmitt, Jérôme Chave. TROLL 4.0: representing water and carbon fluxes, leaf phenology and intraspecific trait variation in a mixed-species individual-based forest dynamics model – Part 1: Model description. 2024. hal-04769295

HAL Id: hal-04769295

<https://hal.inrae.fr/hal-04769295v1>

Preprint submitted on 6 Nov 2024

HAL is a multi-disciplinary open access archive for the deposit and dissemination of scientific research documents, whether they are published or not. The documents may come from teaching and research institutions in France or abroad, or from public or private research centers.

L'archive ouverte pluridisciplinaire **HAL**, est destinée au dépôt et à la diffusion de documents scientifiques de niveau recherche, publiés ou non, émanant des établissements d'enseignement et de recherche français ou étrangers, des laboratoires publics ou privés.



Distributed under a Creative Commons Attribution 4.0 International License

TROLL 4.0: representing water and carbon fluxes, leaf phenology and intraspecific trait variation in a mixed-species individual-based forest dynamics model – Part 1: Model description

Isabelle Maréchaux¹, Fabian Jörg Fischer^{2,3}, Sylvain Schmitt^{1,4,5}, Jérôme Chave²

1. AMAP, Univ Montpellier, CIRAD, CNRS, INRAE, IRD, 34000 Montpellier, France

2. CRBE, Université de Toulouse, CNRS, IRD, Toulouse INP, 118 route de Narbonne 31062 Toulouse, France

3. School of Biological Sciences, University of Bristol, Bristol, BS8 1TQ United Kingdom

4. CIRAD, UPR Forêts et Sociétés, F-34398, Montpellier, France

5. Forêts et Sociétés, Univ Montpellier, CIRAD, Montpellier, France

Correspondence to: Isabelle Maréchaux (isabelle.marechaux@inrae.fr)

Short summary: We describe TROLL 4.0, a simulator of forest dynamics that represents trees in a virtual space at one-meter resolution. Tree birth, growth, death and the underlying physiological processes such as carbon assimilation, water transpiration and leaf phenology depend on plant traits that are measured in the field for many individuals and species. The model is thus capable of jointly simulating forest structure, diversity and ecosystem functioning, a major challenge in modelling vegetation dynamics.

Abstract. TROLL 4.0 is an individual-based forest dynamics model that is capable of jointly simulating forest structure, diversity and ecosystem functioning, including the ecosystem water balance and productivity, leaf area dynamics and the tree community functional and taxonomic composition. It represents ecosystem flux processes in a manner similar to dynamic global vegetation models, while adopting a representation of plant community structure and diversity at a resolution consistent with that used by field ecologists. Specifically, trees are modeled as three-dimensional individuals with a metric-scale spatial representation, providing a detailed description of ecological processes such as competition for resources and tree demography. Carbon assimilation and plant water loss are explicitly represented at tree level using coupled photosynthesis and stomatal conductance models, depending on the micro-environmental conditions experienced by trees. Soil water uptake by trees is also modelled. Physiological and demographic processes are parameterized using plant functional traits measured in the field. Here we provide a detailed description and discussion of the implementation of TROLL 4.0. An evaluation of the model at two tropical forest sites is provided in a companion paper (Schmitt et al., submitted companion paper). TROLL 4.0's representation of processes reflects the state of the art, and we discuss possible developments to improve its predictive capability and its capacity to address challenges in forest monitoring, forest dynamics and carbon cycle research.



32 **1 Introduction**

33 Modelling vegetation dynamics remains a major challenge (Prentice et al., 2015; Song et al., 2021; Mahnken et al.,
34 2022), and the wide variety of modelling concepts that coexist depend on models' initial objectives. Early versions of global
35 vegetation models were developed to provide boundary conditions for energy, carbon and water budgets in global atmospheric
36 models (Sellers et al., 1986, 1997). With the refinement of modeling concepts and computer power, feedback loops between
37 the atmosphere and vegetation have gradually been taken into account (Charney, 1975; Cox et al., 2000; Meir et al., 2006),
38 leading to an improved representation of fluxes of energy, carbon and water across the vegetation layer (Fisher et al., 2015;
39 Moorcroft, 2003; Pitman, 2003). However, dynamic global vegetation models (DGVMs) typically adopt a simplified
40 representation of floristic composition and vegetation structure (Fisher et al., 2014; Prentice et al., 2007). In many of these
41 models, fluxes between vegetation and the atmosphere are still calculated in an average environment per grid cell (e.g. $1^{\circ} \times 1^{\circ}$),
42 for an average leaf of an individual drawn from a dozen of plant functional types (PFTs). The diversity of plant strategies is
43 therefore typically represented by a small number of PFTs even in highly diverse tropical forests (Fisher et al., 2014; Poulter
44 et al., 2011).

45 In parallel, stand-scale process-based models have been developed to better understand the exchanges between
46 vegetation and the atmosphere through an up-scaling of fine-scale ecophysiological processes, and to account for within-stand
47 micro-environmental heterogeneity (Wang and Jarvis, 1990; Gu et al., 1999; Williams et al., 1996; Ogée et al., 2003; Duursma
48 and Medlyn, 2012; Fyllas et al., 2014). These process-based models are conceptually close to DGVMs, but they implement a
49 more detailed representation of plant structure at the stand scale, and they have nurtured some important advances in DGVM-
50 development over the past decades (e.g., Chen et al., 2016). Typically used to assimilate eddy-flux data, they do not include
51 demographic processes however.

52 Forest growth models have a different history as they were initially developed to predict successional dynamics and
53 inform forest management (Watt, 1947; Botkin et al., 1972; Vanclay, 1994; Porté and Bartelink, 2002; Liang and Picard,
54 2013). A key innovation have been gap models that represent recruitment, growth, mortality and competition between
55 individual trees within forest patches. Forest patches are typically the size of a canopy opening created by the fall of a dominant
56 tree (gap, or chablis, Bugmann 2001) and modelled as horizontally homogeneous, with a spatially implicit representation of
57 tree positions. Through the simulation of a large number of patches, gap models can represent spatial heterogeneity due to gap
58 dynamics within stands. Overall, these models adopt a finer representation of vegetation structure than classic DGVMs, but
59 biogeochemical processes are generally modeled more coarsely, using ideal yield curves for tree growth rates combined with
60 limiting factors imposed by the patch environment. Since these empirical relationships can only be parameterized on the basis
61 of a large amount of data – readily available in plantations, but difficult to obtain elsewhere –, gap models typically also use
62 plant functional types to simulate diverse forest stands. The number and definition of these groups has been much discussed
63 in the literature, with no clear consensus (Botkin, 1975; Swaine and Whitmore, 1988; Vanclay, 1991; Köhler and Huth, 1998;



64 Köhler et al., 2000; Gourlet-Fleury et al., 2005; Kazmierczak et al., 2014), and these plant functional types are difficult to
65 transfer from one site to another (Picard and Franc, 2003; Picard et al., 2012).

66 Modelling vegetation from a completely different perspective and building upon flora distribution maps and
67 biogeographic concepts (Humboldt, 1849; Grisebach, 1872), plant species distribution models have been developed for long
68 (SDMs; Guisan et al., 2017). Generally, SDMs first estimate the envelope of environmental conditions for a species based on
69 species occurrence data (Guisan and Thuiller, 2005; Hutchinson, 1957; Soberón, 2007), which is used to infer a probability
70 distribution in space (Elith and Leathwick, 2009). These models require little knowledge on the processes underlying species
71 distribution, which explains their widespread use. However, because these models are statistical in nature, their ability to
72 project future states is unclear, and a great deal of research has been devoted to implementing process-based versions of these
73 SDMs (Chaine and Beaubien, 2001; Ferrier and Guisan, 2006; Morin and Lechowicz, 2008; Morin and Thuiller, 2009;
74 Kearney and Porter, 2009; Dormann et al., 2012; Journé et al., 2020).

75 From this brief and non exhaustive overview it emerges that each research community in vegetation modeling
76 emphasizes one representation of vegetation dimension – functioning, structure or diversity -- to the detriment of the others
77 (Maréchaux et al., 2021). Data availability and computing power partly explain such tradeoffs, and increasing model
78 complexity does not necessarily translate into an increase in reliability and robustness (Mahnken et al., 2022; Prentice et al.,
79 2015). However, a consensus has emerged in the literature that a better integration of plant species diversity, structure and
80 functioning should improve the predictive power of vegetation models (Purves and Pacala, 2008; Thuiller et al., 2008;
81 McMahon et al., 2011; Evans, 2012; Dormann et al., 2012; Mokany et al., 2016; Fisher et al., 2018). For example, tree species
82 diversity influences the productivity and resilience of forest ecosystems (Schnabel et al., 2019), and these biodiversity-
83 ecosystem functioning relationships result from local interactions where competition for resources is a key process (Fichtner
84 et al., 2018; Guillemot et al., 2020; Jourdan et al., 2020; Yu et al., 2024; Nemetscheck *et al.* 2024). Similarly, the fine details
85 of stand structure control the uptake of resources by vegetation (Braghiere et al., 2019, 2021; Brum et al., 2019; Ivanov et al.,
86 2012; De Deurwaerder et al., 2018), and they also determine the response to environmental stresses and disturbances
87 (Blanchard et al., 2023; Jucker et al., 2018; Seidl et al., 2014; De Frenne et al., 2019). More generally, the contribution of
88 vegetation in biogeochemical cycles, albeit typically quantified from stand to global scales (e.g. biomass, productivity),
89 ultimately depends on individual processes (e.g. mortality, Johnson et al., 2016) controlled by fine-scale heterogeneity and the
90 various ecological strategies of species (Poorter et al., 2015).

91 Therefore, recent developments in DGVMs have sought to better represent plant community structure and diversity.
92 Several cohort-based DGVMs have been developed to refine the representation of vegetation heterogeneity (Moorcroft et al.,
93 2001; Fisher et al., 2015; Longo et al., 2019; Smith et al., 2001). Continuous representations of functional diversity have also
94 been proposed using the distribution and co-variation of traits at the individual level or trait-climate relationships (Sakschewski
95 et al., 2015; Verheijen et al., 2015; Scheiter et al., 2013; Pavlick et al., 2013; Berzaghi et al., 2020; Van Bodegom et al., 2014).
96 These developments represent major advances in vegetation modelling, but scale mismatches between field data and model
97 representations limit the ability to assimilate data of various nature and resolution. While inverse modelling approaches can



98 partially alleviate these constraints (Hartig et al., 2012; Dietze et al., 2013; LeBauer et al., 2013; Fer et al., 2018; Lagarrigues
99 et al., 2015), they rely heavily on confidence in the model structure, can therefore raise equifinality issues (Medlyn et al.,
100 2005), and increase rapidly in computational complexity in high-dimensional parameter sets.

101 Finally, most of these challenges are exacerbated for tropical forests, as they are structurally complex (Doughty et al.,
102 2023), support a large number of tree species per hectare (up to several hundred, Wilson et al., 2012), and are more difficult
103 to access for evaluation in the field (Schimel et al., 2015). Given that they provide a range of ecosystem services and play a
104 major role in regional and global biogeochemical cycles (Beer et al., 2010; Bonan, 2008; Pan et al., 2011; Harper et al., 2013),
105 tropical forests and their responses to changing environmental factors have been identified as one of the greatest sources of
106 uncertainty in Earth system models (Koch et al., 2021; Powell et al., 2013; Restrepo-Coupe et al., 2017; Huntingford et al.,
107 2013). Thus, many advances in vegetation modelling have been, and still are, motivated by the challenge of tropical forests.

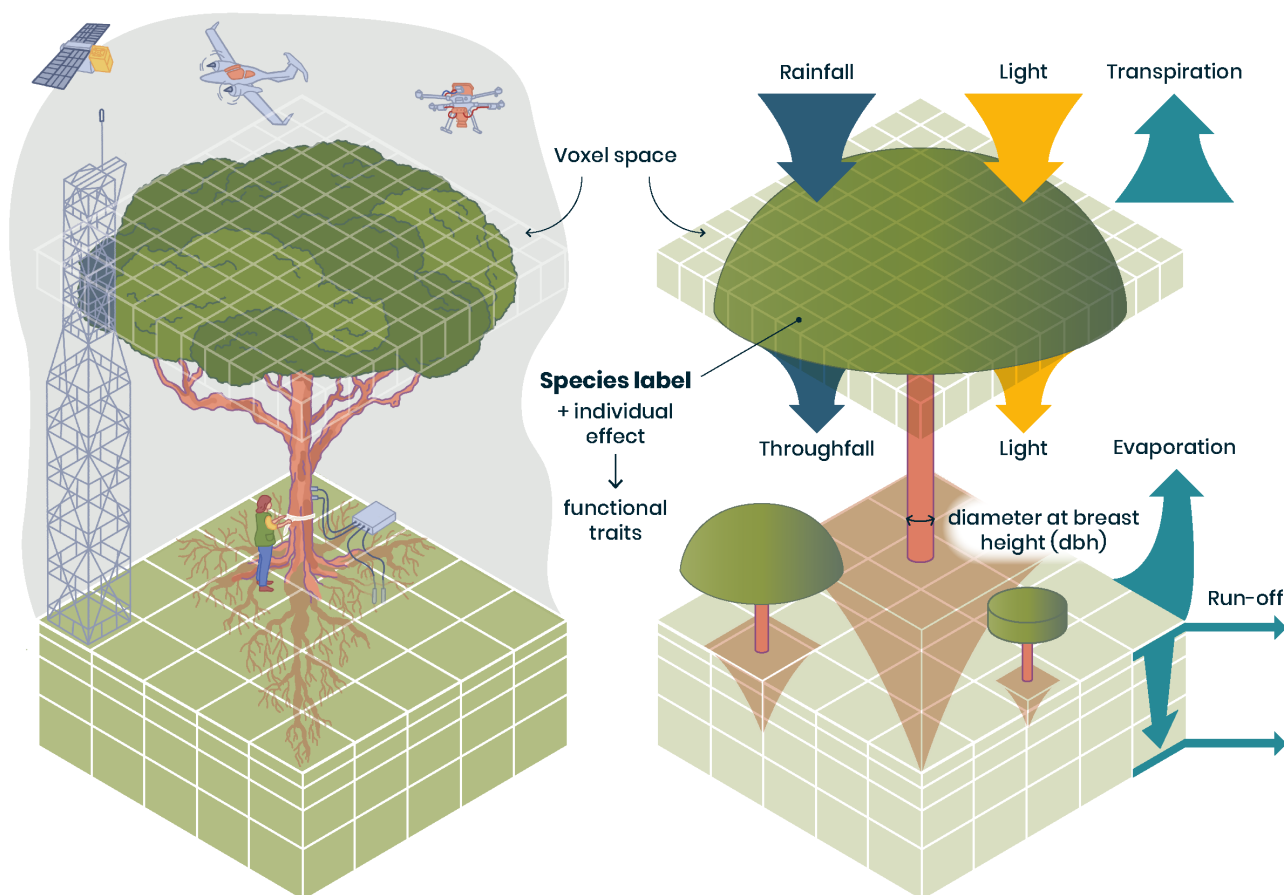
108 Here we describe a major upgrade of the TROLL forest dynamics model (Chave, 1999; Maréchaux and Chave, 2017;
109 Fischer, 2019), referred to here as TROLL 4.0. TROLL 4.0 brings together various modelling traditions, including elements
110 of DGVMs, stand-scale process-based models and forest gap models while adopting a species-level representation of plant
111 diversity, to jointly simulate the functioning, structure and diversity of forest ecosystems, and in particular tropical forests.
112 TROLL is a spatially explicit forest dynamics model, with an individual- and trait-based representation (Fig. 1). Individual
113 trees from 1cm diameter at breast height (*dbh*) are explicitly represented in a three-dimensional space discretized at a resolution
114 of one meter, allowing a fine representation of stand structure and local interactions via explicit competition for resources.
115 Each tree belongs to a species, with a list of mean traits per species provided as input. These traits control the physiological
116 and demographic processes of the tree's functioning and life cycle, from recruitment to growth, to seed dispersal and death.
117 This type of trait-based parameterization is based on recent advances in plant physiology and functional ecology, has been
118 facilitated by the expansion of large databases of functional traits (Díaz et al., 2016, 2022; Kattge et al., 2011, 2020), in
119 particular for tropical trees (Baraloto et al., 2010a; Vleminckx et al., 2021).

120 In TROLL 4.0, carbon assimilation and water loss by transpiration are represented explicitly using a photosynthesis
121 model coupled with a stomatal conductance model. Both take into account variation in micro-environmental conditions
122 between and within tree crowns, as well as the tree's access to soil water. A water cycle is now simulated, with the state and
123 dynamics of soil water explicitly represented and coupled with the vegetation dynamics. The influence of water availability
124 on leaf-level gas exchanges, leaf phenology, tree recruitment and death is parameterized through the leaf water potential at
125 turgor loss point (Bartlett et al., 2012) and mechanistic-based coordination with other hydraulic traits (Bartlett et al., 2016).
126 Carbon that is not consumed by the respiration of living tissues is then allocated to leaf production, carbon storage and tree
127 growth through allometric relationships. Compared to TROLL version 2.3.2 (Maréchaux and Chave, 2017), TROLL 4.0
128 includes other improvements: plant functional traits can vary among trees of the same species; tree crown shapes can be more
129 realistic than cylinders; and leaf density can vary within the tree crowns.

130 In this contribution, we provide a detailed description of the structure and objectives of the TROLL 4.0 model,
131 discussing how new modeling representations are an outcome of the state of knowledge and the availability of data. Finally,



132 we discuss the limitations of the model and future developments. An evaluation of the model's ability to simulate forest
133 structure, diversity and functioning for two Amazonian forest sites is reported in a companion paper (Schmitt et al., submitted
134 companion paper). The model is written in C++ and wrapped in the R environment through a dedicated package named
135 *rcontrol* (Schmitt et al. 2023).
136



137
138 **Figure 1: Representation of individual trees in a spatially explicit environment in TROLL 4.0 (right) allowing direct comparison**
139 **with data of various nature (left). In TROLL 4.0, each tree is composed of a trunk, a crown, whose shape evolves from a cylinder to**
140 **an umbrella as the tree grows, and root biomass that decreases exponentially with soil depth. Tree dimensions are updated at each**
141 **timestep, depending on the net assimilated carbon that is allocated to growth, and following allometric relationships depending on**
142 **tree diameter at breast height (*dbh*). Each tree has a species label associated with plant functional traits, which, together with an**
143 **individual effect randomly attributed at tree birth, determines the tree's functional traits. These traits are used to parameterize**
144 **physiological and demographic processes that govern tree functioning throughout its life cycle. Light diffusion is computed explicitly**
145 **at each time step and within each voxel from the canopy top to the ground. Water balance is also computed at each timestep, and**
146 **the resulting water availability across soil voxels influence tree functioning. With this representation of forest structure, composition**
147 **and functioning, model outputs can be directly compared with a wide range of data, including carbon and water fluxes provided by**
148 **eddy-flux towers, field inventories, and 3D structure estimates from remote sensing (left). In TROLL 4.0, aboveground voxels**
149 **typically have a finer horizontal resolution than belowground voxels, but the latter are vertically finer and increasing in thickness**
150 **with depth (right). This resolution matches the one of fine-scale remote-sensing products or soil water content monitoring (left).**



151

152 **2 Model description**

153 **2.1 Environmental conditions**

154 TROLL 4.0 simulates an idealized forest stand with a typical size of 1 to 100 ha. Parallel computing may be used to simulate
155 several times the same stand, or to simulate several forest stands with different environmental conditions. Climatic drivers are
156 similar to those represented in many DGVMs (air temperature, vapor pressure deficit, wind speed, and light intensity above
157 the canopy, as well as precipitation). The forest ecosystem is divided into an above-ground and below-ground part. Soil is
158 explicitly represented as a water reservoir, but soil nutrients are not modeled. The topography within a stand is assumed to be
159 flat.

160 **2.2 Light availability and aboveground variation in micro-climate**

161 Above ground, the simulated forest stand is represented as a discrete grid of 1m^3 cubic voxels. Light diffuses through the
162 forest's leaf layers from the top of the canopy to the ground, with one recalculation each day. In a given voxel, light availability
163 is the photosynthetic photon flux density in $\mu\text{mol photons m}^{-2} \text{s}^{-1}$ and is computed as a function of the incident light intensity
164 at top canopy ($PPFD_{top}$, see Table A1 for a list of symbols), the cumulated leaf density of voxels above and the (constant) leaf
165 density within the voxel itself. The Beer-Lambert extinction of light within the canopy allows to calculate the incident PPFD
166 (per unit ground area) above any layer at vertical extent v as:

$$167 \quad PPFD(v) = PPFD_{top} \times \exp[-k \times LAI(v)] \quad (1)$$

168 where $LAI(v)$ is the cumulated leaf area above height v , and k is the extinction coefficient. We here define $k =$
169 $k_{geom} \times \text{absorptance}_{leaves}$, where k_{geom} reflects the geometric arrangement of leaves in the voxel (a value of 0.5 reflecting
170 spherical leaf distribution; Ross, 1981) and $\text{absorptance}_{leaves}$, the fraction of absorbed light within a single leaf (Long et al.,
171 1993; Poorter et al., 1995). The absorbed light in a layer a of thickness Δa is then

$$172 \quad PPFD_{abs}(a) = PPFD_{top} \times \exp[-k \times LAI(a)] - PPFD_{top} \times \exp[-k \times LAI(a + \Delta a)] \quad (2)$$

173 Assuming that leaf area per unit ground area ($\text{m}^2 \text{m}^{-2}$), or $dens(a)$, is constant within the layer, this simplifies to:

$$174 \quad PPFD_{abs}(a) = PPFD_{top} \times \exp[-k \times LAI(a)] \times (1 - \exp[-k \times dens(a)]) \quad (3)$$

175 For photosynthesis calculations, absorbed PPFD per unit ground area is converted into absorbed PPFD per unit leaf area by
176 dividing $PPFD_{abs}(a)$ by $dens(a)$.

177 Air microenvironmental variation within the canopy is represented as follows. Nighttime temperature (T_{night}) is
178 assumed constant throughout the night and within the canopy, while temperature (T) and vapor pressure deficit (VPD) vary
179 across voxels depending on the variable $\lambda(v) = \frac{LAI(v)}{LAI_{sat}}$ with LAI_{sat} a threshold LAI and $LAI(v)$ the LAI above voxel v . At
180 height v above ground, we calculate temperature and VPD as follows:



181 $T(v) = T_{top} - \Delta T \times \lambda(v)$ (4)

182 $VPD(v) = VPD_{top} \times [C_{VPD0} + (1 - C_{VPD0}) \sqrt{(1 - \lambda(v))}]$ (5)

183 where ΔT and C_{VPD0} are set parameters and T_{top} and VPD_{top} are values at the top of canopy. For any given layer a of depth
184 Δa , temperatures and VPDs are then calculated by averaging both functions from a to $a + \Delta a$:

185 $T_{mean}(a) = \frac{1}{\Delta a} \int_a^{a+\Delta a} (T_{top} - \frac{\Delta T}{LAI_{sat}} \times LAI(v)) dv$ (6)

186 $VPD_{mean}(a) = \frac{1}{\Delta a} \int_a^{a+\Delta a} VPD_{top} \times [C_{VPD0} + \frac{(1-C_{VPD0})}{\sqrt{LAI_{sat}}} \sqrt{(LAI_{sat} - LAI(v))}] dv$ (7)

187 Equations 6 and 7 can then be simplified using the assumption of constant leaf density within a layer and redefining v with
188 respect to the current layer a , so that $LAI(v) = LAI(a) + dens(a) \times v$.

189 This representation of variation of T and VPD within the canopy is in qualitative agreement with empirical
190 observations of microclimate gradients within tropical forest canopies (Camargo and Kapos, 1995; Shuttleworth, 1985;
191 Shuttleworth et al., 1989, Tymen et al. 2017), with a consistent buffering effect of forest canopies on understory micro-
192 environment (De Frenne et al., 2019), and a strong control by forest structure (Gril et al., 2023b, a; Tymen et al., 2017;
193 Zellweger et al., 2019).

194 Wind speed attenuation inside the canopy is simulated as described in Rau et al. (2022), who explored the effect of
195 wind speed on forest structure in a forest exposed to cyclones using TROLL. Wind speed is usually measured above the canopy
196 and decreases as one approaches the canopy top layer, so wind speed at the top of the canopy is (Monteith & Unsworth 2008):

197 $u(z) = \frac{u_*}{\kappa} \ln\left(\frac{z-d}{z_0}\right), \text{ if } z \geq H$ (8)

198 where $u(z)$ is the horizontal wind speed in $m s^{-1}$ at a height z (in m) above ground, H the height of the top of the canopy (in
199 m), u_* is the friction velocity, κ the von Karman constant ($\kappa=0.40$), d the zero-plane displacement height, here assumed to be
200 equal to $0.8H$, and z_0 the aerodynamic roughness, here assumed to be equal to $0.06H$ (Rau et al., 2022). Within the canopy,
201 wind speed decreases as (Inoue 1963):

202 $u(z) = u(H) \exp\left(-\alpha\left(1 - \frac{z}{H}\right)\right), \text{ if } z < H$ (9)

203 with $\alpha \approx 3$ (Raupach et al., 1996). Wind speed was not computed at the voxel scale, but using the coarser horizontal resolution
204 of the belowground field (see section 2.3 below, e.g. 25x25 m), and a mean top canopy height H was computed as input to Eqs
205 (8) and (9).

206 2.3 Soil water availability

207 In TROLL 4.0, the belowground part of the ecosystem is explicitly represented, and its discretization is specified by the user,
208 including the number and depth of layers, and horizontal dimensions of the cells. Belowground voxels are typically coarser
209 horizontally (e.g. 25m x 25m, as commonly implemented in gap models Bugmann, 2001), but finer vertically, than
210 aboveground 1-m³ voxels. Metric-scale lateral water fluxes are difficult to parameterize and evaluate, and neglecting them



211 here limits the computational burden. Soil layers typically increase in thickness with depth, as in most DGVMs or forest
212 physiological models (Prentice et al., 2015) and in standard soil assessments (e.g. Hengl et al., 2017). In this representation,
213 contrasting root depth and access to water can be represented across individual trees together with potential variation in soil
214 properties and hydraulic state. This approach contrasts with some forest dynamics models that use a single-layer belowground
215 representation (e.g. Gutiérrez et al., 2014; Christoffersen et al., 2016; Fyllas et al., 2014).

216 The water content in each belowground voxel is simulated using a bucket model, which relies on the vertical water
217 balance for each voxel. Neglecting horizontal lateral fluxes, the water balance for a given soil column amounts to:

$$218 \Delta SWC = P - I - Q - E - T - L \quad (10)$$

219 where SWC is the soil water content, P the incident rainfall, I the canopy interception, Q the run-off, E the evaporation from
220 the soil, T the transpiration, i.e. the plant water uptake, and L the leakage. This water balance is established for each soil layer,
221 with inputs from upwards and outputs downwards starting from the top layer ($l=1$): outputs of layer l are inputs for layer $l+1$,
222 with L corresponding to the output of the deepest layer, and $P-I-Q$ to the input of the top layer. Note that this downward
223 iteration neglects: (i) potential hydraulic lift (upward water redistribution, see e.g. Dawson, 1993; Burgess et al., 1998; Oliveira
224 et al., 2005); and (ii) potential interaction with the water table (Costa et al., 2023; Sousa et al., 2022). Further developments
225 could account for these two mechanisms where they are expected to play a significant role. In particular, flooded areas could
226 be easily represented, with a shallower soil depth and a prescribed boundary condition, i.e. a shallower water table. We now
227 describe and discuss each term of the water balance and the corresponding modeling choices.

228 *Rainfall.* Rainfall (P , in mm) is a model input. It is assumed that the total daily rainfall corresponds to a single event
229 of rain per day (one storm, as in, e.g., Rodriguez-Iturbe et al., 1999; Laio et al., 2001; Fischer et al., 2014; Gutiérrez et al.,
230 2014).

231 *Interception.* Rainfall interception by the canopy is simulated using a model where interception depends on LAI, as
232 proposed by Liang et al. (1994):

$$233 I = \min(P, K \times LAI) \quad (11)$$

234 where $K=0.2\text{mm}$ and LAI corresponds to the leaf area index at ground level, averaged across the ground-level aboveground
235 voxels that contribute to a single belowground voxel (typically $625=25^2$ aboveground voxels contribute to one belowground
236 voxel). Similar simple formulations of canopy interception have been used elsewhere (e.g. Liu et al., 2017), and this choice is
237 justified by the lack of relevant data to properly parameterize more complex formulations at most field sites. More complex
238 models of rainfall interception also exist however (Rutter and Morton, 1977; Gash, 1979; Gash et al., 1995).

239 *Run-off and infiltration.* As in most bucket models coupled with a forest dynamics model, the temporal propagation
240 of the wetting front into the soil is not explicitly simulated here, because of the daily timestep and the vertically lumped
241 representation of soil moisture dynamics (e.g., Laio et al., 2001, Guimberteau et al., 2014). When the soil top layer has enough
242 available storage to absorb the totality of the throughfall (i.e. when throughfall is smaller than the layer water content at field
243 capacity minus the current soil water content), it is assumed that the increment in soil water content of that top layer is equal
244 to the throughfall. Otherwise, the excess water percolates to the next layer below. In the absence of an explicit wetting front,



245 runoff occurs only when the superficial layer is already saturated, which is similar to Dunne run-off (Dunne and Black, 1970).
246 More complex formulations of run-off exist (d'Orgeval et al., 2008; Guimberteau et al., 2014; Horton, 1933), but because of
247 the high porosity of many tropical forest soils (Hodnett and Tomasella, 2002; Sander 2002) and the lack of explicit topography
248 in this version, our choice is parsimonious.

249 *Soil evaporation.* We assumed that water evaporates from the top soil layer only, a reasonable assumption if the top
250 soil layer is not too thin. We followed Sellers et al. (1992) under which evaporation from the soil is expressed as (see Merlin
251 et al., 2016 for a review of alternatives):

$$252 \quad E = \frac{M_w}{RT_s} \times \frac{e_s - e_a}{r_{soil} + r_{aero}} \quad (12)$$

253 where E is in $\text{kg m}^{-2} \text{s}^{-1}$, M_w is the molar mass of water vapor ($M_w = 18 \text{ kg mol}^{-1}$), R is the ideal gas constant ($R = 8.31 \text{ J mol}^{-1}$
254 K^{-1}), T_s is the temperature at soil surface in K, e_s is the vapor pressure of the soil surface in Pa, e_a is the vapor pressure of air
255 above the soil surface in Pa, r_{soil} is the soil surface resistance in s m^{-1} , and r_{aero} is the aerodynamic resistance to heat transfer
256 in s m^{-1} . Soil water pressure e_s is a function of the water potential of the top soil belowground voxel ($\psi_{soil,top}$, in MPa; Jones,
257 2013, Eq. (5.14) therein):

$$258 \quad e_s = e_{sat}(T_s) \times \exp\left(\frac{V_w}{RT_s} \times \psi_{soil,top}\right) = e_{sat}(T_s) \times \exp\left(2.17 \times \frac{\psi_{soil,top}}{T_s}\right) \quad (13)$$

259 Where V_w is the partial molal volume of water ($V_w = 18 \times 10^{-6} \text{ m}^3 \text{ mol}^{-1}$), and $e_{sat}(T_s)$ is the saturated vapor pressure at T_s
260 computed following the Buck equation (Jones, 2013, Appendix 4 therein). e_a is by definition equal to $e_{sat}(T_s) - VPD_{ground}$,
261 where the latter is the VPD at ground level in Pa. r_{soil} is computed following Sellers et al. (1992, Eq. (19) therein, see also
262 Merlin et al., 2016, Eq. (12)):

$$263 \quad r_{soil} = \exp\left(8.206 - 4.255 \times \frac{\theta_{top}}{\theta_{fc,top}}\right) \quad (14)$$

264 where θ_{top} is the water content of the top soil belowground voxel and $\theta_{fc,top}$ is its water content at field capacity (in m^3).
265 Aerodynamic resistance r_{aero} is computed as follows (Merlin et al., 2016, Eq. (B10) therein):

$$266 \quad r_{aero} = \frac{1}{\kappa^2 \times u(Z)} \ln\left(\frac{Z}{Z_m}\right)^2 \quad (15)$$

267 with κ again the von Karman constant ($\kappa = 0.40$), $u(Z)$ is the wind speed (in m s^{-1}) at reference height Z , here taken at 1m above
268 ground, and Z_m is the momentum soil roughness in m, set to 0.001m.

269 *Transpiration.* Trees transpire soil water from the belowground voxel they are rooted in (see section 2.4.3). For a
270 given tree, the total daily soil water uptake is the sum of the water transpired by leaves across its crown and across day-time
271 half hours (see section 2.5.2). Soil layers contribute to water uptake as a function of tree-dependent weights, w_l (see Eq. (21),
272 section 2.4.3), which depend on root biomass and on the soil hydraulic state in each layer.

273 For each belowground voxel in layer l , the soil water potential (ψ_l) and the soil hydraulic conductivity (K_l) are
274 computed at each time step from the soil water content in the focal voxel using the van Genuchten-Mualem soil characteristic
275 and hydraulic conductivity curves (Mualem, 1976; van Genuchten, 1980; see Table 1 in Marthews et al., 2014). Parameters of



276 these curves are estimated using regression models (pedotransfer functions) for tropical soils (Hodnett and Tomasella, 2002),
277 except the saturated hydraulic conductivity, which is computed following Cosby et al. (1984; see Table 2 in Marthews et al.,
278 2014). In practice, when only soil texture data is available, TROLL 4.0 contains a default option to apply the texture-based
279 only pedotransfer function provided by Tomasella and Hodnett (1998), coupled to the soil characteristic and hydraulic
280 conductivity curves of Brooks and Corey (1964) (see Tables 1 and 2 in Marthews et al., 2014).

281 **2.4 Representation of trees in the model**

282 **2.4.1 Species affiliation and intra-specific trait variability**

283 In TROLL 4.0, each tree (and seed) is attributed a botanical species defined by a taxonomic binomial. It is assumed that the
284 user has sufficiently good knowledge of the tree species growing in the study area so that a list of species-specific mean plant
285 functional trait values can be provided as input. These are the leaf mass per area (LMA, in g m^{-2}), the leaf area (LA, cm^2), the
286 leaf nitrogen content per dry mass (N, in mg g^{-1}), the leaf phosphorous content per dry mass (P, in mg g^{-1}), the wood specific
287 gravity (wsg, in g cm^{-3}), the leaf water potential at turgor loss point (π_{tlp} , in MPa), and three allometric parameters ($\text{dbh}_{\text{thres}}$,
288 h_{lim} , a_h , all in m; see section 2.4.2). The number of species provided in input is not limited. In addition to mean plant functional
289 trait values, it is possible to input individual trait values from which a trait variance-covariance matrix is computed
290 (alternatively the trait variance-covariance matrix can be prescribed). With this option, for each recruited tree, the trait values
291 are drawn from a distribution rather than attributed the species-specific mean value. For each trait i and tree j , the species-
292 specific mean value is multiplied by a factor $e^{\varepsilon_{i,j}}$ where $\varepsilon_{i,j} \sim N(0, \sigma_i)$ where σ_i the trait-specific standard deviation on a
293 logarithmic scale (lognormal variation). The sole exception is wood specific gravity, which we assume to be normally
294 distributed around the mean with $\varepsilon_{wsg,j} \sim N(0, \sigma_{wsg})$. Trait covariance is only considered for leaf N, leaf P and LMA, and
295 other traits are assumed to be decoupled (Baraloto et al., 2010b). Note that with this implementation, intraspecific variation is
296 not structured in space or time nor heritable, and is thus a surrogate for variability emerging from genetic variation or plasticity
297 (Girard-Tercieux et al., 2023; 2024). A more realistic representation of the latter is left for future version.

298 **2.4.2 Aboveground structure**

299 Above ground, the tree geometry is represented as a three-dimensional object within the voxelized space and consists of a
300 trunk and a crown filled with leaves. The trunk is assumed to be a cylinder characterized by its total height and its diameter
301 (dbh , for diameter at breast height, by analogy with forest inventories). The aboveground dimensions of trees are predicted
302 from their dbh via scaling rules. For tree j with dbh_j , we calculate its height h_j , its crown radius cr_j , and its crown depth cd_j as
303 follows:

$$304 \quad h_j = \frac{h_{\text{lim}} \times \text{dbh}_j}{(a_h + \text{dbh}_j)} \times e^{\varepsilon_{h,j}} \quad (16)$$

$$305 \quad cr_j = e^{a_{cr}} \times \text{dbh}_j^{b_{cr}} \times e^{\varepsilon_{cr,j}} \quad (17)$$



306
$$cd_j = \min\left(\frac{h_j}{2}, (a_{cd} + b_{cd} \times h_j) \times e^{\varepsilon_{cd,j}}\right) \quad (18)$$

307 where h_{lim} and a_h are species-specific coefficients of the Michaelis-Menten function, and a_{cr} , b_{cr} , a_{cd} , and b_{cd} allometric
308 coefficients that are species independent. $\varepsilon_{h,j}$, $\varepsilon_{cr,j}$ and $\varepsilon_{cd,j}$ are variance terms to simulate intraspecific variation with
309 $\varepsilon_{h,j} \sim N(0, \sigma_h)$, $\varepsilon_{cr,j} \sim N(0, \sigma_{cr})$, and $\varepsilon_{cd,j} \sim N(0, \sigma_{cd})$. Tree crown architecture is known to depend on species ecological
310 strategies (Bohlman and O'Brien, 2006; Iida et al., 2012; Poorter et al., 2006; Laurans et al., 2024), but given that crown
311 extents are difficult to measure reliably in the dense canopies of tropical forests, we used a single set of parameters for all the
312 species.

313 In the previous published version (Maréchaux and Chave, 2017), tree crowns were represented as cylinders with
314 homogeneous leaf densities. Since v.3.0, TROLL can also model tree crowns as flexible, umbrella-like shapes with
315 heterogeneous leaf density distributions. Small tree crowns are simulated as cylinders, but consist of up to three separate 1-m
316 layers of leaves (top, intermediate and bottom layer). Each layer can be assigned a percentage of the total leaf area (e.g., 50%,
317 30%, 20%) to reflect gradients in leaf densities from the upmost to lower crown layers (Kitajima et al., 2005), but the default
318 is an equal distribution (33%, 33%, 33%) across all layers. Once a tree surpasses 3 m in crown depth, no new layers are added.
319 Instead, the treetop grows quicker in height than the outer crown parts. As a result, the three 1-m layers are folded around the
320 tree trunk like an umbrella at various stages of opening (see Fig. 1b in Schmitt et al., 2023, and similar tree representations in
321 Strigul et al., 2008). Different functional forms are available to describe height variation from treetop to crown edge, but here
322 we chose a simple linear decrease between the radius at the top of the crown to the radius at the bottom of the crown. The ratio
323 between both radii is controlled through the global parameter *shape_crown*, which varies between 0 (conical shape) and 1
324 (cylinder), and thus allows for various “conifer-like” and “broadleaf-like” shapes in between.

325 We also relax the assumption that tree crowns are homogeneously filled across their horizontal extent. In TROLL
326 4.0, crowns have small 1-m² openings (or gaps) in their crowns, parameterized as percentage of total crown area that is not
327 filled with leaves, f_{gap} . This allows for the modelling of a spatially heterogeneous light environment in the understory (Tymen
328 et al., 2017), with a theoretical range from $f_{gap} = 0\%$ (full crown cover, no openings) to $f_{gap} = 100\%$ (a hypothetical crown with
329 no leaf area). When calibrating TROLL for tropical forests with airborne laser scanning (Fischer et al., 2019), we found a value
330 of $f_{gap} = 15\%$ to be a good approximation for this within-crown gap fraction. If intraspecific variation in crown extent is
331 explicitly modelled, the fraction of crown gaps is rescaled so that the absolute crown cover stays constant (i.e., the fraction of
332 crown gaps is divided by $e^{2\varepsilon_{cr,j}}$). Within species, variation in crown extent is thus assumed as decoupled from variation in leaf
333 area, i.e., reflecting variation in branch angles and directions, but not branch number or biomass.

334 2.4.3 Belowground structure

335 TROLL 4.0 makes the common assumption that total fine root biomass is equal to leaf biomass. Future developments should
336 endeavor to represent a more explicit belowground allocation scheme (Merganičová et al., 2019; Huaraca Huasco et al., 2021).
337 Direct estimates of individual tree root depth and root distribution are rare in moist tropical forests (Canadell et al., 1996;



338 Jackson et al., 1996, 1999; Nepstad et al., 1994; Cusack et al., 2024; Guerrero-Ramírez et al., 2021). Some studies have
339 quantified the depth of tree water uptake using indirect methods, such as predawn leaf water potential, or isotope labeling
340 (Brum et al., 2019; Stahl et al., 2013), but this does not give access to the actual rooting depth. Tree root depth was here
341 assumed to increase with tree size, and was computed as a function of tree *dbh* as follows (Kenzo et al., 2009, Fig. 4 therein):

$$342 \quad RD = 0.35 \times dbh^{0.54} \quad (19)$$

343 with root depth, RD, in m, and diameter at breast height, *dbh*, in cm. As in Xu et al. (2016), the exponent was based on Kenzo
344 et al. (2009), who reported on data from excavated trees in secondary forests in Malaysia. The first parameter (0.35, root depth
345 at *dbh*=1cm) was adjusted to avoid unrealistic water depletion of the top soil layer. In the absence of relevant species-specific
346 data, this allometric equation was assumed to hold for all species, even if root depth is known to be highly plastic (e.g. Rowland
347 et al., 2023). Correlations between rooting depth and leaf phenological habit have been reported, but in drier or more seasonal
348 sites than Amazonian rainforests (Brum et al., 2019; Hasselquist et al., 2010; Smith-Martin et al., 2020), and trait coordination
349 are known to be typically stronger under harsher environmental conditions (Dwyer and Laughlin, 2017; Delhaye et al., 2020).

350 We assumed that vertical tree root distribution follows an exponential profile, as observed empirically at the stand
351 scale (Fisher et al., 2007; Humbel, 1978; Jackson et al., 1996). The fine root biomass in layer *l*, at depths ranging from z_l to
352 z_{l+1} ($> z_l$) is computed as:

$$353 \quad RB_l = RB_t \times \left(\exp\left(-3 \frac{z_l}{RD}\right) - \exp\left(-3 \frac{z_{l+1}}{RD}\right) \right) \quad (20)$$

354 where RB_t is the total tree fine root biomass (in g), RB_l the fine root biomass in layer *l* (in g), RD the tree rooting depth (in m).
355 The factor 3 was determined so that about 95% of the tree biomass is contained between soil surface and RD (note that $-\log(0.05) \approx 3$) (Arora and Boer, 2003). Tree roots are distributed across vertical layers, but do not spread across belowground
356 voxels horizontally. As a result, trees only deplete the water content of the belowground voxels located below their trunk
357 position (see section 2.3).

359 The soil water potential in the root zone, ψ_{root} (in MPa), captures how the plant equilibrates with the soil water state
360 across its root profile. It is computed as the weighted mean of the belowground voxel water potentials across layers. We used
361 the weighting scheme proposed by Williams et al. (2001; see also Bonan et al., 2014; Duursma and Medlyn, 2012), which
362 accounts for the variation of soil water availability and conductance across layers as follows:

$$363 \quad \psi_{root} = \sum_l w_l \times \psi_l \quad \text{with } w_l = \frac{(\psi_l - \psi_{R,min}) \times G_l}{\sum_{ll} (\psi_{ll} - \psi_{R,min}) \times G_{ll}} \quad (21)$$

364 where ψ_l is the soil water potential in layer *l*, and $\psi_{R,min}$ is the root water potential below which there is no water uptake
365 within the layer (minimal root water potential, assumed to be -3 MPa as in Duursma and Medlyn, 2012). G_l , the soil-to-root
366 water conductance in layer *l*, in $\text{mmol H}_2\text{O m}^{-2} \text{ s}^{-1} \text{ MPa}^{-1}$, computed as follows (Gardner, 1964):

$$367 \quad G_l = \frac{2\pi L_{a,l} K_l}{\log\left(\frac{r_s}{r_r}\right)} \quad (22)$$

368 In Eq (22), $L_{a,l}$ is the total root length per unit area in the layer (in m m^{-2}), with the total root length in the layer computed as
369 $RB_l \times SRL$ where SRL is the specific root length, here assumed to be constant (10 m g^{-1} , Bonan et al., 2014; Metcalfe et al.,



370 2008; Weemstra et al., 2016). K_l is the soil hydraulic conductivity of layer l (in $\text{mmol H}_2\text{O m}^{-1} \text{s}^{-1} \text{MPa}^{-1}$, see section 2.3), r_r is
371 the mean fine root radius, here set at 1mm, and r_s is half the mean distance between roots, calculated with the assumption of
372 uniform root spacing in a given layer (Newman, 1969):

$$373 \quad r_s = \frac{1}{\sqrt{\pi L_{v,l}}} \quad (23)$$

374 where $L_{v,l}$ is the total root length per unit soil volume in the layer (in m m^{-3}), computed in the same way as $L_{a,l}$, but also divided
375 by layer depth.

376 A range of other models have been used to infer ψ_{root} using the relative tree root biomass in each layer directly as
377 weights (De Kauwe et al., 2015; Naudts et al., 2015; Powell et al., 2013; Schaphoff et al., 2018; Sakschewski et al., 2021;
378 Verbeeck et al., 2011). However, trees do not uptake water simply as a proportion of root density, but can equilibrate with the
379 wettest soil layers (Schmidhalter, 1997; Duursma and Medlyn, 2012): the contrasting temporal variations in water availability
380 across layers result in seasonal changes in the depth of active water withdrawal (Bruno et al., 2006; Joetzier et al., 2022). For
381 instance, cavitation in the driest part of the soil disconnects roots from the soil (Sperry et al., 2002; see also Fisher et al., 2006).
382 This is likely why deeper roots, although often very rare, disproportionately contribute to sustain forest productivity during
383 dry seasons.

384 2.5 Leaf physiology

385 The carbon assimilated and the water transpired by a tree within a day are the sum of the leaf-level carbon and water fluxes
386 across day-time half hours. Leaf-level carbon assimilation is computed per crown layer of each tree, using the Farquhar-von
387 Caemmerer-Berry model of C_3 photosynthesis (Farquhar et al., 1980, see section 2.5.1), coupled to the model of stomatal
388 conductance of Medlyn et al. (2011; see section 2.5.2) as in Maréchaux and Chave (2017). In TROLL 4.0 the dependences on
389 leaf temperature (T_l), vapor pressure deficit at the leaf surface (VPD_s), and CO_2 concentration at the leaf surface (c_s) are now
390 determined iteratively at the leaf surface, starting from air temperature (T), air vapor pressure deficit (VPD_a) and air CO_2
391 concentration (c_a) averaged across the tree crown layer (see sections 2.2 and 2.4.2) and with transpiration computed using the
392 Penman-Monteith equation (see section 2.5.4).

393 2.5.1 Photosynthesis

394 In Farquhar et al. (1980), leaf-level net carbon assimilation rate (A_n , $\mu\text{mol CO}_2 \text{m}^{-2} \text{s}^{-1}$) is limited by either Rubisco activity
395 (A_v , $\mu\text{mol CO}_2 \text{m}^{-2} \text{s}^{-1}$), or RuBP regeneration (A_j , $\mu\text{mol CO}_2 \text{m}^{-2} \text{s}^{-1}$):

$$396 \quad A_n = \min\{A_v, A_j\} - R_p(T_l) \quad ; \quad A_v = V_{cmax}(T_l, \psi_{pd}) \times \frac{c_i - \Gamma^*}{c_i + K_m(T_l)} \quad ; \quad A_j = \frac{1}{4} \frac{c_i - \Gamma^*(T_l)}{c_i + 2\Gamma^*(T_l)} \quad (24)$$

397 where R_p is the photorespiration rate ($\mu\text{mol C m}^{-2} \text{s}^{-1}$), V_{cmax} is the maximum rate of carboxylation ($\mu\text{mol CO}_2 \text{m}^{-2} \text{s}^{-1}$), c_i the
398 CO_2 partial pressure at carboxylation sites, Γ^* the CO_2 compensation point in the absence of dark respiration, K_m the apparent



399 kinetic constant of the Rubisco (von Caemmerer, 2000), and J the electron transport rate ($\mu\text{mol } e^- \text{ m}^{-2} \text{ s}^{-1}$), which depends on
400 PPFD through:

$$401 \quad J = \frac{1}{2\theta} \left[\alpha \times PPFD + J_{max}(T_l, \psi_{pd}) - \sqrt{\left(\alpha \times PPFD + J_{max}(T_l, \psi_{pd}) \right)^2 - 4\theta \times \alpha \times PPFD \times J_{max}(T_l, \psi_{pd})} \right] \quad (25)$$

402 J_{max} is the maximal electron transport capacity ($\mu\text{mol } e^- \text{ m}^{-2} \text{ s}^{-1}$), θ the curvature factor (unitless), and α the apparent quantum
403 yield to electron transport ($\text{mol } e^- \text{ mol photons}^{-1}$), computed following von Caemmerer (2000) as $\alpha = (1 - LSQ) \times 0.5$, with
404 LSQ the effective spectral quality of light, fixed at 0.15, and the factor 0.5 accounts for the fact that each photosystem absorbs
405 half of the photons.

406 The V_{cmax} and J_{max} parameters depend on leaf properties, leaf temperature (T_l) and water state (through the leaf
407 predawn water potential, ψ_{pd} , see Eq. (37)) and represent a large source of uncertainty in vegetation models (Zaehle et al.,
408 2005; Mercado et al., 2009; Rogers et al., 2017). In tropical forest environments, Domingues et al. (2010) suggested that V_{cmax}
409 and J_{max} are co-limited by the leaf concentration of nitrogen and phosphorus as follows (see also Walker et al., 2014):

$$410 \quad V_{cmax-M}(25^\circ\text{C}) = \min\{-1.56 + 0.43 \times N - 0.37 \times LMA ; -0.80 + 0.45 \times P - 0.25 \times LMA \} \quad (26)$$

$$411 \quad J_{max-M}(25^\circ\text{C}) = \min\{-1.50 + 0.41 \times N - 0.45 \times LMA ; -0.74 + 0.44 \times P - 0.32 \times LMA \} \quad (27)$$

412 with V_{cmax-M} and J_{max-M} the photosynthetic capacities at 25°C of unstressed mature leaves on a leaf dry mass basis, in μmol
413 $\text{CO}_2 \text{ g}^{-1} \text{ s}^{-1}$ and $\mu\text{mol } e^- \text{ g}^{-1} \text{ s}^{-1}$, respectively. N and P are leaf nitrogen and phosphorus concentrations in mg g^{-1} , and LMA is the
414 leaf mass per area in g cm^{-2} . V_{cmax-M} and J_{max-M} can be converted into area-based V_{cmax} and J_{max} by multiplying by LMA.
415 We used this leaf trait-based parameterization of $V_{cmax}(25^\circ\text{C})$ and $J_{max}(25^\circ\text{C})$ in the absence of water stress (as in Fyllas et
416 al., 2014; Mercado et al., 2011). The dependence of V_{cmax} and J_{max} with temperature was given by equations in Bernacchi et
417 al. (2003), and the dependence with water availability was modelled by a function of ψ_{pd} (WSF_{ns} , see section 2.5.3, Eq. (40)):

$$418 \quad V_{cmax}(T_l, \psi_{pd}) = V_{cmax}(25^\circ\text{C}) \times e^{\left(\frac{26.35 - \frac{65.33}{R \times (T_l + 273.15)}}{R \times (T_l + 273.15)} \right)} \times WSF_{ns}(\psi_{pd}) \quad (28)$$

$$419 \quad J_{max}(T_l, \psi_{pd}) = J_{max}(25^\circ\text{C}) \times e^{\left(\frac{17.57 - \frac{43.54}{R \times (T_l + 273.15)}}{R \times (T_l + 273.15)} \right)} \times WSF_{ns}(\psi_{pd}) \quad (29)$$

420 where R is the molar gas constant ($0.008314 \text{ kJ K}^{-1} \text{ mol}^{-1}$), and T_l is the internal leaf temperature in Celsius degrees. The
421 temperature dependence of Γ^* and K_m followed von Caemmerer (2000):

$$422 \quad \Gamma^*(T_l) = 37 \times e^{\frac{23.4 \times (T_l - 25)}{298 \times R \times (273 + T_l)}} \quad (30)$$

$$423 \quad K_m(T_l) = 404 \times e^{\frac{59.36 \times (T_l - 25)}{298 \times R \times (273 + T_l)}} \times \left(1 + \frac{210}{248 \times e^{\frac{35.94 \times (T_l - 25)}{298 \times R \times (273 + T_l)}}} \right) \quad (31)$$

424 Temperature dependencies in Eqs (28)-(31) are consistent with Domingues et al. (2010), following recommendations from
425 Rogers et al. (2017).

426 Leaf photorespiration rate R_p was assumed to be a fixed fraction (40%) of leaf dark respiration rate (Atkin et al.,
427 2000). We used Atkin et al. (2015) ‘broadleaved trees’ empirical model to estimate mature leaf dark respiration rates as a
428 function of plant functional traits:



429 $R_{d-M}(25^{\circ}\text{C}) = 8.5341 - 0.1306 \times N - 0.5670 \times P - 0.0137 \times LMA + 11.1 \times V_{cmax-M} + 0.1876 \times N \times P$ (32)

430 with R_{d-M} the leaf dark respiration rate on a dry mass basis and at reference temperature of 25°C (in $\text{nmol CO}_2 \text{ g}^{-1}\text{s}^{-1}$).

431 Multiplying R_{d-M} by LMA gives the area-based leaf dark respiration R_d (in $\mu\text{mol C m}^{-2} \text{ s}^{-1}$). The temperature dependence of

432 mature leaf dark respiration rates was calculated as (Atkin et al., 2015, Eq. (1) therein; see also Heskell et al. 2016):

433 $R_d(T_l) = R_d(25^{\circ}\text{C}) \times \left[3.09 - 0.043 \times \frac{(T_l+25)}{2} \right]^{\frac{(T_l-25)}{10}}$ (33)

434 Long-term acclimation to temperature is not considered in TROLL 4.0 (Kattge and Knorr, 2007; Smith and Dukes, 2013).

435 2.5.2 Stomatal conductance

436 Carbon assimilation by photosynthesis is limited by the CO_2 partial pressure at carboxylation sites, which is controlled by

437 stomatal transport as modeled by the diffusion equation:

438 $A_n = g_s(c_s - c_i)$ (34)

439 with g_s the stomatal conductance to CO_2 ($\text{mol CO}_2 \text{ m}^{-2} \text{ s}^{-1}$). The representation of stomatal conductance varies greatly across

440 vegetation models (Damour et al., 2010; Bonan et al., 2014; Rogers et al., 2017; see Appendix B, Table B1) and remains an

441 active research topic (Anderegg et al., 2018; Dewar et al., 2018; Lamour et al., 2022; Sperry et al., 2017; Wolf et al., 2016;

442 Sabot et al., 2022). In TROLL 4.0, stomatal conductance to water vapor is simulated as (Medlyn et al., 2011):

443 $g_{sw} = g_0 + 1.6 \times \left(1 + \frac{g_1}{\sqrt{VPD_s}} \right) \times \frac{A_n}{c_s}$ (35)

444 where g_{sw} is the stomatal conductance to water vapor in $\text{mol H}_2\text{O m}^{-2} \text{ s}^{-1}$, 1.6 is the factor needed to convert one mole of CO_2

445 into one mole of H_2O , VPD_s is the vapor pressure deficit at the leaf surface in kPa, A_n is the assimilation rate in $\mu\text{mol CO}_2 \text{ m}^{-2} \text{ s}^{-1}$

446 (Eq. (24) above), c_s is the CO_2 concentration at the leaf surface in ppm, g_0 is the minimum conductance for water vapor

447 in $\text{mol H}_2\text{O m}^{-2} \text{ s}^{-1}$ (Duursma et al., 2019), and g_1 is a model parameter in $\text{kPa}^{1/2}$. Equations 24, 34 and 35 taken together lead

448 to two quadratic equations for c_i , one when Rubisco activity is limiting and one when RuBP regeneration is limiting, and the

449 solution is the highest root.

450 The parameter g_1 varies with species ecological strategies and carbon cost of water use (Domingues et al., 2014;

451 Franks et al., 2018; Héroult et al., 2013; Lin et al., 2015; Wolz et al., 2017). Consequently, it is expected that g_1 should differ

452 across plant functional types (e.g. Xu et al., 2016). Here we assumed a dependence of g_1 with wood density (wsg , in g cm^{-3})

453 as in Lin et al. (2015). We also assumed a dependence with water availability, modelled by a function of ψ_{pd} (WSF_s ; see

454 section 2.5.3):

455 $g_1 = (-3.97 \times wsg + 6.53) \times WSF_s(\psi_{pd})$ (36)

456 This parameterization of g_1 based on wood density is a matter of debate however, and alternatives have been proposed (Wu

457 et al., 2020; Lamour et al., 2023).

458 The parameter g_0 quantifies water fluxes through the leaf cuticle (cuticular conductance) and from stomatal leaks.

459 Although it is increasingly recognized as a key parameter explaining tree water loss in drought conditions (Cochard, 2021;



460 Martin-StPaul et al., 2017), its values and variation with other functional traits is poorly documented (Duursma et al., 2019;
461 Slot et al., 2021; Nemetschek et al., 2024), and we here assumed a fixed value. Note that some previous studies have defined
462 g_0 as cuticular conductance only, ignoring stomatal leak effects, and thus underestimating g_0 .

463 Both g_0 and g_1 were assumed not to depend on temperature in the absence of clear empirical evidence for tropical
464 forest trees (Duursma et al., 2019; Slot et al., 2021; Rogers et al., 2017), but this may be further explored in the future through
465 measurement and experiment (Cochard, 2021).

466 2.5.3 Effect of water availability on leaf-level gas exchange

467 Under water stress, leaf-level gas exchanges and photosynthesis are impaired, but how this is represented varies greatly across
468 models (Appendix B, Table B1; Powell et al., 2013; Trugman et al., 2018; Verhoef and Egea, 2014). A common approach is
469 to define a single integrative water stress factor cumulating all effects along the soil-plant-atmosphere pathway, some of which
470 being difficult to evaluate empirically (e.g. Fischer et al., 2014; Gutiérrez et al., 2014; Krinner et al., 2005; Clark et al., 2011).
471 This factor is then used to modify the parameters of the stomatal conductance and/or photosynthesis models (Egea et al., 2011;
472 Verhoef and Egea, 2014). Depending on models, water stress factors have been assumed to depend on soil water content or on
473 soil water potential in the root zone (De Kauwe et al., 2015; Drake et al., 2017; Joetzjer et al., 2014; Powell et al., 2013;
474 Trugman et al., 2018). Alternatively, some models have implemented a water stress factor as a function of leaf water potential
475 (ψ_{leaf} ; Christoffersen et al., 2016; Duursma and Medlyn, 2012; Kennedy et al., 2019; Xu et al., 2016; see also the pioneer
476 work of Tuzet et al., 2003) or used optimization approaches (Williams et al., 1996; Anderegg et al., 2018; Sabot et al., 2020;
477 Sperry et al., 2017; Wolf et al., 2016), to account for the cost of water uptake and transportation in the plant water column.
478 The shape of such functions remains contentious however (Table B1), resulting in substantial differences in model predictions.

479 Also, there is no consensus on the relative role of stomatal and non-stomatal limitations on leaf CO_2 assimilation
480 under drying conditions, reflecting contrasted experimental results (Drake et al., 2017; Zhou et al., 2014; Keenan et al., 2010;
481 Appendix B, Table B2). Under stomatal limitation, stomatal closure reduces leaf gas exchanges, and the water stress factor is
482 applied on stomatal conductance, or stomatal conductance model parameters (e.g. g_1). Under non-stomatal limitations, drought
483 (leading to increased leaf temperature and/or decreased leaf water potential) impairs the biochemical photosynthesis apparatus,
484 which results in a reduction of photosynthetic capacities, and/or mesophyll conductance (Flexas et al., 2004, 2012). In this
485 latter case, the water stress factor is applied on V_{cmax} and J_{max} (Drake et al., 2017; Keenan et al., 2010). Some models consider
486 only one limitation, and others both (Appendix B, Table B1).

487 In TROLL 4.0, two water stress factors are used, one for stomatal limitation, modifying the g_1 parameter (WSF_s ; Eq.
488 (36)), and one for non-stomatal limitations, modifying the V_{cmax} and J_{max} parameters of the photosynthesis model (WSF_{ns} ; Eq.
489 (28) and (29)). Both water stress factors are assumed to depend on the leaf predawn water potential (ψ_{pd} ; De Kauwe et al.,
490 2015; Verhoef and Egea, 2014), which is a function of the soil water potential in the root zone (ψ_{root} , Eq. (21)) (Stahl et al.,
491 2013, but see Bucci et al., 2004; Donovan et al., 2003) as follows (Jones, 2013; Eq. (4.9) therein):



492 $\psi_{pd} = \psi_{root} - \rho gh \approx \psi_{root} - 0.01 \times h$ (37)

493 where ρ is the density of water, g the gravitational force ($g=9.81 \text{ m s}^{-2}$), and h total tree height in m. Here, WSF_s was computed
494 as (Zhou et al., 2013; De Kauwe et al., 2015):

495 $WSF_s = \exp(b \times \psi_{pd})$ (38)

496 where b is a parameter. To parameterize b , we used the relationship between the leaf water potential at turgor loss point (π_{tlp}
497 in MPa) and the water potential causing 90% of stomatal closure (ψ_{gs90} , in MPa): $\pi_{tlp} = 0.97 \times \psi_{gs90}$ ($P<0.01$, $R^2=0.4$; Fig.
498 1 in Martin-StPaul et al. 2017), and assumed that $WSF_s \approx 0.1$ at ψ_{gs90} (an approximation given the shape of Eq. (35)), leading
499 to:

500 $WSF_s = \exp\left(-2.23 \times \frac{\psi_{pd}}{\pi_{tlp}}\right)$ (39)

501 The link between the leaf water potential at stomatal closure and the leaf water potential at turgor loss point is supported by
502 several studies (Bartlett et al., 2016b; Brodribb et al., 2003; Farrell et al., 2017; Martin-StPaul et al., 2017; Meinzer et al.,
503 2016; Rodriguez-Dominguez et al., 2016; Trueba et al., 2019). The formulation of WSF_s in Eq (39) was preferred over
504 alternatives, such as a linear relationship between WSF_s and ψ_{pd} (Oleson et al., 2008; Powell et al., 2013; Verhoef and Egea,
505 2014). The latter is less supported by data and leads to threshold responses as soil water content declines and similar responses
506 across species, in contrast with empirical evidence (Kursar et al., 2009; Zhou et al., 2013).

507 The water stress factor for non-stomatal limitation (WSF_{ns}) was computed following Xu et al. (2016):

508 $WSF_{ns} = \left(1 + \left(\frac{\psi_{pd}}{\pi_{tlp}}\right)^a\right)^{-1}$ (40)

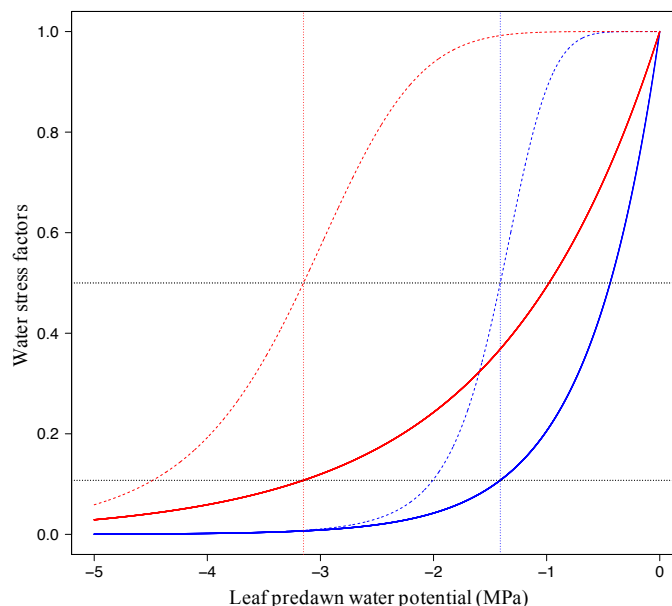
509 with $a=6$ estimated from data reported in Brodribb et al. (2003). In this formula, $WSF_{ns} = 1/2$ when $\psi_{pd} = \pi_{tlp}$, in agreement
510 with empirical findings (Brodribb et al., 2002; Manzoni, 2014).

511 The parameterization of WSF_s and WSF_{ns} based on π_{tlp} is supported by the fact that leaf cells need to maintain turgor
512 to sustain functioning (Hsiao, 1973). These functions do not depend on π_{tlp} when $\psi_{pd} = \pi_{tlp}$, so there is a simple link between
513 the leaf drought tolerance, as informed by π_{tlp} , and the response of leaf-level gas exchange to water availability. Also, these
514 equations predict that the decline of stomatal conductance as water availability decreases precedes that of photochemistry,
515 consistent with observations (Fig. 2; Fatichi et al., 2016; Trueba et al., 2019).

516 Note that, since mesophyll conductance is not explicitly represented here, the effect of water stress on photosynthetic
517 capacities (WSF_{ns}) includes both direct effects on the photosynthetic machinery and indirect effects from the reduction of
518 mesophyll conductance (Drake et al., 2017; Keenan et al., 2010). Alternative shapes of water stress factors could be explored
519 in the future, and a more explicit representation of the water flow through the plant water column could be implemented
520 (Paschalis et al., 2024). In the absence of a clear consensus on the effect of water stress on respiration, TROLL 4.0 does not
521 assume that respiration depends on water availability (Flexas et al., 2006, 2005; Rowland et al., 2018, 2015; Santos et al.,
522 2018; Stahl et al., 2013b).



523



524

525 **Figure 2: Responses of leaf-level gas exchange to water stress, depending on the leaf drought tolerance. Water stress factors for the**
 526 **stomatal conductance parameter g_1 (stomatal limitation, WSF_s , Eq. (39); solid lines) and for the photosynthetic capacities J_{max} and**
 527 **V_{cmax} (non-stomatal limitation, WSF_{ns} , Eq. (40); dashed lines) as a function of leaf predawn water potential (Ψ_{pd} , in MPa). WSF_s**
 528 **are shown for a drought vulnerable species ($\pi_{tlp}=-1.41$ MPa, the least negative value reported in Maréchaux et al., 2015; blue**
 529 **lines), and for a drought tolerant species ($\pi_{tlp}=-3.15$ MPa, the most negative value reported in Maréchaux et al., 2015). Vertical**
 530 **dotted lines: π_{tlp} , horizontal dotted black lines: WSF_s and WSF_{ns} at π_{tlp} .**

531 2.5.4 Leaf energy balance

532 In TROLL 4.0, leaf temperature (T_l), vapor pressure deficit (VPD_s) and CO_2 concentration (c_s) at the leaf surface are computed
 533 through an iterative scheme that solves the leaf energy balance (Medlyn et al., 2007; Wang and Leuning, 1998; Duursma,
 534 2015; Vezy et al., 2018). This is an important step because the leaf boundary layer plays a key role on gas exchanges, and
 535 especially so in dense tropical moist forests, given the large size of tropical tree leaves and the low wind speeds within canopies
 536 (De Kauwe et al., 2017; Jarvis and McNaughton, 1986; Meinzer et al., 1997). The iterative scheme is as follows. Initially, T_l ,
 537 VPD_s and c_s are set equal to surrounding air values (T , VPD and c_a). Leaf photosynthesis (A_n) and stomatal conductance (g_{sw})
 538 are computed using Eqs (24), (34) and (35); next, the boundary layer conductance and radiation conductance are computed;
 539 and finally leaf-level transpiration rate is deduced from the Penman-Monteith equation (Eq. (41) below). After these steps,
 540 new values for T_l , VPD_s and c_s are computed, and the above steps are repeated until leaf temperature converges, i.e., when the
 541 absolute difference between the T_l of two consecutive iteration is lower than $0.01^\circ C$.

542 Leaf-level transpiration rate E_l (in $mol\ H_2O\ m^{-2}\ s^{-1}$) is calculated as:



$$E_l = \frac{1}{\lambda} \times \frac{sR_{ni} + VPD_a g_H C_p M_a}{s + \gamma \frac{g_H}{g_w}} \quad (41)$$

where λ is the latent heat of water vapor (in J mol⁻¹), s is the slope of the (locally linearized) relationship between saturated vapor pressure and temperature (in Pa K⁻¹, see Jones, 2013, Eq. (5.15) therein), R_{ni} is the isothermal net radiation (in J m⁻² s⁻¹), g_H is the total leaf conductance to heat (in mol m⁻² s⁻¹), C_p is the heat capacity of air (1010 J kg⁻¹ K⁻¹), M_a is the molecular mass of air (28.96 × 10⁻³ kg mol⁻¹), γ the psychrometric constant (in Pa K⁻¹), and g_w the total conductance to water vapor (mol H₂O m⁻² s⁻¹). The latent heat of water vapor λ depends on air temperature as follows:

$$\lambda = (2.501 \times 10^3 - 2.365 \times T) \times 18 \quad (42)$$

The isothermal net radiation R_{ni} has two components, the absorbed solar radiation (S_{abs}), including both PAR and NIR wavebands, and the net longwave radiation (Leuning et al., 1995; Appendix D therein):

$$R_{ni} = S_{abs} - B_{n,0} \times k_d \exp(-k_d LAI) \quad (43)$$

where $B_{n,0}$ is the net longwave radiation at the top of the canopy, and $k_d \exp(-k_d LAI)$ accounts for its extinction within the canopy, with k_d set equal to 0.8. To account for the absorbed NIR radiation at a given height within the canopy in S_{abs} , we used the relationship reported by Kume et al. (2011; Fig. 4 therein) that links the transmitted NIR to the transmitted and incident PAR, and assumed a leaf absorptance in the NIR equal to 0.1. $B_{n,0}$ is then computed as the absorbed minus the emitted longwave radiation:

$$B_{n,0} = \varepsilon_l (1 - \varepsilon_a) \sigma T_{top}^4 \quad (44)$$

where T_{top} is the top canopy air temperature in K, σ is the Stefan-Boltzmann constant ($\sigma = 5.67 \times 10^{-8}$ W m⁻² K⁻⁴), ε_l is the emissivity of the canopy leaves, here assumed to be 1, and ε_a the emissivity of the atmosphere. Several models exist for ε_a , with varying performance depending on the sky conditions (Marthews et al., 2012). We here used Dilley and O'Brien (1998), which compromises between parsimony and performance across sky conditions (Marthews et al., 2012; Tables 2 and 5 therein).

g_H , the total leaf conductance to heat, has three components, the boundary layer conductance for free convection g_{bHf} , the boundary layer for forced convection g_{bHu} , and the radiation conductance g_r (Leuning et al., 1995; Jones, 2013):

$$g_H = 2 \times (g_{bHf} + g_{bHu} + g_r) \quad (45)$$

where the factor 2 accounts for the two sides of the leaves. g_{bHf} , the boundary layer conductance for free convection, is given by:

$$g_{bHf} = 0.5 \times D_H \times \left(\frac{1.6 \times 10^8 \times |T_l - T|}{w_l} \right)^{0.25} \times \frac{P_{ress}}{RT} \quad (46)$$

where D_H is the molecular diffusivity to heat ($D_H = 21.5 \times 10^{-6}$ m² s⁻¹), P_{ress} the atmospheric pressure (in Pa), R the universal gas constant ($R = 8.314$ J mol⁻¹ K⁻¹) and T the temperature of surrounding air in K. Leaf width w_l (in m) is estimated as the square root of leaf area ($w_l = \sqrt{LA}$). g_{bHu} , the boundary layer for forced convection (in mol m⁻² s⁻¹), is given by:

$$g_{bHu} = 0.003 \times \sqrt{\frac{u}{w_l}} \times \frac{P_{ress}}{RT} \quad (47)$$



573 where u is the wind speed in m s^{-1} (see Eq. (9)). g_r , the radiation conductance in $\text{mol m}^{-2} \text{s}^{-1}$ varies with T_a as follows (Jones,
 574 2013, p.101 therein):

$$575 \quad g_r = \frac{4 \times \epsilon_l \sigma T^3}{c_p M_a} \quad (48)$$

576 g_w the total conductance to water vapor has two components that represent hydraulic resistances in series: the stomatal
 577 conductance (g_{sw} , in $\text{mol H}_2\text{O m}^{-2} \text{s}^{-1}$, Eq. (35)) and the boundary layer conductance (g_{bw} in $\text{mol H}_2\text{O m}^{-2} \text{s}^{-1}$) to water vapor:

$$578 \quad g_w = \frac{g_{bw} \times g_{sw}}{g_{bw} + g_{sw}} \quad (49)$$

$$579 \quad \text{with } g_{bw} = 1.075 \times (g_{bHf} + g_{bHu}) \quad (50)$$

580 where 1.075 accounts for the relative diffusivities of heat and water vapor in air. Equations (49) and (50) assume that all leaves
 581 are hypostomatous (stomates on the ground-facing side of the leaves only), a reasonable assumption in tropical forests (Drake
 582 et al., 2019; Muir, 2015).

583 2.6 Carbon allocation

584 2.6.1. Net carbon uptake: whole-tree integration and respiration

585 At each daily timestep, the individual tree net primary productivity of carbon, NPP_{ind} (in gC), is obtained by the following
 586 balance equation (Fig. 3):

$$587 \quad NPP_{ind} = GPP_{ind} - R_{maintenance} - R_{growth} \quad (51)$$

588 GPP_{ind} (in gC) is computed each half hour as the carbon assimilation rate A_n (Eq. (19)), multiplied by the leaf area in each
 589 tree crown layer (LA_l , in m^2), then summed over tree crown layers and cumulated across the day.

590 Young leaves and old leaves have been reported to have lower photosynthetic capacities and activities than mature
 591 leaves (Doughty and Goulden, 2008; Kitajima et al., 2002, 1997b; Wu et al., 2016; Albert et al., 2018; Menezes et al., 2021).
 592 For each tree, total leaf area (LA_t) is partitioned into three leaf age pools: young, mature and old leaves, so that $LA_t = LA_{young}$
 593 $+ LA_{mature} + LA_{old}$ (all in m^2). These three leaf age pools are assumed to be uniformly distributed within the tree crown. In
 594 young and old leaves, net assimilation rate is a fraction $\rho < 1$ of that of mature leaves, so that:

$$595 \quad GPP_{ind} = C_{GPP} \times \frac{(\rho \times LA_{young} + LA_{mature} + \rho \times LA_{old})}{LA_t} \sum_l \sum_t A_n(t, l) \times LA_l \quad (52)$$

596 where the factor C_{GPP} is a conversion factor, t depicts the daytime half-hours and l the tree crown layers. Here we assume that
 597 the carbon uptake efficiency ρ relative to mature leaves is the same in young and old leaves and $\rho = 0.5$, a value consistent
 598 with observations.

599 TROLL 4.0 partitions autotrophic respiration into maintenance respiration and growth respiration, even if both come
 600 from the same biochemical pathways (Amthor, 1984; Thornley and Cannell, 2000). Maintenance respiration ($R_{maintenance}$) has
 601 seldom been documented for stem and roots and is inferred empirically (Cavaleri et al., 2008; Meir et al., 2001; Slot et al.,
 602 2013; Weerasinghe et al., 2014). Nighttime leaf maintenance respiration is computed using Eqs (32) and (33), using the mean



603 nighttime temperature. As stomatal conductance and dark respiration vary less with leaf age than carbon assimilation rate
 604 (Albert et al., 2018; Kitajima et al., 2002; Villar et al., 1995), we assumed that young and old leaves have respiration and
 605 transpiration rate equal to $q' = 0.75$ that of mature leaves, leading to lower water use efficiency than mature leaves. Tree-level
 606 nighttime leaf respiration and daytime transpiration are computed as follows at each timestep:

$$607 \quad X_{ind} = C_X \times \frac{(q' \times LA_{young} + LA_{mature} + q' \times LA_{old})}{LA_t} \sum_l (\sum_i X(i, l)) \times LA_l \quad (53)$$

608 where X_{ind} is either the carbon respired by leaves during the night or the total water transpired by the tree, in gC or m³
 609 respectively, X being the leaf dark respiration (Eqs. (32) and (33)) or the leaf-level transpiration rate (Eq. (41)) respectively,
 610 and C_X is a conversion factor.

611 Stem maintenance respiration (R_{stem} , in $\mu\text{mol C s}^{-1}$) was modeled assuming a constant respiration rate per volume of
 612 sapwood ($39.6 \mu\text{mol m}^{-3} \text{ s}^{-1}$, Ryan et al., 1994), so that:

$$613 \quad R_{stem} = C_{sresp} \times 39.6 \times SA \times (h - cd) \quad (54)$$

614 where SA is the tree sapwood area (in m²) and C_{sresp} is a conversion factor. Stem respiration response to temperature was
 615 modeled using a Q_{10} value of 2.0 (Meir and Grace, 2002; Ryan et al., 1994), and using mean daytime and nighttime
 616 temperatures. Stahl et al. (2011) reported that R_{stem} varies among individual trees, even when controlling for sapwood volume.
 617 However, in absence of a clear understanding of the drivers, Eq. (54) is a parsimonious choice. In TROLL 4.0, sapwood area
 618 is computed dynamically. We used an inversion of the pipe model to derive sapwood area from the tree's leaf area (LA_t , in
 619 m²), height (h , in m) and wood density following Fyllas et al. (2014; Eqs (7) and (8) therein):

$$620 \quad SA = C_{SA} \frac{2 \times LA_t}{\lambda_1 + \lambda_2 \times h + \delta_1 + \delta_2 \times wsg} \quad (55)$$

621 with $\lambda_1 = 0.066 \text{ m}^2 \text{ cm}^{-2}$, $\lambda_2 = 0.017 \text{ m cm}^{-2}$, $\delta_1 = -0.018 \text{ m}^2 \text{ cm}^{-2}$, and $\delta_2 = 1.6 \text{ cm}^3 \text{ g}^{-1}$, and C_{SA} a conversion factor. In addition
 622 to Eq. (55), there are both lower and upper limits on sapwood extent. Sapwood has a minimum thickness of 0.5 cm and any
 623 newly grown wood is always considered sapwood, irrespective of leaf area. TROLL 4.0 also imposes an upper limit on
 624 sapwood growth based on stem diameter growth, so that increases in living tissue cannot exceed increases in total tissue.

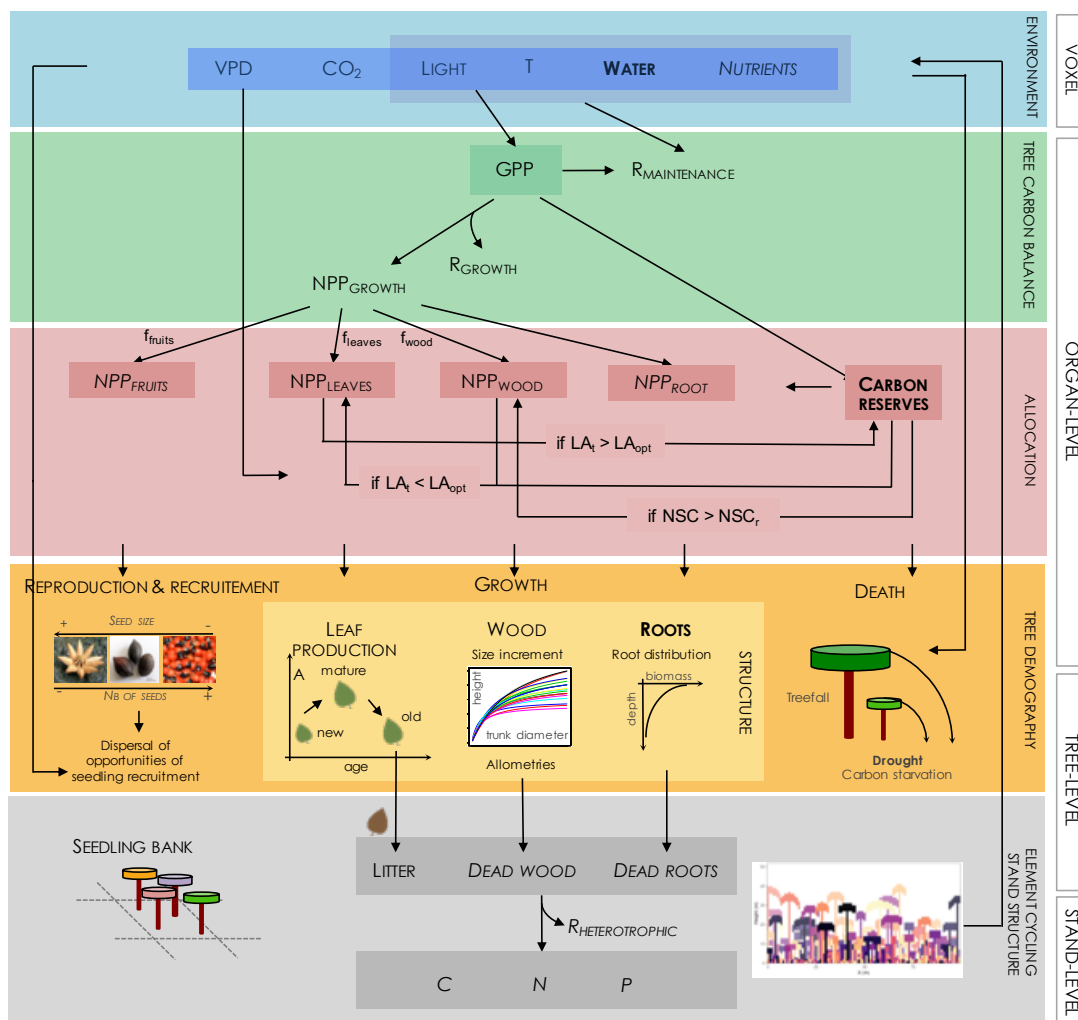
625 Other contributions of maintenance respiration were prescribed as proportions of leaf and stem maintenance
 626 respiration. Fine root maintenance respiration was assumed to be half of leaf maintenance respiration (Malhi, 2012), and coarse
 627 root and branch maintenance respirations were assumed to account for half of stem respiration (Asao et al., 2015; Cavaleri et
 628 al., 2006; Meir and Grace, 2002).

629 Growth respiration (R_{growth}) was assumed to account for 30% of the carbon uptake by photosynthesis (gross primary
 630 productivity) minus the maintenance respiration (Cannell and Thornley, 2000). These assumptions are commonly made in the
 631 literature, but remain a major source of uncertainty in the carbon flux modeling (Atkin et al., 2014; Huntingford et al., 2013).

632 Contrary to the last published version of TROLL, in which the allocation of NPP_{ind} to plant organs was fully prescribed
 633 by fixed factors ($f_{canopy} = f_{leaves} + f_{fruit} + f_{twigs}$ and f_{wood} , Maréchaux and Chave, 2017), the allocation scheme implemented in
 634 TROLL 4.0 can now be additionally modulated depending on the current tree state and it includes an explicit carbon storage
 635 compartment (sections 2.6.2 and 2.6.3; Fig. 3).



636



637

638 **Figure 3: Diagram of structures and processes driving individual and community dynamics, as investigated under the modeling**
 639 **approach adopted in TROLL 4.0. Elements in bold letters refer to novel implementation in comparison to the previous published**
 640 **version, while italic letters refer to elements still not included in this present version. Abiotic environment is modeled at the voxel**
 641 **scale and drive C assimilation in the leaves (gross primary productivity, GPP) and maintenance respiration rates of the different**
 642 **plant organs ($R_{\text{MAINTENANCE}}$). The C amount resulting from the balance between GPP and $R_{\text{MAINTENANCE}}$ can be used for tissue**
 643 **production (NPP_{FRUITS} , NPP_{LEAVES} , NPP_{WOOD} and NPP_{ROOTS}) or stored (**CARBON RESERVES**) in the different tree organs. Both**
 644 **allocations induce metabolic costs (R_{GROWTH} and R_{STORAGE} ; but the latter is not represented nor included). **CARBON RESERVES****
 645 **represents non-structural carbohydrates (NSC), mainly stored as sugar or starch, and its maximal storage capacity is given by NSC_r .**
 646 **Allocation to these different compartments follows a hierarchical scheme initialized by default proportions (f_{fruits} , f_{leaves} , f_{wood}). If the**
 647 **tree leaf area (LA_t) exceeds the optimal leaf area (LA_{opt} , a function of both tree properties and its micro-environment), then the**
 648 **surplus of NPP_{LEAVES} is allocated to carbon reserves. If the tree leaf area is lower than optimal, then NPP_{WOOD} , and if further needed,**
 649 **carbon reserves, are mobilized for leaf production. If carbon reserves surpass storage capacity (NSC_r), then stored carbohydrates**
 650 **are used for woody growth. C allocated to tissue production leads to an increment of trunk diameter and height following allometric**
 651 **relationships, and the production of new young leaves and roots. Simultaneously with tissue turnover, this leads to the update of leaf**
 652 **density and root biomass distribution, influencing both abiotic environment (eg. light diffusion and water interception) and light**
 653 **and element acquisition, and thus carbon assimilation and metabolism. C allocated to reproduction leads to the production of seeds,**
 654 **which are dispersed randomly. This generates a spatially-explicit seedling bank, from which winners are locally recruited depending**



655 on both light and water availability. Tree death may be triggered by environmental or mechanical constraints, or carbon starvation.
656 In a future version, litter decomposition, wood decay and nutrient mineralization, could lead to soil nutrient availability for plant
657 uptake, and take place through the action of soil microorganisms, which activity, and hence respiration ($R_{\text{HETEROTROPHIC}}$), depends
658 particularly on temperature and soil moisture.
659

660 2.6.2 Leaf production and leaf shedding

661 Leaf phenology is a key driver of the variation of tropical forest productivity (Manoli et al., 2018; Restrepo-Coupe et al., 2013;
662 Wu et al., 2017). However, its underlying drivers remain poorly understood, and its representation in vegetation models
663 remains challenging (Chen et al., 2020; Restrepo-Coupe et al., 2017). In ORCHIDEE, Chen et al. (2020, 2021) proposed a leaf
664 phenological scheme in which the production of young leaves is partly controlled by incident shortwave radiation, while the
665 shedding of old leaves is controlled by vapor pressure deficit. This scheme reproduces the simultaneous increase in leaf
666 production and litterfall observed in many Amazonian rainforest sites where productivity increases during the dry season
667 (Chave et al., 2010; Wagner et al., 2016; Yang et al., 2021), but not the observed seasonality in productivity at some sites (e.g.
668 GUYAFLUX eddy-flux site in French Guiana, Chen et al., 2020). Additionally, this scheme overlooks the contrasted leaf
669 phenological patterns observed across canopy individuals within and across species within communities (Nicolini et al., 2012;
670 Loubry, 1994). In ED2, Xu et al. (2016) implemented a leaf phenological scheme driven by water availability in the root zone
671 in a seasonally dry tropical forest. Since leaf shedding is often triggered by drought-induced loss of leaf turgor in these systems
672 (Sobrado, 1986), leaf shedding and production are assumed to depend on the difference between leaf predawn water potential
673 and leaf water potential at turgor loss point. However, such a scheme cannot simulate the simultaneous leaf production and
674 shedding observed in moist tropical forests.

675 In TROLL 4.0, we propose an alternative approach. At each timestep, the optimal tree total leaf area (LA_{opt}) is
676 estimated as the leaf area beyond which producing more leaves leads to a net carbon loss due to self-shading and respiration
677 costs. LA_{opt} depends on tree crown size and leaf area density (section 2.4.2), leaf photosynthetic capacities and respiration rate
678 (section 2.5.1), and local light environment. At each timestep, the amount of carbon allocated to the production of new young
679 leaves, NPP_{leaves} , and to woody growth, NPP_{wood} , are determined by default as: $NPP_{\text{leaves}} = f_{\text{leaves}} \times NPP_{\text{ind}}$, with
680 $f_{\text{leaves}} = 0.68 \times f_{\text{canopy}}$ (Chave et al., 2008, 2010; Maréchaux and Chave, 2017), and $NPP_{\text{wood}} = 0.6 \times f_{\text{wood}} \times NPP_{\text{ind}}$,
681 where the factor 0.6 accounts for the fact that about 40% of woody NPP is actually used for branch fall repair (Malhi et al.,
682 2011). When leaf area LA_t exceeds LA_{opt} , NPP_{leaves} is reduced so that $LA_t = LA_{\text{opt}}$. Second, if the carbon allocated to leaf
683 production is not sufficient to compensate leaf loss, then the carbon attributed by default to tree woody growth is mobilized
684 for leaf production until leaf loss is compensated. If not sufficient, the tree carbon storage (see section 2.6.3) is then also
685 mobilized. Hence this scheme prioritizes the maintenance of the assimilating tissues over woody growth (Schipper et al.,
686 2015). The variation of leaf area for each leaf age pool is then computed as follows:

$$687 \Delta LA_{\text{young}} = \frac{2 \times NPP_{\text{leaves}}}{LMA} - \frac{LA_{\text{young}}}{\tau_{\text{young}}}$$



$$\Delta LA_{mature} = \frac{LA_{young}}{\tau_{young}} - \frac{LA_{mature}}{\tau_{mature}}$$

$$\Delta LA_{old} = \frac{LA_{mature}}{\tau_{mature}} - \frac{LA_{old}}{\tau_{old}} \quad (56)$$

where τ_{young} , τ_{mature} , τ_{old} are the residence times in each class (in yr), so that $LL = \tau_{young} + \tau_{mature} + \tau_{old}$ with LL the maximal tree leaf lifespan (in yr). LL is inferred from the tree LMA, using the following empirical relationships (Schmitt, 2017):

$$LL = \frac{1}{12} \max(3, 12.755 \times \exp(0.007 \times LMA - 0.565 \times N)) \quad (57)$$

τ_{young} was fixed to $\min(LL/3, 1/12)$ yr (Doughty and Goulden, 2008; Wu et al., 2016), and τ_{mature} as a third of total leaf lifespan.

The loss term LA_{old}/τ_{old} corresponds to the rate of leaf litterfall at each timestep. In the previous TROLL version, litterfall resulted from the dynamics of leaf biomass with $\tau_{old} = LL - \tau_{young} - \tau_{mature}$. This leaf shedding scheme is passive and does not simulate the observed seasonality in leaf litterfall. Here we propose a new approach to simulate leaf shedding. We first observed that within species and sites, canopy trees can shed their leaves at different times, suggesting that causal environmental drivers should display fine-scale heterogeneity in space (unlike atmospheric shortwave radiation and vapor pressure deficit). In addition, old leaves display nutrient resorption before abscission (Albert et al., 2018; Kitajima et al., 1997a; Urbina et al., 2021); similarly, solute translocation from older to younger leaves can lower osmotic potential and leaf water potential at turgor loss point, thus increasing the drought tolerance of younger leaves to the detriment of older leaves (Pantin et al., 2012). We therefore used predawn leaf water potential as a trigger of leaf shedding as in Xu et al., (2016), but with different thresholds for leaves of different ages, older leaves being more susceptible to a small decrease in tree water availability, while younger leaves can maintain turgor and grow at the same time. More specifically, we defined the following threshold:

$$\psi_{T,o} = \min(a_{T,o} \times \pi_{tlp} - 0.01 \times h - b_{T,o}) \quad (58)$$

The first term in $\psi_{T,o}$ with $a_{T,o} < 1$ represents old leaves' lower ability to maintain turgor as soil dries. The second term modulates this susceptibility to drought depending on tree height (Bennett et al., 2015): it induces a susceptibility to a (small) decrease $b_{T,o} > 0$ in soil water availability for large trees, while preventing them from constantly shedding their old leaves at fast pace (see Eq. (37)). τ_{old} is then updated using a multiplying factor f_o ($0.001 \leq f_o \leq 1$). Initially, $\tau'_{old} = f_o \tau_{old}$ with $f_o = 1$, which is updated daily as follows: $f'_o = f_o - \delta_o$ when $\psi_{pd} < \psi_{T,o}$ and $f'_o = f_o + \delta_o$ when $\psi_{pd} > \psi_{T,o}$, always assuming that f_o has 0.001 as a lower bound, and 1 as an upper bound.

We assumed no variation of π_{tlp} with tree height (Maréchaux et al., 2016). The threshold $\psi_{T,o}$ jointly depends on π_{tlp} and tree height h to account for drought tolerance and tree height on leaf-level water stress. Practically, the tree height above which old leaves becomes susceptible to a small decrease in soil water availability is $H_{T,o} = -100 \times (a_{T,o} \pi_{tlp} + b_{T,o})$ in m: 28 m at $\pi_{tlp} = -1.5$ MPa and 58m at $\pi_{tlp} = -3$ MPa (when $a_{T,o} = 0.2$ and $b_{T,o} = 0.02$). While this scheme is based on process-based observations, parameters $a_{T,o}$, $b_{T,o}$, and δ_o are currently calibrated (see Schmitt et al., submitted companion paper).



719 2.6.3 Carbon storage

720 In TROLL 4.0, trees can store carbon explicitly in non-structural carbohydrates. The maximal amount of carbon a tree can
721 store and remobilize is determined as follows:

$$722 \quad NSC_r = 1000 \times 0.5 \times 0.05 \times 1.25 \times AGB \quad (59)$$

723 where NSC_r stands for non-structural carbohydrates (in gC), AGB is the tree aboveground biomass (in kg), and 1000×0.5
724 converts biomass in kg into C in g (Elias and Potvin, 2003). It is assumed that NSC can account for 10% of the tree biomass,
725 half of which is mobilizable (Martínez-Vilalta et al., 2016), hence the factor 0.05. The other half of NSC supports critical
726 metabolic functions or is no longer accessible. The factor 1.25 accounts for an additional 25% biomass storage in coarse roots,
727 so $1.25 \times AGB$ is total tree biomass (Ledo et al., 2018). AGB is computed following (Chave et al., 2014; Eq. (5) therein):

$$728 \quad AGB = 0.0559 \times wsg \times dbh^2 \times h \quad (60)$$

729 where dbh is in cm, h in m and wsg in $g\ cm^{-3}$. The NSC storage compartment is filled by the potential carbon surplus resulting
730 from the allocation to leaf production, i.e. $f_{leaves} \times NPP_{ind} - NPP_{leaves}$, if positive. If the storage compartment has reached
731 its maximal capacity NSC_r , then the surplus is allocated to woody growth.

732 2.6.4 Growth

733 The net primary production allocated to woody growth, NPP_{wood} , depends on the outcome of allocation to leaf
734 production and carbon reserves (see sections 2.6.2 and 2.6.3; Fig. 3). In TROLL 4.0, hydraulic control on carbon assimilation
735 and leaf phenology both influence carbon allocation to trunk growth (e.g. Doughty et al., 2014; Farrior et al., 2013;
736 Friedlingstein et al., 1999), but turgor-mediated processes are not explicitly modeled (Coussement et al., 2018; Peters et al.,
737 2023; Muller et al., 2011; Körner, 2015). NPP_{wood} is converted into an increment of stem volume, ΔV in m^3 , as follows:

$$738 \quad \Delta V = 10^{-6} \times \frac{NPP_{wood}}{0.5 \times wsg} \times Senesc(dbh) \quad (61)$$

739 where the factor 0.5 converts dry biomass units into carbon units (Elias and Potvin, 2003). The function $Senesc(dbh)$ is
740 designed so that the largest trees cannot allocate carbon as efficiently into growth, reflecting empirical evidence of a size-
741 related relative growth decline in trees (Yoda et al., 1965; Ryan et al., 1997; Mencuccini et al., 2005; Woodruff and Meinzer,
742 2011; Stephenson et al., 2014). We assumed that trees cannot exceed a trunk diameter of $dbh_{max} = \frac{3}{2} dbh_{thresh}$, where
743 dbh_{thresh} depends on species-specific information provided by the user (see section 2.4.1), so that:

$$744 \quad Senesc(dbh) = \begin{cases} 1 & \text{when } dbh \leq dbh_{thresh} \\ \max\left(0; 3 - 2\frac{dbh}{dbh_{thresh}}\right) & \text{when } dbh > dbh_{thresh} \end{cases} \quad (62)$$

745 Trunk diameter growth increment Δdbh (in m), is computed from ΔV as follows. $V = C \pi \left(\frac{dbh}{2}\right)^2 h$, where C is a form
746 factor (Chave et al. 2014, Eq. (5) therein). The term h (in m) is total tree height inferred from the dbh following Eq. (16), this
747 leads to an expression of V as a function of dbh only. This function can be inverted to estimate Δdbh as a function of ΔV ,
748 which is known from Eq. (61). Tree height and crown dimensions are then updated using Eqs (16), (17) and (18).



749 2.7 Tree demography

750 2.7.1 Seed production, dispersal and recruitment

751 The starting point for a tree life cycle, as represented in TROLL 4.0 is an event of seed dispersal into the seed bank. On each
752 1x1 m ground site and for each species s , a ‘seed’ bank stores all the seeds dispersed from the mature trees as well as from an
753 external seed rain. The seed bank is updated once a year. Here, our conceptual ‘seeds’ represent opportunities of seedling
754 recruitment rather than as true seeds, since not all seed dispersal events are modeled explicitly, and the seed-to-seedling
755 transition is implicit.

756 In TROLL 4.0 trees are assumed to become fertile above a diameter threshold dbh_{mature} that depends on the tree
757 maximal size (Visser et al., 2016) as follows:

$$758 \quad dbh_{mature} = 0.5 \times dbh_{thresh} \quad (63)$$

759 This relationship is drawn from direct observations of reproductive status of tree species in the tropical forest of Barro Colorado
760 Island, Panama, with maximal tree dbh spanning a range of 0.05 to 2 m (see Fig. S9 in Visser et al., 2016; $R^2=0.81$, $n=60$
761 species). The number of reproduction opportunities per mature tree, n_s , is assumed fixed and equal for all individuals, and its
762 value is user-defined. This assumption of a fixed reproductive opportunity per tree is predicated on the fact that there is a trade-
763 off between seed number and seed size, itself related to seed and seedling survival. Thus, the probability of germination does
764 not depend strongly on seed size or on the number of produced seeds and can be assumed a zero-sum game (Coomes and
765 Grubb, 2003; Moles et al., 2004; Moles and Westoby, 2006). Each of the n_s events is scattered away from the tree in a random
766 direction and at a distance randomly drawn from a Rayleigh distribution, thus allowing for potential long-dispersal events.
767 Although seed dispersal distance is known to vary depending on dispersal syndrome and plant traits (Tamme et al., 2014;
768 Seidler and Plotkin, 2006; Muller-Landau et al., 2008), the scale parameter σ_{disp} of the distribution is here fixed across species
769 and individuals.

770 The intensity of the external seed rain is quantified by N_{tot} (in number of incoming seeds per hectare) and its species
771 composition is defined by the relative abundances of species $f_{reg,s}$, both being user-defined. Hence, for each species s , $n_{ext,s}$
772 events of dispersal due to seeds immigrating from the outside occurred, with:

$$773 \quad n_{ext,s} = N_{tot} \times f_{reg,s} \times n_{ha} \quad (64)$$

774 with n_{ha} the number of hectares of the simulated plot. These reproduction opportunities are uniformly distributed within the
775 simulated area.

776 If several species are competing for recruitment in a local seed bank, one of the species is picked at random as the
777 winner out of all the seeds present, as in a lottery model (Chesson and Warner, 1981). The recruitment event occurs only if
778 ground-level light availability is sufficiently high. To test if this condition is met, the seedling is first attributed individual trait
779 values depending on the species-specific averages (see section 2.4.1). These traits values are then used to determine the
780 maximum LAI (LAI_{max}) the seedling would support under average environmental conditions, with LAI_{max} defined as the



781 threshold beyond which the seedling leaf assimilation would be less than respiration (see section 2.6.2). The seedling can be
782 recruited if the site LAI at ground level is lower than LAI_{max} .

783 Water availability is also key to seedling performance (Engelbrecht et al., 2006; Johnson et al., 2017; Kupers et al.,
784 2019), hence TROLL 4.0 now implements an additional water-dependent dependence on seedling establishment (Craine et al.,
785 2012; Paine et al., 2018). Seedling recruitment is possible only if top-layer soil water potential is less negative than half the
786 turgor loss point ($\pi_{tlp}/2$). Such parameterization is motivated by the fact that, at turgor loss point, the seedlings would not
787 germinate, and a certain level of turgor is needed for germination and growth (Bradford, 1990; Daws et al., 2008; Coussement
788 et al., 2018; Hsiao, 1973; Fatichi et al., 2016).

789 If both conditions on light and water availability are met, the newly recruited tree is initialized with a $dbh=0.01m$, a
790 total leaf area $LA_t = 0.25 \times LA_{opt}$ distributed across the three leaf age pools in proportion to their relative span (τ_{young}/LL ,
791 τ_{mature}/LL , τ_{old}/LL ; see section 2.6.2), and a carbon storage compartment filled at half its maximum NSC_r (see section 2.6.3).

792 The assumptions here made on tree reproduction largely reflect limited knowledge on these processes, which remains
793 major sources of uncertainty in current models (König et al., 2022; Hanbury-Brown et al., 2022; Díaz-Yáñez et al., 2024).

794 2.7.2 Mortality

795 Mortality processes also play a key role in forest structure and carbon balance (Sevanto et al., 2014; Friend et al., 2014; Johnson
796 et al., 2016; Esquivel-Muelbert et al., 2020; McDowell et al., 2022). TROLL 4.0 explicitly represents several important
797 mechanisms of tree mortality. At each timestep, individual tree death rate (in events yr^{-1} ; Sheil et al. 1995) is:

$$798 d = d_b + d_{starv} + d_{treefall} + d_{drought} \quad (65)$$

799 where d_b is a background death rate, d_{starv} represents death due to carbohydrate shortage (carbon starvation), $d_{treefall}$
800 represents death due to treefall (including trees indirectly killed by neighboring fallen trees), and $d_{drought}$ the drought-induced
801 tree mortality.

802 Background mortality d_b encapsulates death events that are not attributed to any specific mechanism in the model.
803 Mortality rate is known to vary greatly among species, and we here assume that it is negatively correlated with tree wood
804 density, as observed pan-tropically (King et al., 2006; Kraft et al., 2010; Poorter et al., 2008; Wright et al., 2010). This
805 dependence illustrates a trade-off between investment into construction costs and risk of mortality (Chave et al., 2009). We
806 assumed the following relationship:

$$807 d_b = m \times \left(1 - \frac{wsg}{wsg_{lim}}\right) \quad (66)$$

808 where m (in events yr^{-1}) is the reference background mortality rate for a species with low wood density and is user-specified.
809 wsg_{lim} is a value large enough so that d_b always remains positive (here set at 1 g cm^{-3}).



810 A tree can also die because of carbohydrate shortage in case of prolonged stress (d_{starv} in Eq. (65)). In TROLL 4.0
811 that includes an explicit carbohydrate storage compartment, the tree dies of carbon starvation when this compartment is empty
812 and $NPP_{ind} \leq 0$ (Eq. (51)).

813 Tree death may be caused by treefalls (term $d_{treefall}$ in Eq. (65)). To simulate this process, we first define a stochastic
814 threshold θ , depending on the tree maximal height, and prescribed at tree birth. Then, the tree can fall with a probability equal
815 to $1 - \frac{\theta}{h}$ (Chave, 1999) each month. As TROLL 4.0 uses a daily timestep, this probability is uniformly distributed across the
816 days of one month. The parameter θ is computed for each tree, as follows:

$$817 \theta = h_{max} \times (1 - v_T \times |\zeta|) \quad (67)$$

818 where h_{max} is maximal tree height (i.e. the tree height computed using Eq. (16) at dbh_{max}), v_T is a variance term, $|\zeta|$ is the
819 absolute value of a random Gaussian variable with zero mean and unit standard deviation. v_T is modified at tree level so that
820 high risks of treefall ($> 99.5^{\text{th}}$ percentile of the Gaussian variable) occur at the same height for all individuals of the same
821 species. This implicitly introduces a growth-mortality trade-off, as more slender trees (larger ratio of height to trunk diameter)
822 should reach this height threshold quicker. The orientation of tree falls is random. Trees on the trajectory of the falling tree can
823 be damaged, especially if they are smaller than the fallen tree (van der Meer and Bongers, 1996). To model this effect, an
824 individual variable $hurt$ is defined. If a tree is within the trajectory of the fallen stem or of the fallen crown, its variable $hurt$ is
825 updated to h and $\frac{h-CR}{2}$, respectively, if it was lower, where h and CR are the tree height and crown radius of the fallen tree,
826 respectively. The probability to die due to another treefall is then $1 - \frac{1}{2} \frac{h}{hurt \times e^{\varepsilon_{h,j}}}$, where h is the height of the focal tree and
827 $e^{\varepsilon_{h,j}}$ (see Eq. (16)) accounts for the fact that slender individuals (higher tree height deviation) would be more vulnerable to
828 treefall. Such tree can either fall and itself damage other trees or dies standing, depending on the user choice. The $hurt$ variable
829 is reset to zero at each timestep.

830 Finally, prolonged drought is also a source of mortality. Drought-induced mortality is triggered when the leaf predawn
831 water potential ψ_{pd} is below a lethal level (ψ_{lethal}), and ψ_{lethal} is computed from the leaf water potential at turgor loss point,
832 using the relationship provided by the global meta-analysis of Bartlett et al. (2016; $P=0.03$, $R^2=0.31$, $n=15$ species from tropical
833 dry and moist biomes), as follows:

$$834 \psi_{lethal} = -0.9842 + 3.1795 \times \pi_{ttp} \quad (68)$$

835 3 Modelling protocol

836 3.1 Model inputs

837 TROLL 4.0 requires five input files to run a simulation: (i) global parameters, (ii) species parameters, (iii) soil characteristics,
838 and finally, meteorological drivers varying at (iv) half-hour and (v) daily step.



839 The global input file contains parameters that define the simulation set-up (e.g. the number of timesteps, size of the
840 simulated plot and of the belowground voxels), and values for biophysical parameters that remain constant throughout the
841 simulation and are not species- or tree-specific. These include the light attenuation coefficient, allocation parameters, minimal
842 death rate, and more (see Table A1). Parameter values can be varied across simulations, to test model sensitivity, transfer
843 across sites, or any other reason. The species input file contains mean functional traits for at least one species and with no
844 upper bound (see Table A1). Functional trait values can be prescribed from local field measurements, or retrieved from global
845 trait databases (e.g. Kattge et al., 2020; Díaz et al., 2022).

846 The soil input file contains the soil variables needed for the pedotransfer functions, i.e. soil texture (proportion of silt,
847 clay and sand), soil organic matter content, dry bulk density, soil pH, and cation exchange capacity, for each soil layer, with
848 thickness of each layer. The number of soil layers is at least one, and is not theoretically limited. Lacking local soil data, model
849 users may retrieve soil parameters from online databases (e.g. Poggio et al., 2021), bearing in mind the uncertainties of such
850 products, especially in tropical areas (Khan et al., 2024).

851 Meteorological drivers are provided in two files, depending on their temporal resolution in the model. Daytime
852 temperature, vapor pressure deficit, incident irradiance and wind speed at a reference height above the canopy are provided
853 for every half-hour, while average nighttime temperature and cumulative rainfall are provided at a daily timestep. Such data
854 can typically be retrieved from meteorological stations embedded in eddy-flux towers, or from global products (Muñoz-Sabater
855 et al., 2021), as in Schmitt et al. (2023).

856 **3.2 Initial conditions**

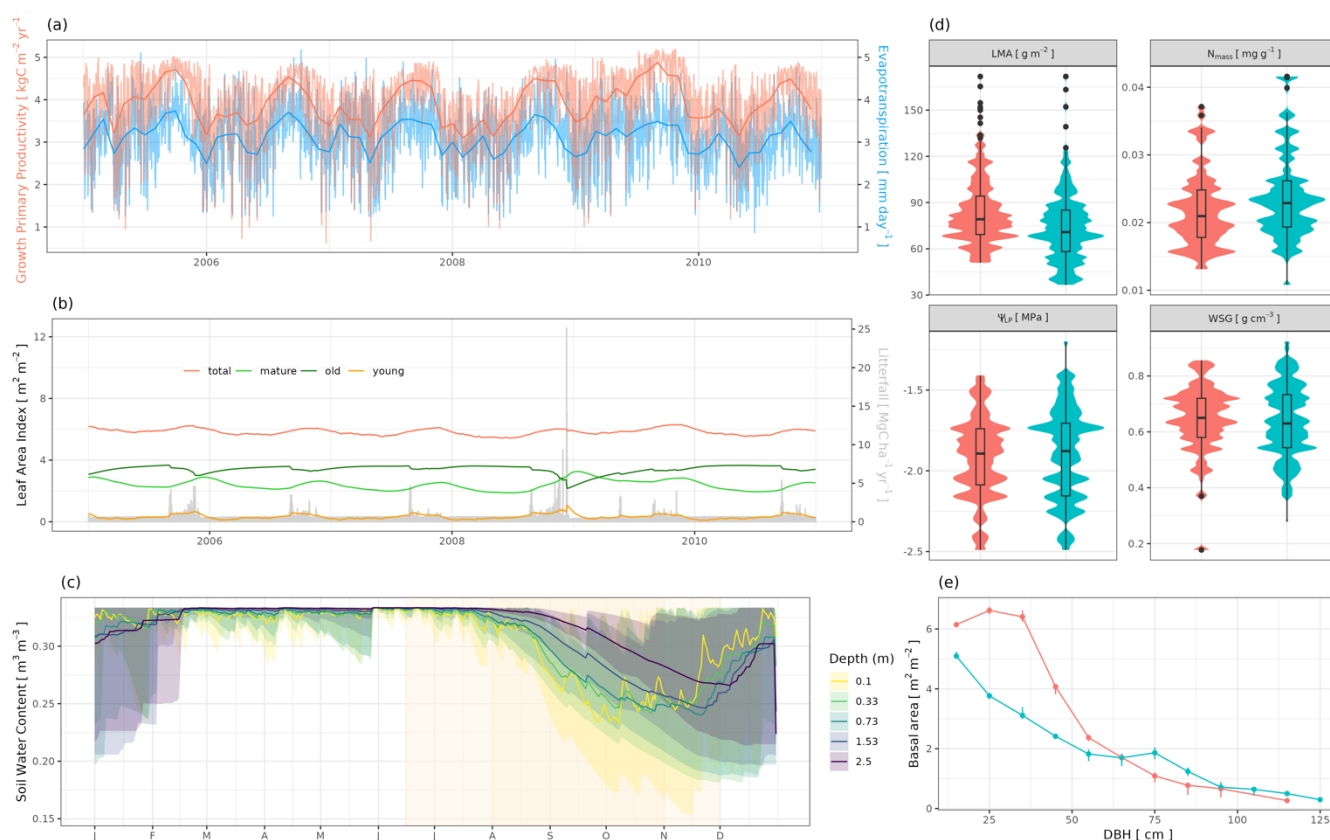
857 Two types of initial conditions are useful in most practical settings, and are implemented in TROLL 4.0. First, the user can
858 simulate forest regeneration from bare ground. In this case, forest succession is initiated by the external seed rain, the
859 composition and intensity of which are user-defined (see above). The steady-state forest composition and structure are thus
860 emergent properties of the community assembly mechanisms embedded in the model, and the user-specified seed rain. The
861 second option is to prescribe an initial forest state. This requires that an initial forest state be provided as an additional input
862 file. The code is designed to adapt to the level of information provided by the inventory file, from a minimal requirement of
863 tree *dbh* to the full list of individual variables for each tree. For individual variables missing in the input file, these are either
864 computed from the model relationships or drawn at random. This second initial condition matches a real site forest state given
865 the available data, but will require careful calibration to maintain the forest state over a longer time period (e.g. Fischer et al.,
866 2019). A more common use case is to restart new simulations from an output of a previous simulation, e.g., to perform virtual
867 experiments controlling the initial state.

868 **3.3 Standard outputs**

869 TROLL 4.0 provides a range of outputs related to forest structure, forest composition and diversity, and ecosystem functioning
870 (e.g., carbon and water fluxes; Fig. 4). It simulates forest structure and composition and provides outputs comparable to those



871 measured in the field: tree size distribution, tree spatial distribution, biomass accumulation curve, functional trait distribution,
 872 canopy height and leaf area index maps (Maréchaux and Chave, 2017), and more generally all information that can be retrieved
 873 from a detailed field inventory or a meter-scale airborne laser scanning survey (Fischer et al., 2019). In TROLL 4.0, other
 874 outputs are also available: litterfall fluxes, carbon and water fluxes comparable to the one provided by eddy-flux towers, soil
 875 water state (content and water potential). An evaluation of these outputs for two Amazonian forest sites is provided in a
 876 companion paper (Schmitt et al., submitted companion paper).
 877



878
 879 **Figure 4: Examples of outputs provided by TROLL 4.0 and related to ecosystem functioning, diversity and structure. (a) Temporal**
 880 **variations of gross primary productivity (red) and evapotranspiration (blue) within and across years. (b) Variation in total leaf area**
 881 **index (red line) and leaf area index per leaf age cohort (young, mature, old; yellow, light green and dark green lines, respectively),**
 882 **together with litterfall (grey bars), within and across years. (c) Mean seasonal variations of water content in soil layers of different**
 883 **depths, with the vertical yellow band in the background depicting the dry season. (d) Distribution of functional traits. (e)**
 884 **Distributions of basal area per diameter class. Panels (a), (b) and (c) show outputs for an Amazonian forest site (Paracou), panels**
 885 **(d) and (e) show outputs for two Amazonian sites (Paracou, red; Tapajos, blue), see Schmitt et al., submitted companion paper. for**
 886 **details on simulation set-ups.**



887 **4 Discussion**

888 TROLL 4.0 is a novel generation of forest growth models designed to bridge the gap between traditional forest growth
889 models and process-based models informed by ecophysiology. It includes an integration of processes underlying ecosystem
890 fluxes closer to a modern DGVM than most other forest growth simulators. It also includes representation of plant community
891 structure and diversity at a resolution similar to that used by ecologists in the field. This enables a direct comparison with a
892 range of field data, including forest inventories, trait distribution, fine- and large-scale remote-sensing products, or eddy-
893 covariance data. Here we discuss the assumptions of the water cycle newly included in the model, as well as transferability
894 and limitations of the current model version.

895 **4.1 Simulating water fluxes and forest responses to water availability**

896 Previous versions of TROLL assume that water availability does not limit ecosystem fluxes and dynamics, a strong but
897 reasonable assumption in a light-limited forest like in Eastern Amazonia (Guan et al., 2015; Wagner et al., 2016; Maréchaux
898 and Chave, 2017). However, such a simplification does not allow to account for drought-induced inter-annual variability in
899 forest dynamics (Bonal et al., 2008; Aguilos et al., 2018; Leitold et al., 2018) or to transfer the model to sites where water
900 availability is limiting. As droughts will be important drivers for tropical ecosystems in the future (Duffy et al., 2015), such a
901 simplification does not allow to project future states of forest under climate change.

902 In TROLL 4.0, we implemented a full water cycle. We introduced a belowground field with a hydraulic state coupled
903 to the vegetation, and a representation of the response of leaf gas exchanges to local atmospheric conditions and their control
904 by the leaf boundary layer. This detailed representation is commonplace DGVMs (Prentice et al., 2007) but to our knowledge,
905 it is new for an individual-based spatially explicit forest dynamic simulator. This paves the way for explorations and projections
906 of the independent effects of soil water availability and atmospheric demand on ecosystem functioning (Novick et al., 2016;
907 Santos et al., 2018), community composition and structure (Esquivel-Muelbert et al., 2019; Fauset et al., 2012; Slik, 2004;
908 Feeley et al., 2011).

909 These developments have striven to follow the parsimonious principle: more complex representations do not
910 systematically result in increased model reliability and robustness, especially if the additional parameters are poorly
911 constrained (Mahnken et al., 2022; Prentice et al., 2015). The soil hydraulic state is simulated using a bucket model (Budyko,
912 1961; Manabe 1969; Vargas Godoy et al., 2021). In the future, more complex representations of soil water dynamics could be
913 implemented at finer temporal and spatial resolutions, such as the implementation of Richards' equation (Richards, 1931), and
914 integration of lateral flows, but this would be at a serious computational cost. These could be compared with the current simpler
915 representation to assess the relevance of increasing complexity in various contexts and soil data availability (Van Nes and
916 Scheffer, 2005). However, two aspects were considered to be needed in the current version, based on biological considerations.
917 First, we implemented a multi-layer soil model, a more detailed representation compared with other models using a bucket
918 model approach (e.g. Fischer et al., 2014; Laio et al., 2001). This was motivated by the need to account for contrasting rooting



919 strategies and access to water among coexisting plants, which is an under-explored, but likely key, aspect of community
920 dynamics in forests (Brum et al., 2019; De Deurwaerder et al., 2018; Ivanov et al., 2012). Second, we assumed that the depth
921 of tree water uptake is not only controlled by the distribution of root biomass (as in Naudts et al., 2015; Sakschewski et al.,
922 2021; Paschalis et al., 2024), but also by soil water state and its vertical variation (as in Williams et al., 1996; Duursma and
923 Medlyn, 2012). These improvements are relevant to the temporal variation of water retrieval depth (Bruno et al., 2006) and
924 the sustained dry-season productivity in rainforest ecosystems (Restrepo-Coupe et al., 2017).

925 The control of leaf gas exchange by water availability has been implemented by means of multiplicative soil water
926 stress factors. Although the use of such factors has been debated (Powell et al., 2013; Joetzjer et al., 2014), it has been preferred
927 over a more explicit representation of the water flow through the plant column (e.g. Yao et al., 2022; Christoffersen et al.,
928 2016; Cochard et al., 2021; De Cáceres et al., 2023). Although the stem hydraulic traits that would be needed for parameterizing
929 an explicit plant water flow module have been increasingly measured over the past decades, data availability for tropical tree
930 species remains low in regards to the actual number of species coexisting in these communities. Alternatively, correlative
931 relationships have been used to infer these traits from more easily measured traits (Christoffersen et al., 2016; Xu et al., 2016).
932 However, these are context dependent (Brodrribb, 2017; Rosas et al., 2019) and have at best low statistical support in rainforest
933 communities that are loosely constrained by water availability (Dwyer and Laughlin, 2017; Delhayé et al., 2020; Maréchaux
934 et al., 2020). Innovative methods alleviate the difficulties of robustly measuring the vulnerability of tropical trees to embolism
935 (Cochard et al., 2016; Sergent et al., 2020; Garcia et al., 2023), and this could provide a key motivation for a more explicit
936 module of plant water flow in TROLL (Kennedy et al., 2019; Paschalis et al., 2024). Such developments could be necessary
937 to correctly represent the legacy of drought in forest ecosystems (Paschalis et al., 2024; Anderegg et al., 2015). However, two
938 important aspects were taken into account in the implementation of the multiplicative water stress factors in TROLL 4.0. These
939 factors were parameterized based on soil water potential as independent variable, and not soil water content, the former directly
940 controlling water availability for plants, while the effect of soil water content is strongly mediated by soil properties (Novick
941 et al., 2022). Also, different water stress factors were used for stomatal and non-stomatal limitations, in order to capture the
942 sequence of effects of decreasing water availability on plant function (Trueba et al., 2019; Fatichi et al., 2016; Hsiao, 1973).

943 The effects of water availability on plant function and tree demography were implemented through trait-based
944 parameterization, which allows a range of responses between trees and species. This was made possible through the use of leaf
945 water potential at turgor loss point ($\pi_{t_{lp}}$), a leaf-level trait that is mechanistically linked to plant responses to water availability
946 (Bartlett et al., 2016b) and that is measurable at the community scale in diverse systems through a well-validated method
947 (Maréchaux et al., 2016; Griffin-Nolan et al., 2019; Sun et al., 2020; Bartlett et al., 2012a). Leaf water potential at turgor loss
948 point varies greatly across species within Amazonian forest communities (Maréchaux et al., 2015; Ziegler et al., 2019), and
949 this diversity explains contrasting responses to water availability at the leaf and plant levels (Martin-StPaul et al., 2017;
950 Maréchaux et al., 2018; Powell et al., 2017), and species distribution at local, regional and global scales (Bartlett et al., 2016a;
951 Baltzer et al., 2008; Lenz et al., 2006; Bartlett et al., 2012b). The relationships implemented here involving $\pi_{t_{lp}}$ have a
952 mechanistic basis, as discussed above. However, the relationships controlling the effect of water availability on (1) leaf



953 shedding, (2) seed germination and seedling recruitment, and (3) drought-induced mortality would deserve in-depth
954 exploration. More generally, these three processes remain key aspects of community dynamics and ecosystem functioning in
955 high need of sustained empirical investigation (Albert et al., 2019; Díaz-Yáñez et al., 2024; McDowell et al., 2022).

956 **4.2 Model-data integration, transferability and limitations**

957 TROLL 4.0 simulates forest structure and diversity, while expanding the types of data with which its results can be compared
958 (Schmitt et al., submitted companion paper). The individual-based species-specific representation of forest yields virtual forest
959 inventories, including the location of each individual, their botanical identity, and their dimensions, and virtual airborne laser
960 scanning point clouds (Fischer et al., 2019; Schmitt et al., 2023). TROLL 4.0 additionally provides water, carbon and litter
961 flux dynamics that are directly comparable to eddy-flux tower data and litter trap monitoring at fine temporal resolutions, and
962 this specificity has numerous advantages.

963 Data-driven knowledge can be directly assimilated in TROLL 4.0, offering new perspectives for inference or
964 calibration (Dietze et al., 2013; Fer et al., 2018; Hartig et al., 2012; LeBauer et al., 2013; Fischer et al., 2019). TROLL 4.0 can
965 help inform the development of DGVMs, in which the representation of vegetation does not allow this type of assimilation
966 (Fischer et al., 2019). TROLL 4.0 is also easy to use and test by field ecologists as it simulates trees, not cohorts, PFTs, or gap
967 patches: it can reproduce classical experiments in community or ecosystem ecology (e.g. Crawford et al., 2021; Schmitt et al.,
968 2020) while overcoming known empirical challenges such as low repeatability (Schnitzer and Carson, 2016) or limited spatial
969 footprint (Estes et al., 2018). TROLL 4.0 can be compared with data under the control of different biophysical processes
970 supporting a more robust evaluation, and limiting equifinality issues (Franks et al., 1997; Medlyn et al., 2005). Finally, the
971 model is parameterized based on traits directly measured in the field improving model transferability (Rau et al., 2022a).

972 The individual-scale and spatially-explicit representation of TROLL 4.0 comes with a computational burden. For a
973 reference 4-ha area starting from bare ground, and 600 years of simulation, the computational cost of TROLL 4.0 is about
974 1820 min, compared with version TROLL2.3 (Maréchaux and Chave 2017) about 12 min. While the shift from a monthly to
975 a daily timestep explains the multiplication by a factor of 30 between the two versions, the addition of a belowground field
976 and of an iterative scheme to simulate leaf gas exchanges explains for a great part the remaining factor of five. Several
977 developments should reduce this computational cost: tree demographic processes do not need to be simulated at the daily
978 timestep and could be represented at a monthly resolution; vegetation models already implement such nested time scales
979 (Moorcroft, 2006). We are also confident that further computer time reduction will be brought about by code optimization.
980 Finally, several strategies can be implemented to up-scale the outputs of individual-based models at reduced computational
981 costs, especially by leveraging large scale remote sensing products (Rödig et al., 2017; Sato et al., 2007; Shugart et al., 2015).

982 **4.3 Current and future developments**

983 TROLL 4.0 is a reflection on the state of the art and knowledge gaps in plant physiology and ecology, resulting in an
984 unbalanced representation across processes. TROLL is being continuously developed, as knowledge and data availability



985 progress, specific questions to address with the model emerge, or important limitations are identified. In a companion paper
986 (Schmitt et al., submitted companion paper), we use data from forest inventories, litter traps, eddy-flux towers and remote
987 sensing products to evaluate and discuss the performance and limitations of TROLL 4.0 at two forest sites. We here mention
988 several on-going or future developments.

989 Empirical findings suggest that the contribution of undisturbed tropical forests to the global carbon sink is declining
990 (Hubau et al., 2020; Qie et al., 2017), pointing to the need of integrated modelling to understand and predict such trends (Yao
991 et al., 2023, 2024; Koch et al., 2021). Among the possible steps forward with TROLL 4.0 are an improved representation of
992 stomatal conductance and its coupling with photosynthesis (Lamour et al., 2022, 2023; Dewar et al., 2018), as well as
993 respiration response and acclimation to climatic drivers (Smith and Dukes, 2013; Collalti et al., 2020; Slot et al., 2013; Rowland
994 et al., 2015). Improvements on the carbon budget would also be important, with more explicit carbon allocation to reproductive
995 organs and belowground structures, under the control of environmental drivers (Fig. 3). However, such developments would
996 rely on limited empirical or experimental knowledge belowground (Cusack et al., 2024) and scarce information on tree
997 reproductive strategies (Igarashi et al., 2024; Vacchiano et al., 2018; Norden et al., 2007). An improved representation and
998 evaluation of drought-induced tree mortality would be another important step forward as it might play a key role in the observed
999 changing dynamics and functional and floristic turnover (Esquivel-Muelbert et al., 2019; Feeley et al., 2011; Hubau et al.,
1000 2020; Qie et al., 2017). Information provided by long-term through fall exclusion experiments would offer interesting
1001 opportunities for model development and evaluation (Powell et al., 2013; Yao et al., 2022).

1002 Tropical forest disturbance by land use change, fire regimes, and other degradations are an important source of C
1003 emissions (Lapola et al., 2023), and they must be represented in models. For instance, it is important to understand how edge
1004 effects affect the forest microclimate, and consequently forest dynamics, functioning and composition (Camargo and Kapos,
1005 1995; Nunes et al., 2022). To this end, micro-climate models could be coupled to or embedded within TROLL (Gril et al.,
1006 2023a; Maclean and Klinges, 2021). Fragmentation also impacts seed dispersal, and thus seed rain and seed bank intensity and
1007 composition (Warneke et al., 2022; Cubiña and Aide, 2001). Improving TROLL's representation of seed dispersal ability and
1008 germination as a function of plant trait and dispersal mode is key to capture the effect of forest loss and fragmentation on forest
1009 functioning and biodiversity (Seidler and Plotkin, 2006; Muller-Landau et al., 2008; Tamme et al., 2014; Chase et al., 2020;
1010 Riva and Fahrig, 2023). More generally, one overarching objective is to improve model's representation of processes involved
1011 in forest regeneration, to simulate secondary forest dynamics and resilience to disturbances (Hanbury-Brown et al., 2022; Díaz-
1012 Yáñez et al., 2024; Poorter et al., 2023; Albrich et al., 2020).

1013 Finally, TROLL 4.0 includes major developments that should facilitate its transferability across sites. The explicit
1014 integration of the ecosystem water balance and vegetation responses to soil water availability now allows to consider spatio-
1015 temporal extrapolation along water stress gradients. The integration of soil topography and heterogeneity would also be an
1016 important advance for improved genericity. As nutrient availability is being altered by human activities (Peñuelas et al., 2013),
1017 the explicit integration of a nutrient cycle with nitrogen and phosphorous colimitation will be a useful advance in the future



1018 (Fernández-Martínez et al., 2014; Turner et al., 2018). Similarly, the extension of tree functioning responses to a broader range
1019 of temperatures, should support the transferability of TROLL to temperate and boreal forests.

1020 5. Conclusion

1021 TROLL 4.0 represents an advance over previous versions as it bridges across forest model types, while maintaining a
1022 representation consistent with field ecology and ecosystem science. TROLL 4.0 simulates the responses of tropical forests to
1023 water availability through the explicit representation of water dynamics belowground and its coupling with leaf-level gas
1024 exchanges and demographic processes. This comes at a computational cost, and a future task is to conduct code optimization
1025 and parallelization, and up-scaling in combination with remote-sensing products. The representation of processes in TROLL
1026 4.0 mirrors an unbalanced state of the art, but its ability to dialogue with a range of data of various nature, makes it a valuable
1027 tool to take up the fundamental and applied research challenges on tropical forests. TROLL 4.0 has benefited from observations
1028 and field experiments that feed the development of models (Medlyn et al., 2015; Paschalis et al., 2020), while modeling
1029 exercises inform and guide empirical approaches (Medlyn et al., 2016; Norby et al., 2016; Pacala and Rees, 1998). This is
1030 possible because of the fine scale representation of forest structure and diversity and the trait-based parameterization of
1031 processes in the model.

1032

1033

1034 *Code and data availability.* The code of TROLL 4.0 is available at <https://github.com/TROLL-code/TROLL>, a DOI will be
1035 linked to this repository upon publication. Additionally, TROLL 4.0 can be set-up and run, and its outputs can be analyzed
1036 with an updated version of the R package rcontroll: <https://github.com/sylvainschmitt/rcontroll/tree/TROLLV4>, also available
1037 in R through the command `devtools::install_github("sylvainschmitt/rcontroll", ref = "TROLLV4")`.

1038

1039 *Supplement.* The supplement related to this article will be available online upon publication acceptance.

1040

1041 *Author contributions.* IM led TROLL 4.0, and designed the implementation of the water cycle and its coupling to vegetation.
1042 FJF co-led TROLL 4.0 and designed the new implementation of intra-specific variability and crown shapes. SS and JC
1043 contributed ideas and discussions. IM wrote the paper with contributions from all authors.

1044

1045 *Competing interests.* The authors declare that they have no conflict of interest.

1046

1047 *Acknowledgements.* We acknowledge Nicolas Martin-StPaul and Rémi Vezy for useful discussions on the representation of
1048 gas exchanges and water fluxes in models; Nicolas Barbier, Gregoire Vincent, and James Ball for sharing data and useful



1049 discussions on leaf phenology; Philippe Verley and Thomas Arsouze for IT support; and Marie Boscher for help in designing
1050 figure 1. This work was carried out with the support of MESO@LR-Platform at the University of Montpellier.

1051

1052 *Financial support.* This research has been supported by fundings from ANR (the French National Research Agency) under the
1053 "Investissements d'avenir" program with the references ANR-16-IDEX-0006, ANR-10-LABX-25-01, ANR-10-LABX-0041,
1054 the Amazonian Landscapes in Transition ANR project (ALT), CNES Biomass-Valo project, and ESA CCI-BIOMASS.

1055 **References**

1056 Aguilos, M., Hérault, B., Burban, B., Wagner, F., and Bonal, D.: What drives long-term variations in carbon flux and balance
1057 in a tropical rainforest in French Guiana?, *Agricultural and Forest Meteorology*, 253–254, 114–123,
1058 <https://doi.org/10.1016/j.agrformet.2018.02.009>, 2018.

1059 Albert, L. P., Restrepo-Coupe, N., Smith, M. N., Wu, J., Chavana-Bryant, C., Prohaska, N., Taylor, T. C., Martins, G. A.,
1060 Ciais, P., Mao, J., Arain, M. A., Li, W., Shi, X., Ricciuto, D. M., Huxman, T. E., McMahon, S. M., and Saleska, S. R.:
1061 Cryptic phenology in plants: Case studies, implications, and recommendations, *Global Change Biology*, 25, 3591–3608,
1062 <https://doi.org/10.1111/gcb.14759>, 2019.

1063 Albert, L. P., Wu, J., Prohaska, N., de Camargo, P. B., Huxman, T. E., Tribuzy, E. S., Ivanov, V. Y., Oliveira, R. S., Garcia,
1064 S., Smith, M. N., Oliveira Junior, R. C., Restrepo-Coupe, N., da Silva, R., Stark, S. C., Martins, G. A., Penha, D. V., and
1065 Saleska, S. R.: Age-dependent leaf physiology and consequences for crown-scale carbon uptake during the dry season in
1066 an Amazon evergreen forest, *New Phytologist*, 218, <https://doi.org/10.1111/nph.15056>, 2018.

1067 Albrich, K., Rammer, W., Turner, M. G., Ratajczak, Z., Braziunas, K. H., Hansen, W. D., and Seidl, R.: Simulating forest
1068 resilience: A review, *Global Ecology and Biogeography*, 29, 2082–2096, <https://doi.org/10.1111/geb.13197>, 2020.

1069 Amthor, J. S.: The role of maintenance respiration in plant growth, *Plant, Cell & Environment*, 7, 561–569,
1070 <https://doi.org/10.1111/1365-3040.ep11591833>, 1984.

1071 Anderegg, W. R. L., Schwalm, C., Biondi, F., Camarero, J. J., Koch, G., Litvak, M., Ogle, K., Shaw, J. D., Shevliakova, E.,
1072 Williams, A. P., Wolf, A., Ziaco, E., and Pacala, S.: Pervasive drought legacies in forest ecosystems and their implications
1073 for carbon cycle models, *Science*, 349, 528–532, <https://doi.org/10.1126/science.aab1833>, 2015.

1074 Anderegg, W. R. L., Wolf, A., Arango-Velez, A., Choat, B., Chmura, D. J., Jansen, S., Kolb, T., Li, S., Meinzer, F., Pita, P.,
1075 Dios, V. R. de, Sperry, J. S., Wolfe, B. T., and Pacala, S.: Plant water potential improves prediction of empirical stomatal
1076 models, *PLOS ONE*, 12, e0185481, <https://doi.org/10.1371/journal.pone.0185481>, 2017.

1077 Anderegg, W. R. L., Wolf, A., Arango-Velez, A., Choat, B., Chmura, D. J., Jansen, S., Kolb, T., Li, S., Meinzer, F. C., Pita,
1078 P., Dios, V. R. de, Sperry, J. S., Wolfe, B. T., and Pacala, S.: Woody plants optimise stomatal behaviour relative to hydraulic
1079 risk, *Ecology Letters*, 21, 968–977, <https://doi.org/10.1111/ele.12962>, 2018.



- 1080 Arora, V. K. and Boer, G. J.: A Representation of Variable Root Distribution in Dynamic Vegetation Models, *Earth Interact.*,
1081 7, 1–19, [https://doi.org/10.1175/1087-3562\(2003\)007<0001:AROVRD>2.0.CO;2](https://doi.org/10.1175/1087-3562(2003)007<0001:AROVRD>2.0.CO;2), 2003.
- 1082 Asao, S., Bedoya-Arrieta, R., and Ryan, M. G.: Variation in foliar respiration and wood CO₂ efflux rates among species and
1083 canopy layers in a wet tropical forest, *Tree Physiol*, 35, 148–159, <https://doi.org/10.1093/treephys/tpu107>, 2015.
- 1084 Atkin, O. K., Evans, J. R., Ball, M. C., Lambers, H., and Pons, T. L.: Leaf respiration of snow gum in the light and dark.
1085 Interactions between temperature and irradiance., *Plant Physiol.*, 122, 915–924, <https://doi.org/10.1104/pp.122.3.915>,
1086 2000.
- 1087 Atkin, O. K., Meir, P., and Turnbull, M. H.: Improving representation of leaf respiration in large-scale predictive climate–
1088 vegetation models, *New Phytol*, 202, 743–748, <https://doi.org/10.1111/nph.12686>, 2014.
- 1089 Atkin, O. K., Bloomfield, K. J., Reich, P. B., Tjoelker, M. G., Asner, G. P., Bonal, D., Bönisch, G., Bradford, M. G., Cernusak,
1090 L. A., Cosio, E. G., Creek, D., Crous, K. Y., Domingues, T. F., Dukes, J. S., Egerton, J. J. G., Evans, J. R., Farquhar, G.
1091 D., Fyllas, N. M., Gauthier, P. P. G., Gloor, E., Gimeno, T. E., Griffin, K. L., Guerrieri, R., Heskell, M. A., Huntingford,
1092 C., Ishida, F. Y., Kattge, J., Lambers, H., Liddell, M. J., Lloyd, J., Lusk, C. H., Martin, R. E., Maksimov, A. P., Maximov,
1093 T. C., Malhi, Y., Medlyn, B. E., Meir, P., Mercado, L. M., Mirotchnick, N., Ng, D., Niinemets, Ü., O’Sullivan, O. S.,
1094 Phillips, O. L., Poorter, L., Poot, P., Prentice, I. C., Salinas, N., Rowland, L. M., Ryan, M. G., Sitch, S., Slot, M., Smith,
1095 N. G., Turnbull, M. H., VanderWel, M. C., Valladares, F., Veneklaas, E. J., Weerasinghe, L. K., Wirth, C., Wright, I. J.,
1096 Wythers, K. R., Xiang, J., Xiang, S., and Zaragoza-Castells, J.: Global variability in leaf respiration in relation to climate,
1097 plant functional types and leaf traits, *New Phytol*, 206, 614–636, <https://doi.org/10.1111/nph.13253>, 2015.
- 1098 Baltzer, J. L., Davies, S. J., Bunyavejchewin, S., and Noor, N. S. M.: The role of desiccation tolerance in determining tree
1099 species distributions along the Malay–Thai Peninsula, *Functional Ecology*, 22, 221–231, <https://doi.org/10.1111/j.1365-2435.2007.01374.x>, 2008.
- 1100
- 1101 Baraloto, C., Paine, C. E. T., Patiño, S., Bonal, D., Hérault, B., and Chave, J.: Functional trait variation and sampling strategies
1102 in species-rich plant communities, *Functional Ecology*, 24, 208–216, <https://doi.org/10.1111/j.1365-2435.2009.01600.x>,
1103 2010a.
- 1104 Baraloto, C., Timothy Paine, C. E., Poorter, L., Beauchene, J., Bonal, D., Domenach, A.-M., Hérault, B., Patiño, S., Roggy,
1105 J.-C., and Chave, J.: Decoupled leaf and stem economics in rain forest trees, *Ecology Letters*, 13, 1338–1347,
1106 <https://doi.org/10.1111/j.1461-0248.2010.01517.x>, 2010b.
- 1107 Bartlett, M. K., Scoffoni, C., Ardy, R., Zhang, Y., Sun, S., Cao, K., and Sack, L.: Rapid determination of comparative drought
1108 tolerance traits: using an osmometer to predict turgor loss point, *Methods Ecol. Evol.*, 3, 880–888,
1109 <https://doi.org/10.1111/j.2041-210X.2012.00230.x>, 2012a.
- 1110 Bartlett, M. K., Scoffoni, C., and Sack, L.: The determinants of leaf turgor loss point and prediction of drought tolerance of
1111 species and biomes: a global meta-analysis, *Ecology Letters*, 15, 393–405, <https://doi.org/10.1111/j.1461-0248.2012.01751.x>, 2012b.
- 1112



- 1113 Bartlett, M. K., Zhang, Y., Yang, J., Kreidler, N., Sun, S.-W., Lin, L., Hu, Y.-H., Cao, K.-F., and Sack, L.: Drought tolerance
1114 as a driver of tropical forest assembly: resolving spatial signatures for multiple processes, *Ecology*, 97, 503–514,
1115 <https://doi.org/10.1890/15-0468.1>, 2016a.
- 1116 Bartlett, M. K., Klein, T., Jansen, S., Choat, B., and Sack, L.: The correlations and sequence of plant stomatal, hydraulic, and
1117 wilting responses to drought, *PNAS*, 113, 13098–13103, <https://doi.org/10.1073/pnas.1604088113>, 2016b.
- 1118 Beer, C., Reichstein, M., Tomelleri, E., Ciais, P., Jung, M., Carvalhais, N., Rödenbeck, C., Arain, M. A., Baldocchi, D., Bonan,
1119 G. B., Bondeau, A., Cescatti, A., Lasslop, G., Lindroth, A., Lomas, M., Luysaert, S., Margolis, H., Oleson, K. W.,
1120 Rouspard, O., Veenendaal, E., Viovy, N., Williams, C., Woodward, F. I., and Papale, D.: Terrestrial gross carbon dioxide
1121 uptake: global distribution and covariation with climate, *Science*, 329, 834–838, <https://doi.org/10.1126/science.1184984>,
1122 2010.
- 1123 Bennett, A. C., McDowell, N. G., Allen, C. D., and Anderson-Teixeira, K. J.: Larger trees suffer most during drought in forests
1124 worldwide, *Nature Plants*, 1, <https://doi.org/10.1038/nplants.2015.139>, 2015.
- 1125 Bernacchi, C. J., Pimentel, C., and Long, S. P.: In vivo temperature response functions of parameters required to model RuBP-
1126 limited photosynthesis, *Plant, Cell & Environment*, 26, 1419–1430, <https://doi.org/10.1046/j.0016-8025.2003.01050.x>,
1127 2003.
- 1128 Berzaghi, F., Wright, I. J., Kramer, K., Oddou-Muratorio, S., Bohn, F. J., Reyer, C. P. O., Sabaté, S., Sanders, T. G. M., and
1129 Hartig, F.: Towards a New Generation of Trait-Flexible Vegetation Models, *Trends in Ecology & Evolution*, 35, 191–205,
1130 <https://doi.org/10.1016/j.tree.2019.11.006>, 2020.
- 1131 Blanchard, G., Barbier, N., Vieilledent, G., Ibanez, T., Hequet, V., McCoy, S., and Birnbaum, P.: UAV-Lidar reveals that
1132 canopy structure mediates the influence of edge effects on forest diversity, function and microclimate, *Journal of Ecology*,
1133 111, 1411–1427, <https://doi.org/10.1111/1365-2745.14105>, 2023.
- 1134 Bohlman, S. and O'Brien, S.: Allometry, adult stature and regeneration requirement of 65 tree species on Barro Colorado
1135 Island, Panama, *Journal of Tropical Ecology*, 22, 123–136, <https://doi.org/10.1017/S0266467405003019>, 2006.
- 1136 Bonal, D., Bosc, A., Ponton, S., Goret, J.-Y., Burban, B., Gross, P., Bonnefond, J.-M., Elbers, J., Longdoz, B., Epron, D.,
1137 Guehl, J.-M., and Granier, A.: Impact of severe dry season on net ecosystem exchange in the Neotropical rainforest of
1138 French Guiana, *Global Change Biology*, 14, 1917–1933, <https://doi.org/10.1111/j.1365-2486.2008.01610.x>, 2008.
- 1139 Bonan, G. B.: Forests and Climate Change: Forcings, Feedbacks, and the Climate Benefits of Forests, *Science*, 320, 1444–
1140 1449, <https://doi.org/10.1126/science.1155121>, 2008.
- 1141 Bonan, G. B., Williams, M., Fisher, R. A., and Oleson, K. W.: Modeling stomatal conductance in the earth system: linking
1142 leaf water-use efficiency and water transport along the soil–plant–atmosphere continuum, *Geosci. Model Dev.*, 7, 2193–
1143 2222, <https://doi.org/10.5194/gmd-7-2193-2014>, 2014.
- 1144 Botkin, D. B.: Functional groups of organisms in model ecosystems, *Ecosystem Analysis and Prediction*, 98–102, 1975.
- 1145 Botkin, D. B., Janak, J. F., and Wallis, J. R.: Some Ecological Consequences of a Computer Model of Forest Growth, *Journal*
1146 *of Ecology*, 60, 849–872, <https://doi.org/10.2307/2258570>, 1972.



- 1147 Bradford, K. J.: A Water Relations Analysis of Seed Germination Rates, *Plant Physiol.*, 94, 840–849,
1148 <https://doi.org/10.1104/pp.94.2.840>, 1990.
- 1149 Braghieri, R. K., Quaipe, T., Black, E., He, L., and Chen, J. M.: Underestimation of Global Photosynthesis in Earth System
1150 Models Due to Representation of Vegetation Structure, *Global Biogeochemical Cycles*, 33, 1358–1369,
1151 <https://doi.org/10.1029/2018GB006135>, 2019.
- 1152 Braghieri, R. K., Wang, Y., Doughty, R., Sousa, D., Magney, T., Widlowski, J.-L., Longo, M., Bloom, A. A., Worden, J.,
1153 Gentine, P., and Frankenberg, C.: Accounting for canopy structure improves hyperspectral radiative transfer and sun-
1154 induced chlorophyll fluorescence representations in a new generation Earth System model, *Remote Sensing of*
1155 *Environment*, 261, 112497, <https://doi.org/10.1016/j.rse.2021.112497>, 2021.
- 1156 Brodrribb, T. J.: Progressing from ‘functional’ to mechanistic traits, *New Phytol*, 215, 9–11, <https://doi.org/10.1111/nph.14620>,
1157 2017.
- 1158 Brodrribb, T. J., Holbrook, N. M., and Gutiérrez, M. V.: Hydraulic and photosynthetic co-ordination in seasonally dry tropical
1159 forest trees, *Plant, Cell & Environment*, 25, 1435–1444, <https://doi.org/10.1046/j.1365-3040.2002.00919.x>, 2002.
- 1160 Brodrribb, T. J., Holbrook, N. M., Edwards, E. J., and Gutiérrez, M. V.: Relations between stomatal closure, leaf turgor and
1161 xylem vulnerability in eight tropical dry forest trees, *Plant, Cell & Environment*, 26, 443–450,
1162 <https://doi.org/10.1046/j.1365-3040.2003.00975.x>, 2003.
- 1163 Brooks, R. H. and Corey, A. T.: Hydraulic properties of porous media. Hydrology Paper No. 3, Civil Engineering Department,
1164 Colorado State University., Fort Collins, 1964.
- 1165 Brum, M., Vadeboncoeur, M. A., Ivanov, V., Asbjornsen, H., Saleska, S., Alves, L. F., Penha, D., Dias, J. D., Aragão, L. E.
1166 O. C., Barros, F., Bittencourt, P., Pereira, L., and Oliveira, R. S.: Hydrological niche segregation defines forest structure
1167 and drought tolerance strategies in a seasonal Amazon forest, *Journal of Ecology*, 107, 318–333,
1168 <https://doi.org/10.1111/1365-2745.13022>, 2019.
- 1169 Bruno, R. D., da Rocha, H. R., de Freitas, H. C., Goulden, M. L., and Miller, S. D.: Soil moisture dynamics in an eastern
1170 Amazonian tropical forest, *Hydrol. Process.*, 20, 2477–2489, <https://doi.org/10.1002/hyp.6211>, 2006.
- 1171 Bucci, S., Scholz, F. G., Goldstein, G., Meinzer, F. C., Hinojosa, J. A., Hoffman, W. A., and Franco, A. C.: Processes
1172 preventing nocturnal equilibration between leaf and soil water potential in tropical savanna woody species., *Tree*
1173 *Physiology*, 24, 1119–1127, 2004.
- 1174 Budyko, M. I.: The Heat Balance of the Earth’s Surface, *Soviet Geography*, 1961.
- 1175 Bugmann, H.: A review of forest gap models, *Climatic Change*, 51, 259–305, <https://doi.org/10.1023/A:1012525626267>, 2001.
- 1176 Burgess, S. S. O., Adams, M. A., Turner, N. C., and Ong, C. K.: The redistribution of soil water by tree root systems, *Oecologia*,
1177 115, 306–311, <https://doi.org/10.1007/s004420050521>, 1998.
- 1178 von Caemmerer, S.: Biochemical models of leaf photosynthesis, Csiro Publishing, 184 pp., 2000.
- 1179 Camargo, J. L. C. and Kapos, V.: Complex edge effects on soil moisture and microclimate in central Amazonian forest, *Journal*
1180 *of Tropical Ecology*, 11, 205–221, 1995.



- 1181 Canadell, J., Jackson, R. B., Ehleringer, J. R., Mooney, H. A., Sala, O. E., and Schulze, E. D.: Maximum rooting depth of
1182 vegetation types at the global scale, *Oecologia*, 108, 583–595, <https://doi.org/10.1007/BF00329030>, 1996.
- 1183 Cannell, M. G. R. and Thornley, J. H. M.: Modelling the components of plant respiration: some guiding principles, *Ann Bot*,
1184 85, 45–54, <https://doi.org/10.1006/anbo.1999.0996>, 2000.
- 1185 Cavaleri, M. A., Oberbauer, S. F., and Ryan, M. G.: Wood CO₂ efflux in a primary tropical rain forest, *Global Change Biology*,
1186 12, 2442–2458, <https://doi.org/10.1111/j.1365-2486.2006.01269.x>, 2006.
- 1187 Cavaleri, M. A., Oberbauer, S. F., and Ryan, M. G.: Foliar and ecosystem respiration in an old-growth tropical rain forest,
1188 *Plant, Cell & Environment*, 31, 473–483, <https://doi.org/10.1111/j.1365-3040.2008.01775.x>, 2008.
- 1189 Charney, J. G.: Dynamics of deserts and drought in the Sahel, *Q.J.R. Meteorol. Soc.*, 101, 193–202,
1190 <https://doi.org/10.1002/qj.49710142802>, 1975.
- 1191 Chase, J. M., Blowes, S. A., Knight, T. M., Gerstner, K., and May, F.: Ecosystem decay exacerbates biodiversity loss with
1192 habitat loss, *Nature*, 584, 238–243, <https://doi.org/10.1038/s41586-020-2531-2>, 2020.
- 1193 Chave: Study of structural, successional and spatial patterns in tropical rain forests using TROLL, a spatially explicit forest
1194 model, *Ecological Modelling*, 124, 233–254, [https://doi.org/10.1016/S0304-3800\(99\)00171-4](https://doi.org/10.1016/S0304-3800(99)00171-4), 1999.
- 1195 Chave, J., Olivier, J., Bongers, F., Châtelet, P., Forget, P.-M., van der Meer, P., Norden, N., Riéra, B., and Charles-Dominique,
1196 P.: Above-ground biomass and productivity in a rain forest of eastern South America, *Journal of Tropical Ecology*, 24,
1197 355–366, <https://doi.org/10.1017/S0266467408005075>, 2008.
- 1198 Chave, J., Coomes, D., Jansen, S., Lewis, S. L., Swenson, N. G., and Zanne, A. E.: Towards a worldwide wood economics
1199 spectrum, *Ecology Letters*, 12, 351–366, <https://doi.org/10.1111/j.1461-0248.2009.01285.x>, 2009.
- 1200 Chave, J., Navarrete, D., Almeida, S., Álvarez, E., Aragão, L. E. O. C., Bonal, D., Châtelet, P., Silva-Espejo, J. E., Goret, J.-
1201 Y., von Hildebrand, P., Jiménez, E., Patiño, S., Peñuela, M. C., Phillips, O. L., Stevenson, P., and Malhi, Y.: Regional and
1202 seasonal patterns of litterfall in tropical South America, *Biogeosciences*, 7, 43–55, <https://doi.org/10.5194/bg-7-43-2010>,
1203 2010.
- 1204 Chave, J., Réjou-Méchain, M., Búrquez, A., Chidumayo, E., Colgan, M. S., Delitti, W. B. C., Duque, A., Eid, T., Fearnside,
1205 P. M., Goodman, R. C., Henry, M., Martínez-Yrizar, A., Mugasha, W. A., Muller-Landau, H. C., Mencuccini, M., Nelson,
1206 B. W., Ngomanda, A., Nogueira, E. M., Ortiz-Malavassi, E., Péliissier, R., Ploton, P., Ryan, C. M., Saldarriaga, J. G., and
1207 Vieilledent, G.: Improved allometric models to estimate the aboveground biomass of tropical trees, *Glob Change Biol*, 20,
1208 3177–3190, <https://doi.org/10.1111/gcb.12629>, 2014.
- 1209 Chen, X., Maignan, F., Viovy, N., Bastos, A., Goll, D., Wu, J., Liu, L., Yue, C., Peng, S., Yuan, W., Conceição, A. C. da,
1210 O’Sullivan, M., and Ciais, P.: Novel Representation of Leaf Phenology Improves Simulation of Amazonian Evergreen
1211 Forest Photosynthesis in a Land Surface Model, *Journal of Advances in Modeling Earth Systems*, 12, e2018MS001565,
1212 <https://doi.org/10.1029/2018MS001565>, 2020.
- 1213 Chen, X., Ciais, P., Maignan, F., Zhang, Y., Bastos, A., Liu, L., Bacour, C., Fan, L., Gentine, P., Goll, D., Green, J., Kim, H.,
1214 Li, L., Liu, Y., Peng, S., Tang, H., Viovy, N., Wigneron, J.-P., Wu, J., Yuan, W., and Zhang, H.: Vapor Pressure Deficit



- 1215 and Sunlight Explain Seasonality of Leaf Phenology and Photosynthesis Across Amazonian Evergreen Broadleaved Forest,
1216 Global Biogeochemical Cycles, 35, e2020GB006893, <https://doi.org/10.1029/2020GB006893>, 2021.
- 1217 Chen, Y., Ryder, J., Bastrikov, V., McGrath, M. J., Naudts, K., Otto, J., Otlé, C., Peylin, P., Polcher, J., Valade, A., Black,
1218 A., Elbers, J. A., Moors, E., Foken, T., van Gorsel, E., Haverd, V., Heinesch, B., Tiedemann, F., Knohl, A., Launiainen,
1219 S., Loustau, D., Ogée, J., Vessala, T., and Luysaert, S.: Evaluating the performance of land surface model ORCHIDEE-
1220 CAN v1.0 on water and energy flux estimation with a single- and multi-layer energy budget scheme, Geoscientific Model
1221 Development, 9, 2951–2972, <https://doi.org/10.5194/gmd-9-2951-2016>, 2016.
- 1222 Chesson, P. L. and Warner, R. R.: Environmental variability promotes coexistence in lottery competitive systems, The
1223 American Naturalist, 117, 923–943, 1981.
- 1224 Christoffersen, B. O., Gloor, M., Fauset, S., Fyllas, N. M., Galbraith, D. R., Baker, T. R., Rowland, L., Fisher, R. A., Binks,
1225 O. J., Sevanto, S. A., Xu, C., Jansen, S., Choat, B., Mencuccini, M., McDowell, N. G., and Meir, P.: Linking hydraulic
1226 traits to tropical forest function in a size-structured and trait-driven model (TFS v.1-Hydro), Geoscientific Model
1227 Development Discussions, 0, 1–60, <https://doi.org/10.5194/gmd-2016-128>, 2016.
- 1228 Chuine, I. and Beaubien, E. G.: Phenology is a major determinant of tree species range, Ecology Letters, 4, 500–510,
1229 <https://doi.org/10.1046/j.1461-0248.2001.00261.x>, 2001.
- 1230 Clark, D. B., Mercado, L. M., Sitch, S., Jones, C. D., Gedney, N., Best, M. J., Pryor, M., Rooney, G. G., Essery, R. L. H.,
1231 Blyth, E., Boucher, O., Harding, R. J., Huntingford, C., and Cox, P. M.: The Joint UK Land Environment Simulator
1232 (JULES), model description – Part 2: Carbon fluxes and vegetation dynamics, Geosci. Model Dev., 4, 701–722,
1233 <https://doi.org/10.5194/gmd-4-701-2011>, 2011.
- 1234 Cochard, H.: A new mechanism for tree mortality due to drought and heatwaves, Peer Community Journal, 1,
1235 <https://doi.org/10.24072/pcjournal.45>, 2021.
- 1236 Cochard, H., Torres-Ruiz, J. M., and Delzon, S.: Let plant hydraulics catch the wave, Journal of Plant Hydraulics, 3, 002,
1237 2016.
- 1238 Cochard, H., Pimont, F., Ruffault, J., and Martin-StPaul, N.: SurEau: a mechanistic model of plant water relations under
1239 extreme drought, Annals of Forest Science, 78, 55, <https://doi.org/10.1007/s13595-021-01067-y>, 2021.
- 1240 Collalti, A., Tjoelker, M. G., Hoch, G., Mäkelä, A., Guidolotti, G., Heskell, M., Petit, G., Ryan, M. G., Battipaglia, G.,
1241 Matteucci, G., and Prentice, I. C.: Plant respiration: Controlled by photosynthesis or biomass?, Global Change Biology,
1242 26, 1739–1753, <https://doi.org/10.1111/gcb.14857>, 2020.
- 1243 Coomes, D. A. and Grubb, P. J.: Colonization, tolerance, competition and seed-size variation within functional groups, Trends
1244 in Ecology & Evolution, 18, 283–291, [https://doi.org/10.1016/S0169-5347\(03\)00072-7](https://doi.org/10.1016/S0169-5347(03)00072-7), 2003.
- 1245 Cosby, B. J., Hornberger, G. M., Clapp, R. B., and Ginn, T. R.: A Statistical Exploration of the Relationships of Soil Moisture
1246 Characteristics to the Physical Properties of Soils, Water Resources Research, 20, 682–690,
1247 <https://doi.org/10.1029/WR020i006p00682>, 1984.



- 1248 Costa, F. R. C., Schiatti, J., Stark, S. C., and Smith, M. N.: The other side of tropical forest drought: do shallow water table
1249 regions of Amazonia act as large-scale hydrological refugia from drought?, *New Phytologist*, 237, 714–733,
1250 <https://doi.org/10.1111/nph.17914>, 2023.
- 1251 Coussement, J. R., De Swaef, T., Lootens, P., Roldán-Ruiz, I., and Steppe, K.: Introducing turgor-driven growth dynamics
1252 into functional–structural plant models, *Ann Bot*, 121, 849–861, <https://doi.org/10.1093/aob/mcx144>, 2018.
- 1253 Cox, P. M., Betts, R. A., Jones, C. D., Spall, S. A., and Totterdell, I. J.: Acceleration of global warming due to carbon-cycle
1254 feedbacks in a coupled climate model, *Nature*, 408, 184–187, <https://doi.org/10.1038/35041539>, 2000.
- 1255 Craine, J. M., Engelbrecht, B. M. J., Lusk, C. H., McDowell, N. G., and Poorter, H.: Resource limitation, tolerance, and the
1256 future of ecological plant classification, *Frontiers in Plant Science*, 3, <https://doi.org/10.3389/fpls.2012.00246>, 2012.
- 1257 Crawford, M. S., Barry, K. E., Clark, A. T., Fariior, C. E., Hines, J., Ladouceur, E., Lichstein, J. W., Maréchaux, I., May, F.,
1258 Mori, A. S., Reineking, B., Turnbull, L. A., Wirth, C., and Rüger, N.: The function-dominance correlation drives the
1259 direction and strength of biodiversity–ecosystem functioning relationships, *Ecology Letters*, 24, 1762–1775,
1260 <https://doi.org/10.1111/ele.13776>, 2021.
- 1261 Cubiña, A. and Aide, T. M.: The Effect of Distance from Forest Edge on Seed Rain and Soil Seed Bank in a Tropical Pasture,
1262 *BIOTROPICA*, 33, 260–267, [https://doi.org/10.1646/0006-3606\(2001\)033\[0260:TEODFF\]2.0.CO;2](https://doi.org/10.1646/0006-3606(2001)033[0260:TEODFF]2.0.CO;2), 2001.
- 1263 Cusack, D. F., Christoffersen, B., Smith-Martin, C. M., Andersen, K. M., Cordeiro, A. L., Fleischer, K., Wright, S. J., Guerrero-
1264 Ramírez, N. R., Lugli, L. F., McCulloch, L. A., Sanchez-Julia, M., Batterman, S. A., Dallstream, C., Fortunel, C., Toro,
1265 L., Fuchslueger, L., Wong, M. Y., Yaffar, D., Fisher, J. B., Arnaud, M., Diatterich, L. H., Addo-Danso, S. D., Valverde-
1266 Barrantes, O. J., Weemstra, M., Ng, J. C., and Norby, R. J.: Toward a coordinated understanding of hydro-biogeochemical
1267 root functions in tropical forests for application in vegetation models, *New Phytologist*, n/a,
1268 <https://doi.org/10.1111/nph.19561>, 2024.
- 1269 Damour, G., Simonneau, T., Cochard, H., and Urban, L.: An overview of models of stomatal conductance at the leaf level,
1270 *Plant, Cell & Environment*, 33, 1419–1438, <https://doi.org/10.1111/j.1365-3040.2010.02181.x>, 2010.
- 1271 Daws, M. I., Crabtree, L. M., Dalling, J. W., Mullins, C. E., and Burslem, D. F. R. P.: Germination Responses to Water
1272 Potential in Neotropical Pioneers Suggest Large-seeded Species Take More Risks, *Ann Bot*, 102, 945–951,
1273 <https://doi.org/10.1093/aob/mcn186>, 2008.
- 1274 Dawson, T. E.: Hydraulic lift and water use by plants: implications for water balance, performance and plant-plant interactions,
1275 *Oecologia*, 95, 565–574, <https://doi.org/10.1007/BF00317442>, 1993.
- 1276 De Cáceres, M., Molowny-Horas, R., Cabon, A., Martínez-Vilalta, J., Mencuccini, M., García-Valdés, R., Nadal-Sala, D.,
1277 Sabaté, S., Martin-StPaul, N., Morin, X., D’Adamo, F., Batllori, E., and Améztegui, A.: MEDFATE 2.9.3: a trait-enabled
1278 model to simulate Mediterranean forest function and dynamics at regional scales, *Geoscientific Model Development*, 16,
1279 3165–3201, <https://doi.org/10.5194/gmd-16-3165-2023>, 2023.



- 1280 De Deurwaerder, H., Hervé-Fernández, P., Stahl, C., Burban, B., Petronelli, P., Hoffman, B., Bonal, D., Boeckx, P., and
1281 Verbeeck, H.: Liana and tree below-ground water competition—evidence for water resource partitioning during the dry
1282 season, *Tree Physiol*, 38, 1071–1083, <https://doi.org/10.1093/treephys/tpy002>, 2018.
- 1283 De Frenne, P., Zellweger, F., Rodríguez-Sánchez, F., Scheffers, B. R., Hylander, K., Luoto, M., Vellend, M., Verheyen, K.,
1284 and Lenoir, J.: Global buffering of temperatures under forest canopies, *Nat Ecol Evol*, 3, 744–749,
1285 <https://doi.org/10.1038/s41559-019-0842-1>, 2019.
- 1286 De Kauwe, M. G., Zhou, S.-X., Medlyn, B. E., Pitman, A. J., Wang, Y.-P., Duursma, R. A., and Prentice, I. C.: Do land surface
1287 models need to include differential plant species responses to drought? Examining model predictions across a mesic-xeric
1288 gradient in Europe, *Biogeosciences*, 12, 7503–7518, <https://doi.org/10.5194/bg-12-7503-2015>, 2015.
- 1289 De Kauwe, M. G., Medlyn, B. E., Knauer, J., and Williams, C. A.: Ideas and perspectives: how coupled is the vegetation to
1290 the boundary layer?, *Biogeosciences*, 14, 4435–4453, <http://dx.doi.org/10.5194/bg-14-4435-2017>, 2017.
- 1291 Delhaye, G., Bauman, D., Séleck, M., Ilunga wa Ilunga, E., Mahy, G., and Meerts, P.: Interspecific trait integration increases
1292 with environmental harshness: A case study along a metal toxicity gradient, *Functional Ecology*, 34, 1428–1437,
1293 <https://doi.org/10.1111/1365-2435.13570>, 2020.
- 1294 Dewar, R., Mauranen, A., Mäkelä, A., Hölttä, T., Medlyn, B., and Vesala, T.: New insights into the covariation of stomatal,
1295 mesophyll and hydraulic conductances from optimization models incorporating nonstomatal limitations to photosynthesis,
1296 *New Phytologist*, 217, 571–585, <https://doi.org/10.1111/nph.14848>, 2018.
- 1297 Díaz, S., Kattge, J., Cornelissen, J. H. C., Wright, I. J., Lavorel, S., Dray, S., Reu, B., Kleyer, M., Wirth, C., Colin Prentice, I.,
1298 Garnier, E., Bönisch, G., Westoby, M., Poorter, H., Reich, P. B., Moles, A. T., Dickie, J., Gillison, A. N., Zanne, A. E.,
1299 Chave, J., Joseph Wright, S., Sheremet'ev, S. N., Jactel, H., Baraloto, C., Cerabolini, B., Pierce, S., Shipley, B., Kirkup,
1300 D., Casanoves, F., Joswig, J. S., Günther, A., Falczuk, V., Rüger, N., Mahecha, M. D., and Gorné, L. D.: The global
1301 spectrum of plant form and function, *Nature*, 529, 167–171, <https://doi.org/10.1038/nature16489>, 2016.
- 1302 Díaz, S., Kattge, J., Cornelissen, J. H. C., Wright, I. J., Lavorel, S., Dray, S., Reu, B., Kleyer, M., Wirth, C., Prentice, I. C.,
1303 Garnier, E., Bönisch, G., Westoby, M., Poorter, H., Reich, P. B., Moles, A. T., Dickie, J., Zanne, A. E., Chave, J., Wright,
1304 S. J., Sheremetiev, S. N., Jactel, H., Baraloto, C., Cerabolini, B. E. L., Pierce, S., Shipley, B., Casanoves, F., Joswig, J. S.,
1305 Günther, A., Falczuk, V., Rüger, N., Mahecha, M. D., Gorné, L. D., Amiaud, B., Atkin, O. K., Bahn, M., Baldocchi, D.,
1306 Beckmann, M., Blonder, B., Bond, W., Bond-Lamberty, B., Brown, K., Burrascano, S., Byun, C., Campetella, G.,
1307 Cavender-Bares, J., Chapin, F. S., Choat, B., Coomes, D. A., Cornwell, W. K., Craine, J., Craven, D., Dainese, M., de
1308 Araujo, A. C., de Vries, F. T., Domingues, T. F., Enquist, B. J., Fagúndez, J., Fang, J., Fernández-Méndez, F., Fernandez-
1309 Piedade, M. T., Ford, H., Forey, E., Freschet, G. T., Gachet, S., Gallagher, R., Green, W., Guerin, G. R., Gutiérrez, A. G.,
1310 Harrison, S. P., Hattingh, W. N., He, T., Hickler, T., Higgins, S. I., Higuchi, P., Ilic, J., Jackson, R. B., Jalili, A., Jansen,
1311 S., Koike, F., König, C., Kraft, N., Kramer, K., Kreft, H., Kühn, I., Kurokawa, H., Lamb, E. G., Laughlin, D. C., Leishman,
1312 M., Lewis, S., Louault, F., Malhado, A. C. M., Manning, P., Meir, P., Mencuccini, M., Messier, J., Miller, R., Minden, V.,



- 1313 Molofsky, J., et al.: The global spectrum of plant form and function: enhanced species-level trait dataset, *Sci Data*, 9, 755,
1314 <https://doi.org/10.1038/s41597-022-01774-9>, 2022.
- 1315 Díaz-Yáñez, O., Käber, Y., Anders, T., Bohn, F., Braziunas, K. H., Brúna, J., Fischer, R., Fischer, S. M., Hetzer, J., Hickler,
1316 T., Hochauer, C., Lexer, M. J., Lischke, H., Mairota, P., Merganič, J., Merganičová, K., Mette, T., Mina, M., Morin, X.,
1317 Nieberg, M., Rammer, W., Reyer, C. P. O., Scheiter, S., Scherrer, D., and Bugmann, H.: Tree regeneration in models of
1318 forest dynamics: A key priority for further research, *Ecosphere*, 15, e4807, <https://doi.org/10.1002/ecs2.4807>, 2024.
- 1319 Dietze, M. C., Lebauer, D. S., and Kooper, R.: On improving the communication between models and data, *Plant, Cell &*
1320 *Environment*, 36, 1575–1585, <https://doi.org/10.1111/pce.12043>, 2013.
- 1321 Dilley, A. C. and O’Brien, D. M.: Estimating downward clear sky long-wave irradiance at the surface from screen temperature
1322 and precipitable water, *Quarterly Journal of the Royal Meteorological Society*, 124, 1391–1401,
1323 <https://doi.org/10.1002/qj.49712454903>, 1998.
- 1324 Domingues, T. F., Meir, P., Feldpausch, T. R., Saiz, G., Veenendaal, E. M., Schrod, F., Bird, M., Djagbletey, G., Hien, F.,
1325 Compaore, H., Diallo, A., Grace, J., and Lloyd, J.: Co-limitation of photosynthetic capacity by nitrogen and phosphorus in
1326 West Africa woodlands, *Plant, Cell & Environment*, 33, 959–980, <https://doi.org/10.1111/j.1365-3040.2010.02119.x>,
1327 2010.
- 1328 Domingues, T. F., Martinelli, L. A., and Ehleringer, J. R.: Seasonal patterns of leaf-level photosynthetic gas exchange in an
1329 eastern Amazonian rain forest, *Plant Ecology & Diversity*, 7, 189–203, <https://doi.org/10.1080/17550874.2012.748849>,
1330 2014.
- 1331 Donovan, L. A., Richards, J. H., and Linton, M. J.: Magnitude and mechanisms of disequilibrium between predawn plant and
1332 soil water potentials, *Ecology*, 84, 463–470, [https://doi.org/10.1890/0012-9658\(2003\)084\[0463:MAMODB\]2.0.CO;2](https://doi.org/10.1890/0012-9658(2003)084[0463:MAMODB]2.0.CO;2),
1333 2003.
- 1334 Dormann, C. F., Schymanski, S. J., Cabral, J., Chuine, I., Graham, C., Hartig, F., Kearney, M., Morin, X., Römermann, C.,
1335 Schröder, B., and Singer, A.: Correlation and process in species distribution models: bridging a dichotomy, *Journal of*
1336 *Biogeography*, 39, 2119–2131, <https://doi.org/10.1111/j.1365-2699.2011.02659.x>, 2012.
- 1337 Doughty, C. E. and Goulden, M. L.: Seasonal patterns of tropical forest leaf area index and CO₂ exchange, *J. Geophys. Res.*,
1338 113, G00B06, <https://doi.org/10.1029/2007JG000590>, 2008.
- 1339 Doughty, C. E., Gaillard, C., Burns, P., Keany, J. M., Abraham, A. J., Malhi, Y., Aguirre-Gutierrez, J., Koch, G., Jantz, P.,
1340 Shenkin, A., and Tang, H.: Tropical forests are mainly unstratified especially in Amazonia and regions with lower fertility
1341 or higher temperatures, *Environ. Res.: Ecology*, 2, 035002, <https://doi.org/10.1088/2752-664X/ace723>, 2023.
- 1342 Drake, J. E., Power, S. A., Duursma, R. A., Medlyn, B. E., Aspinwall, M. J., Choat, B., Creek, D., Eamus, D., Maier, C.,
1343 Pfautsch, S., Smith, R. A., Tjoelker, M. G., and Tissue, D. T.: Stomatal and non-stomatal limitations of photosynthesis for
1344 four tree species under drought: A comparison of model formulations, *Agricultural and Forest Meteorology*, 247, 454–466,
1345 <https://doi.org/10.1016/j.agrformet.2017.08.026>, 2017.



- 1346 Drake, P. L., Boer, H. J. de, Schymanski, S. J., and Veneklaas, E. J.: Two sides to every leaf: water and CO₂ transport in
1347 hypostomatous and amphistomatous leaves, *New Phytologist*, 222, 1179–1187, <https://doi.org/10.1111/nph.15652>, 2019.
- 1348 Duffy, P. B., Brando, P., Asner, G. P., and Field, C. B.: Projections of future meteorological drought and wet periods in the
1349 Amazon, *PNAS*, 112, 13172–13177, <https://doi.org/10.1073/pnas.1421010112>, 2015.
- 1350 Dunne, T. and Black, R. D.: An Experimental Investigation of Runoff Production in Permeable Soils, *Water Resources*
1351 *Research*, 6, 478–490, <https://doi.org/10.1029/WR006i002p00478>, 1970.
- 1352 Duursma, R. A.: Plantecophys - An R Package for Analysing and Modelling Leaf Gas Exchange Data, *PLOS ONE*, 10,
1353 e0143346, <https://doi.org/10.1371/journal.pone.0143346>, 2015.
- 1354 Duursma, R. A. and Medlyn, B. E.: MAESPA: a model to study interactions between water limitation, environmental drivers
1355 and vegetation function at tree and stand levels, with an example application to [CO₂] × drought interactions, *Geoscientific*
1356 *Model Development*, 5, 919–940, <https://doi.org/10.5194/gmd-5-919-2012>, 2012.
- 1357 Duursma, R. A., Blackman, C. J., Lopéz, R., Martin-StPaul, N. K., Cochard, H., and Medlyn, B. E.: On the minimum leaf
1358 conductance: its role in models of plant water use, and ecological and environmental controls, *New Phytologist*, 221, 693–
1359 705, <https://doi.org/10.1111/nph.15395>, 2019.
- 1360 Dwyer, J. M. and Laughlin, D. C.: Constraints on trait combinations explain climatic drivers of biodiversity: the importance
1361 of trait covariance in community assembly, *Ecol Lett*, 20, 872–882, <https://doi.org/10.1111/ele.12781>, 2017.
- 1362 Egea, G., Verhoef, A., and Vidale, P. L.: Towards an improved and more flexible representation of water stress in coupled
1363 photosynthesis–stomatal conductance models, *Agricultural and Forest Meteorology*, 151, 1370–1384,
1364 <https://doi.org/10.1016/j.agrformet.2011.05.019>, 2011.
- 1365 Elias, M. and Potvin, C.: Assessing inter- and intra-specific variation in trunk carbon concentration for 32 neotropical tree
1366 species, *Can. J. For. Res.*, 33, 1039–1045, <https://doi.org/10.1139/x03-018>, 2003.
- 1367 Elith, J. and Leathwick, J. R.: Species Distribution Models: Ecological Explanation and Prediction Across Space and Time,
1368 *Annual Review of Ecology, Evolution, and Systematics*, 40, 677–697,
1369 <https://doi.org/10.1146/annurev.ecolsys.110308.120159>, 2009.
- 1370 Engelbrecht, B. M. J., Dalling, J. W., Pearson, T. R. H., Wolf, R. L., Galvez, D. A., Koehler, T., Tyree, M. T., and Kursar, T.
1371 A.: Short dry spells in the wet season increase mortality of tropical pioneer seedlings, *Oecologia*, 148, 258–269,
1372 <https://doi.org/10.1007/s00442-006-0368-5>, 2006.
- 1373 Esquivel-Muelbert, A., Baker, T. R., Dexter, K. G., Lewis, S. L., Brienen, R. J. W., Feldpausch, T. R., Lloyd, J., Monteagudo-
1374 Mendoza, A., Arroyo, L., Álvarez-Dávila, E., Higuchi, N., Marimon, B. S., Marimon-Junior, B. H., Silveira, M., Vilanova,
1375 E., Gloor, E., Malhi, Y., Chave, J., Barlow, J., Bonal, D., Cardozo, N. D., Erwin, T., Fauset, S., Hérault, B., Laurance, S.,
1376 Poorter, L., Qie, L., Stahl, C., Sullivan, M. J. P., Steege, H. ter, Vos, V. A., Zuidema, P. A., Almeida, E., Oliveira, E. A.
1377 de, Andrade, A., Vieira, S. A., Aragão, L., Araujo-Murakami, A., Arets, E., C, G. A. A., Baraloto, C., Camargo, P. B.,
1378 Barroso, J. G., Bongers, F., Boot, R., Camargo, J. L., Castro, W., Moscoso, V. C., Comiskey, J., Valverde, F. C., Costa, A.
1379 C. L. da, Pasquel, J. del A., Fiore, A. D., Duque, L. F., Elias, F., Engel, J., Llampazo, G. F., Galbraith, D., Fernández, R.



- 1380 H., Coronado, E. H., Hubau, W., Jimenez-Rojas, E., Lima, A. J. N., Umetsu, R. K., Laurance, W., Lopez-Gonzalez, G.,
1381 Lovejoy, T., Cruz, O. A. M., Morandi, P. S., Neill, D., Vargas, P. N., Camacho, N. C. P., Gutierrez, A. P., Pardo, G.,
1382 Peacock, J., Peña-Claros, M., Peñuela-Mora, M. C., Petronelli, P., Pickavance, G. C., Pitman, N., Prieto, A., Quesada, C.,
1383 Ramírez-Angulo, H., Réjou-Méchain, M., Correa, Z. R., Roopsind, A., Rudas, A., Salomão, R., Silva, N., Espejo, J. S.,
1384 Singh, J., Stropp, J., Terborgh, J., Thomas, R., Toledo, M., Torres-Lezama, A., Gamarra, L. V., Meer, P. J. van de, Heijden,
1385 G. van der, et al.: Compositional response of Amazon forests to climate change, *Global Change Biology*, 25, 39–56,
1386 <https://doi.org/10.1111/gcb.14413>, 2019.
- 1387 Esquivel-Muelbert, A., Phillips, O. L., Brien, R. J. W., Fauset, S., Sullivan, M. J. P., Baker, T. R., Chao, K.-J., Feldpausch,
1388 T. R., Gloor, E., Higuchi, N., Houwing-Duistermaat, J., Lloyd, J., Liu, H., Malhi, Y., Marimon, B., Marimon Junior, B. H.,
1389 Monteagudo-Mendoza, A., Poorter, L., Silveira, M., Torre, E. V., Dávila, E. A., del Aguila Pasquel, J., Almeida, E., Loayza,
1390 P. A., Andrade, A., Aragão, L. E. O. C., Araujo-Murakami, A., Arets, E., Arroyo, L., C. G. A. A., Baisie, M., Baraloto, C.,
1391 Camargo, P. B., Barroso, J., Blanc, L., Bonal, D., Bongers, F., Boot, R., Brown, F., Burban, B., Camargo, J. L., Castro,
1392 W., Moscoso, V. C., Chave, J., Comiskey, J., Valverde, F. C., da Costa, A. L., Cardozo, N. D., Di Fiore, A., Dourdain, A.,
1393 Erwin, T., Llampazo, G. F., Vieira, I. C. G., Herrera, R., Honorio Coronado, E., Huamantupa-Chuquimaco, I., Jimenez-
1394 Rojas, E., Killeen, T., Laurance, S., Laurance, W., Levesley, A., Lewis, S. L., Ladvat, K. L. L. M., Lopez-Gonzalez, G.,
1395 Lovejoy, T., Meir, P., Mendoza, C., Morandi, P., Neill, D., Nogueira Lima, A. J., Vargas, P. N., de Oliveira, E. A.,
1396 Camacho, N. P., Pardo, G., Peacock, J., Peña-Claros, M., Peñuela-Mora, M. C., Pickavance, G., Pipoly, J., Pitman, N.,
1397 Prieto, A., Pugh, T. A. M., Quesada, C., Ramirez-Angulo, H., de Almeida Reis, S. M., Rejou-Machain, M., Correa, Z. R.,
1398 Bayona, L. R., Rudas, A., Salomão, R., Serrano, J., Espejo, J. S., Silva, N., Singh, J., Stahl, C., Stropp, J., Swamy, V.,
1399 Talbot, J., ter Steege, H., et al.: Tree mode of death and mortality risk factors across Amazon forests, *Nature*
1400 *Communications*, 11, 5515, <https://doi.org/10.1038/s41467-020-18996-3>, 2020.
- 1401 Estes, L., Elsen, P. R., Treuer, T., Ahmed, L., Caylor, K., Chang, J., Choi, J. J., and Ellis, E. C.: The spatial and temporal
1402 domains of modern ecology, *Nature Ecology & Evolution*, 1, <https://doi.org/10.1038/s41559-018-0524-4>, 2018.
- 1403 Evans, M. R.: Modelling ecological systems in a changing world, *Phil. Trans. R. Soc. B*, 367, 181–190,
1404 <https://doi.org/10.1098/rstb.2011.0172>, 2012.
- 1405 Farquhar, G. D., Caemmerer, S. von, and Berry, J. A.: A biochemical model of photosynthetic CO₂ assimilation in leaves of
1406 C₃ species, *Planta*, 149, 78–90, 1980.
- 1407 Farrell, C., Szota, C., and Arndt, S. K.: Does the turgor loss point characterize drought response in dryland plants?, *Plant, Cell*
1408 *& Environment*, 40, 1500–1511, <https://doi.org/10.1111/pce.12948>, 2017.
- 1409 Fatichi, S., Pappas, C., and Ivanov, V. Y.: Modeling plant–water interactions: an ecohydrological overview from the cell to
1410 the global scale, *WIREs Water*, 3, 327–368, <https://doi.org/10.1002/wat2.1125>, 2016.
- 1411 Fauset, S., Baker, T. R., Lewis, S. L., Feldpausch, T. R., Affum-Baffoe, K., Foli, E. G., Hamer, K. C., and Swaine, M. D.:
1412 Drought-induced shifts in the floristic and functional composition of tropical forests in Ghana, *Ecol Lett*, 15, 1120–1129,
1413 <https://doi.org/10.1111/j.1461-0248.2012.01834.x>, 2012.



- 1414 Feeley, K. J., Davies, S. J., Perez, R., Hubbell, S. P., and Foster, R. B.: Directional changes in the species composition of a
1415 tropical forest, *Ecology*, 92, 871–882, 2011.
- 1416 Fer, I., Kelly, R., Moorcroft, P. R., Richardson, A. D., Cowdery, E. M., and Dietze, M. C.: Linking big models to big data:
1417 efficient ecosystem model calibration through Bayesian model emulation, *Biogeosciences*, 15, 5801–5830,
1418 <https://doi.org/10.5194/bg-15-5801-2018>, 2018.
- 1419 Fernández-Martínez, M., Vicca, S., Janssens, I. A., Sardans, J., Luysaert, S., Campioli, M., Chapin Iii, F. S., Ciais, P., Malhi,
1420 Y., Obersteiner, M., Papale, D., Piao, S. L., Reichstein, M., Rodà, F., and Peñuelas, J.: Nutrient availability as the key
1421 regulator of global forest carbon balance, *Nature Clim. Change*, 4, 471–476, <https://doi.org/10.1038/nclimate2177>, 2014.
- 1422 Ferrier, S. and Guisan, A.: Spatial modelling of biodiversity at the community level, *Journal of Applied Ecology*, 43, 393–
1423 404, <https://doi.org/10.1111/j.1365-2664.2006.01149.x>, 2006.
- 1424 Fichtner, A., Härdtle, W., Bruelheide, H., Kunz, M., Li, Y., and Oheimb, G.: Neighbourhood interactions drive overyielding
1425 in mixed-species tree communities, *Nature Communications*, 9, 1144, <https://doi.org/10.1038/s41467-018-03529-w>, 2018.
- 1426 Fischer, F. J.: Inferring the structure and dynamics of tropical rain forests with individual-based forest growth models, Doctoral
1427 Dissertation, Université Paul Sabatier-Toulouse III., 2019.
- 1428 Fischer, F. J., Maréchaux, I., and Chave, J.: Improving plant allometry by fusing forest models and remote sensing, *New*
1429 *Phytologist*, 223, 1159–1165, <https://doi.org/10.1111/nph.15810>, 2019.
- 1430 Fischer, F. J., Labrière, N., Vincent, G., Hérault, B., Alonso, A., Memiaghe, H., Bissiengou, P., Kenfack, D., Saatchi, S., and
1431 Chave, J.: A simulation method to infer tree allometry and forest structure from airborne laser scanning and forest
1432 inventories, *Remote Sensing of Environment*, 251, 112056, <https://doi.org/10.1016/j.rse.2020.112056>, 2020.
- 1433 Fischer, R., Armstrong, A., Shugart, H. H., and Huth, A.: Simulating the impacts of reduced rainfall on carbon stocks and net
1434 ecosystem exchange in a tropical forest, *Environmental Modelling & Software*, 52, 200–206,
1435 <https://doi.org/10.1016/j.envsoft.2013.10.026>, 2014.
- 1436 Fisher, J. B., Huntzinger, D. N., Schwalm, C. R., and Sitch, S.: Modeling the Terrestrial Biosphere, *Annual Review of*
1437 *Environment and Resources*, 39, 91–123, <https://doi.org/10.1146/annurev-environ-012913-093456>, 2014.
- 1438 Fisher, R. A., Williams, M., Do Vale, R. L., Da Costa, A. L., and Meir, P.: Evidence from Amazonian forests is consistent
1439 with isohydric control of leaf water potential, *Plant, Cell & Environment*, 29, 151–165, <https://doi.org/10.1111/j.1365-3040.2005.01407.x>, 2006.
- 1441 Fisher, R. A., Williams, M., Da Costa, A. L., Malhi, Y., Da Costa, R. F., Almeida, S., and Meir, P.: The response of an Eastern
1442 Amazonian rain forest to drought stress: results and modelling analyses from a throughfall exclusion experiment, *Global*
1443 *Change Biology*, 13, 2361–2378, <https://doi.org/10.1111/j.1365-2486.2007.01417.x>, 2007.
- 1444 Fisher, R. A., Muszala, S., Versteinstein, M., Lawrence, P., Xu, C., McDowell, N. G., Knox, R. G., Koven, C., Holm, J., Rogers,
1445 B. M., Spessa, A., Lawrence, D., and Bonan, G.: Taking off the training wheels: the properties of a dynamic vegetation
1446 model without climate envelopes, *CLM4.5(ED)*, *Geosci. Model Dev.*, 8, 3593–3619, [https://doi.org/10.5194/gmd-8-3593-](https://doi.org/10.5194/gmd-8-3593-2015)
1447 2015, 2015.



- 1448 Fisher, R. A., Koven, C. D., Anderegg, W. R. L., Christoffersen, B. O., Dietze, M. C., Farrior, C. E., Holm, J. A., Hurtt, G. C.,
1449 Knox, R. G., Lawrence, P. J., Lichstein, J. W., Longo, M., Matheny, A. M., Medvigy, D., Muller-Landau, H. C., Powell,
1450 T. L., Serbin, S. P., Sato, H., Shuman, J. K., Smith, B., Trugman, A. T., Viskari, T., Verbeeck, H., Weng, E., Xu, C., Xu,
1451 X., Zhang, T., and Moorcroft, P. R.: Vegetation demographics in Earth System Models: A review of progress and priorities,
1452 *Global Change Biology*, 24, 35–54, <https://doi.org/10.1111/gcb.13910>, 2018.
- 1453 Flexas, J., Bota, J., Loreto, F., Cornic, G., and Sharkey, T. D.: Diffusive and Metabolic Limitations to Photosynthesis under
1454 Drought and Salinity in C3 Plants, *Plant Biol (Stuttg)*, 6, 269–279, <https://doi.org/10.1055/s-2004-820867>, 2004.
- 1455 Flexas, J., Galmes, J., Ribas-Carbo, M., and Medrano, H.: The Effects of Water Stress on Plant Respiration, in: *Plant*
1456 *Respiration*, Springer, Dordrecht, 85–94, https://doi.org/10.1007/1-4020-3589-6_6, 2005.
- 1457 Flexas, J., Bota, J., Galmés, J., Medrano, H., and Ribas-Carbó, M.: Keeping a positive carbon balance under adverse conditions:
1458 responses of photosynthesis and respiration to water stress, *Physiologia Plantarum*, 127, 343–352,
1459 <https://doi.org/10.1111/j.1399-3054.2006.00621.x>, 2006.
- 1460 Flexas, J., Barbour, M. M., Brendel, O., Cabrera, H. M., Carriquí, M., Díaz-Espejo, A., Douthe, C., Dreyer, E., Ferrio, J. P.,
1461 Gago, J., Gallé, A., Galmés, J., Kodama, N., Medrano, H., Niinemets, Ü., Peguero-Pina, J. J., Pou, A., Ribas-Carbó, M.,
1462 Tomás, M., Tosens, T., and Warren, C. R.: Mesophyll diffusion conductance to CO₂: An unappreciated central player in
1463 photosynthesis, *Plant Science*, 193–194, 70–84, <https://doi.org/10.1016/j.plantsci.2012.05.009>, 2012.
- 1464 Franks, P. J., Bonan, G. B., Berry, J. A., Lombardozzi, D. L., Holbrook, N. M., Herold, N., and Oleson, K. W.: Comparing
1465 optimal and empirical stomatal conductance models for application in Earth system models, *Global Change Biology*, 24,
1466 5708–5723, <https://doi.org/10.1111/gcb.14445>, 2018.
- 1467 Franks, S. W., Beven, K. J., Quinn, P. F., and Wright, I. R.: On the sensitivity of soil-vegetation-atmosphere transfer (SVAT)
1468 schemes: equifinality and the problem of robust calibration, *Agricultural and Forest Meteorology*, 86, 63–75,
1469 [https://doi.org/10.1016/S0168-1923\(96\)02421-5](https://doi.org/10.1016/S0168-1923(96)02421-5), 1997.
- 1470 Friend, A. D., Lucht, W., Rademacher, T. T., Kerbin, R., Betts, R., Cadule, P., Ciais, P., Clark, D. B., Dankers, R., Falloon,
1471 P. D., Ito, A., Kahana, R., Kleidon, A., Lomas, M. R., Nishina, K., Ostberg, S., Pavlick, R., Peylin, P., Schaphoff, S.,
1472 Vuichard, N., Warszawski, L., Wiltshire, A., and Woodward, F. I.: Carbon residence time dominates uncertainty in
1473 terrestrial vegetation responses to future climate and atmospheric CO₂, *Proc. Natl. Acad. Sci. U. S. A.*, 111, 3280–3285,
1474 <https://doi.org/10.1073/pnas.1222477110>, 2014.
- 1475 Fyllas, N. M., Gloor, E., Mercado, L. M., Sitch, S., Quesada, C. A., Domingues, T. F., Galbraith, D. R., Torre-Lezama, A.,
1476 Vilanova, E., Ramírez-Angulo, H., Higuchi, N., Neill, D. A., Silveira, M., Ferreira, L., Aymard C., G. A., Malhi, Y.,
1477 Phillips, O. L., and Lloyd, J.: Analysing Amazonian forest productivity using a new individual and trait-based model (TFS
1478 v.1), *Geosci. Model Dev.*, 7, 1251–1269, <https://doi.org/10.5194/gmd-7-1251-2014>, 2014.
- 1479 Garcia, M. N., Domingues, T. F., Oliveira, R. S., and Costa, F. R. C.: The biogeography of embolism resistance across resource
1480 gradients in the Amazon, *Global Ecology and Biogeography*, 32, 2199–2211, <https://doi.org/10.1111/geb.13765>, 2023.



- 1481 Gardner, W. R.: Relation of Root Distribution to Water Uptake and Availability, *Agronomy Journal*, 56, 41–45,
1482 <https://doi.org/10.2134/agronj1964.00021962005600010013x>, 1964.
- 1483 Gash, J. H. C.: An analytical model of rainfall interception by forests, *Q.J.R. Meteorol. Soc.*, 105, 43–55,
1484 <https://doi.org/10.1002/qj.49710544304>, 1979.
- 1485 Gash, J. H. C., Lloyd, C. R., and Lachaud, G.: Estimating sparse forest rainfall interception with an analytical model, *Journal*
1486 *of Hydrology*, 170, 79–86, [https://doi.org/10.1016/0022-1694\(95\)02697-N](https://doi.org/10.1016/0022-1694(95)02697-N), 1995.
- 1487 van Genuchten, M. Th.: A Closed-form Equation for Predicting the Hydraulic Conductivity of Unsaturated Soils¹, *Soil Science*
1488 *Society of America Journal*, 44, 892–898, <https://doi.org/10.2136/sssaj1980.03615995004400050002x>, 1980.
- 1489 Girard-Tercieux, C., Maréchaux, I., Clark, A. T., Clark, J. S., Courbaud, B., Fortunel, C., Guillemot, J., Künstler, G., le Maire,
1490 G., Pélassier, R., Rüger, N., and Vieilledent, G.: Rethinking the nature of intraspecific variability and its consequences on
1491 species coexistence, *Ecology and Evolution*, 13, e9860, <https://doi.org/10.1002/ece3.9860>, 2023.
- 1492 Girard-Tercieux, C., Vieilledent, G., Clark, A., Clark, J. S., Courbaud, B., Fortunel, C., Kunstler, G., Pélassier, R., Rüger, N.,
1493 and Maréchaux, I.: Beyond variance: simple random distributions are not a good proxy for intraspecific variability in
1494 systems with environmental structure, *Peer Community Journal*, 4, <https://doi.org/10.24072/pcjournal.360>, 2024.
- 1495 Gourlet-Fleury, S., Blanc, L., Picard, N., Sist, P., Dick, J., Nasi, R., Swaine, M. D., and Forni, E.: Grouping species for
1496 predicting mixed tropical forest dynamics: looking for a strategy, *Annals of Forest Science*, 62, 12,
1497 <https://doi.org/10.1051/forest:2005084>, 2005.
- 1498 Griffin-Nolan, R. J., Ocheltree, T. W., Mueller, K. E., Blumenthal, D. M., Kray, J. A., and Knapp, A. K.: Extending the
1499 osmometer method for assessing drought tolerance in herbaceous species, *Oecologia*, 189, 353–363,
1500 <https://doi.org/10.1007/s00442-019-04336-w>, 2019.
- 1501 Gril, E., Spicher, F., Greiser, C., Ashcroft, M. B., Pincebourde, S., Durrieu, S., Nicolas, M., Richard, B., Decocq, G., Marrec,
1502 R., and Lenoir, J.: Slope and equilibrium: A parsimonious and flexible approach to model microclimate, *Methods in*
1503 *Ecology and Evolution*, 14, 885–897, <https://doi.org/10.1111/2041-210X.14048>, 2023a.
- 1504 Gril, E., Laslier, M., Gallet-Moron, E., Durrieu, S., Spicher, F., Le Roux, V., Brasseur, B., Haesen, S., Van Meerbeek, K.,
1505 Decocq, G., Marrec, R., and Lenoir, J.: Using airborne LiDAR to map forest microclimate temperature buffering or
1506 amplification, *Remote Sensing of Environment*, 298, 113820, <https://doi.org/10.1016/j.rse.2023.113820>, 2023b.
- 1507 Grisebach, A.: Die Vegetation der Erde nach ihrer klimatischen Anordnung: Ein Abriss der vergleichenden Geographie der
1508 Pflanzen. Bd. I und II., Verlag von Wilhelm Engelmann, Leipzig, 1872.
- 1509 Gu, L., Shugart, H. H., Fuentes, J. D., Black, T. A., and Shewchuk, S. R.: Micrometeorology, biophysical exchanges and
1510 NEE decomposition in a two-story boreal forest — development and test of an integrated model, *Agricultural and Forest*
1511 *Meteorology*, 94, 123–148, [https://doi.org/10.1016/S0168-1923\(99\)00006-4](https://doi.org/10.1016/S0168-1923(99)00006-4), 1999.
- 1512 Guan, K., Pan, M., Li, H., Wolf, A., Wu, J., Medvigy, D., Caylor, K. K., Sheffield, J., Wood, E. F., Malhi, Y., Liang, M.,
1513 Kimball, J. S., Saleska, S. R., Berry, J., Joiner, J., and Lyapustin, A. I.: Photosynthetic seasonality of global tropical forests
1514 constrained by hydroclimate, *Nature Geosci*, 8, 284–289, <https://doi.org/10.1038/ngeo2382>, 2015.



- 1515 Guerrero-Ramírez, N. R., Mommer, L., Freschet, G. T., Iversen, C. M., McCormack, M. L., Kattge, J., Poorter, H., van der
1516 Plas, F., Bergmann, J., Kuyper, T. W., York, L. M., Bruelheide, H., Laughlin, D. C., Meier, I. C., Roumet, C., Semchenko,
1517 M., Sweeney, C. J., van Ruijven, J., Valverde-Barrantes, O. J., Aubin, I., Catford, J. A., Manning, P., Martin, A., Milla, R.,
1518 Minden, V., Pausas, J. G., Smith, S. W., Soudzilovskaia, N. A., Ammer, C., Butterfield, B., Craine, J., Cornelissen, J. H.
1519 C., de Vries, F. T., Isaac, M. E., Kramer, K., König, C., Lamb, E. G., Onipchenko, V. G., Peñuelas, J., Reich, P. B., Rillig,
1520 M. C., Sack, L., Shipley, B., Tedersoo, L., Valladares, F., van Bodegom, P., Weigelt, P., Wright, J. P., and Weigelt, A.:
1521 Global root traits (GRooT) database, *Global Ecology and Biogeography*, 30, 25–37, <https://doi.org/10.1111/geb.13179>,
1522 2021.
- 1523 Guillemot, J., Kunz, M., Schnabel, F., Fichtner, A., Madsen, C. P., Gebauer, T., Härdtle, W., von Oheimb, G., and Potvin, C.:
1524 Neighbourhood-mediated shifts in tree biomass allocation drive overyielding in tropical species mixtures, *New Phytologist*,
1525 228, 1256–1268, <https://doi.org/10.1111/nph.16722>, 2020.
- 1526 Guimberteau, M., Ducharne, A., Ciais, P., Boisier, J.-P., Peng, S., De Weirdt, M., and Verbeeck, H.: Testing conceptual and
1527 physically based soil hydrology schemes against observations for the Amazon Basin, *Geoscientific Model Development*,
1528 7, 1115–1136, <https://doi.org/10.5194/gmd-7-1115-2014>, 2014.
- 1529 Guisan, A. and Thuiller, W.: Predicting species distribution: offering more than simple habitat models, *Ecology Letters*, 8,
1530 993–1009, <https://doi.org/10.1111/j.1461-0248.2005.00792.x>, 2005.
- 1531 Guisan, A., Thuiller, W., and Zimmermann, N. E.: *Habitat Suitability and Distribution Models: with Applications in R*,
1532 Cambridge University Press, 513 pp., 2017.
- 1533 Gutiérrez, A. G., Armesto, J. J., Díaz, M. F., and Huth, A.: Increased Drought Impacts on Temperate Rainforests from Southern
1534 South America: Results of a Process-Based, Dynamic Forest Model, *PLOS ONE*, 9, e103226,
1535 <https://doi.org/10.1371/journal.pone.0103226>, 2014.
- 1536 Hanbury-Brown, A. R., Ward, R. E., and Kueppers, L. M.: Forest regeneration within Earth system models: current process
1537 representations and ways forward, *New Phytologist*, 235, 20–40, <https://doi.org/10.1111/nph.18131>, 2022.
- 1538 Harper, A., Baker, I. T., Denning, A. S., Randall, D. A., Dazlich, D., and Branson, M.: Impact of evapotranspiration on dry
1539 season climate in the Amazon forest, *Journal of Climate*, 27, 574–591, <https://doi.org/10.1175/JCLI-D-13-00074.1>, 2013.
- 1540 Hartig, F., Dyke, J., Hickler, T., Higgins, S. I., O’Hara, R. B., Scheiter, S., and Huth, A.: Connecting dynamic vegetation
1541 models to data – an inverse perspective, *Journal of Biogeography*, 39, 2240–2252, <https://doi.org/10.1111/j.1365-2699.2012.02745.x>, 2012.
- 1543 Hasselquist, N. J., Allen, M. F., and Santiago, L. S.: Water relations of evergreen and drought-deciduous trees along a
1544 seasonally dry tropical forest chronosequence, *Oecologia*, 164, 881–890, <https://doi.org/10.1007/s00442-010-1725-y>,
1545 2010.
- 1546 Hengl, T., Jesus, J. M. de, Heuvelink, G. B. M., Gonzalez, M. R., Kilibarda, M., Blagotić, A., Shangguan, W., Wright, M. N.,
1547 Geng, X., Bauer-Marschallinger, B., Guevara, M. A., Vargas, R., MacMillan, R. A., Batjes, N. H., Leenaars, J. G. B.,



- 1548 Ribeiro, E., Wheeler, I., Mantel, S., and Kempen, B.: SoilGrids250m: Global gridded soil information based on machine
1549 learning, *PLOS ONE*, 12, e0169748, <https://doi.org/10.1371/journal.pone.0169748>, 2017.
- 1550 Hérault, A., Lin, Y.-S., Bourne, A., Medlyn, B. E., and Ellsworth, D. S.: Optimal stomatal conductance in relation to
1551 photosynthesis in climatically contrasting Eucalyptus species under drought, *Plant, Cell & Environment*, 36, 262–274,
1552 <https://doi.org/10.1111/j.1365-3040.2012.02570.x>, 2013.
- 1553 Heskell, M. A., O’Sullivan, O. S., Reich, P. B., Tjoelker, M. G., Weerasinghe, L. K., Penillard, A., Egerton, J. J. G., Creek, D.,
1554 Bloomfield, K. J., Xiang, J., Sinca, F., Stangl, Z. R., Torre, A. M. la, Griffin, K. L., Huntingford, C., Hurry, V., Meir, P.,
1555 Turnbull, M. H., and Atkin, O. K.: Convergence in the temperature response of leaf respiration across biomes and plant
1556 functional types, *PNAS*, 201520282, <https://doi.org/10.1073/pnas.1520282113>, 2016.
- 1557 Hodnett, M. G. and Tomasella, J.: Marked differences between van Genuchten soil water-retention parameters for temperate
1558 and tropical soils: a new water-retention pedo-transfer functions developed for tropical soils, *Geoderma*, 108, 155–180,
1559 [https://doi.org/10.1016/S0016-7061\(02\)00105-2](https://doi.org/10.1016/S0016-7061(02)00105-2), 2002.
- 1560 Horton, R. E.: The role of infiltration in the hydrologic cycle, *Eos, Transactions American Geophysical Union*, 14, 446–460,
1561 <https://doi.org/10.1029/TR014i001p00446>, 1933.
- 1562 Hsiao, T. C.: Plant Responses to Water Stress, *Annual Review of Plant Physiology*, 24, 519–570,
1563 <https://doi.org/10.1146/annurev.pp.24.060173.002511>, 1973.
- 1564 Huaraca Huasco, W., Riutta, T., Girardin, C. A. J., Hanco Pacha, F., Puma Vilca, B. L., Moore, S., Rifai, S. W., del Aguila-
1565 Pasquel, J., Araujo Murakami, A., Freitag, R., Morel, A. C., Demissie, S., Doughty, C. E., Oliveras, I., Galiano Cabrera,
1566 D. F., Durand Baca, L., Farfán Amézquita, F., Silva Espejo, J. E., da Costa, A. C. L., Oblitas Mendoza, E., Quesada, C. A.,
1567 Evouna Ondo, F., Edzang Ndong, J., Jeffery, K. J., Mihindou, V., White, L. J. T., N’ssi Bengone, N., Ibrahim, F., Addo-
1568 Danso, S. D., Duah-Gyamfi, A., Djaney Djagbletey, G., Owusu-Afryie, K., Amissah, L., Mbou, A. T., Marthews, T. R.,
1569 Metcalfe, D. B., Aragão, L. E. O., Marimon-Junior, B. H., Marimon, B. S., Majalap, N., Adu-Bredu, S., Abernethy, K. A.,
1570 Silman, M., Ewers, R. M., Meir, P., and Malhi, Y.: Fine root dynamics across pantropical rainforest ecosystems, *Global
1571 Change Biology*, 27, 3657–3680, <https://doi.org/10.1111/gcb.15677>, 2021.
- 1572 Hubau, W., Lewis, S. L., Phillips, O. L., Affum-Baffoe, K., Beeckman, H., Cuní-Sanchez, A., Daniels, A. K., Ewango, C. E.
1573 N., Fauset, S., Mukinzi, J. M., Sheil, D., Sonké, B., Sullivan, M. J. P., Sunderland, T. C. H., Taedoumg, H., Thomas, S. C.,
1574 White, L. J. T., Abernethy, K. A., Adu-Bredu, S., Amani, C. A., Baker, T. R., Banin, L. F., Baya, F., Begne, S. K., Bennett,
1575 A. C., Benedet, F., Bitariho, R., Bocko, Y. E., Boeckx, P., Boundja, P., Brienen, R. J. W., Brncic, T., Chezeaux, E.,
1576 Chuyong, G. B., Clark, C. J., Collins, M., Comiskey, J. A., Coomes, D. A., Dargie, G. C., de Haulleville, T., Kamdem, M.
1577 N. D., Doucet, J.-L., Esquivel-Muelbert, A., Feldpausch, T. R., Fofanah, A., Foli, E. G., Gilpin, M., Gloor, E., Gonmadje,
1578 C., Gourlet-Fleury, S., Hall, J. S., Hamilton, A. C., Harris, D. J., Hart, T. B., Hockemba, M. B. N., Hladik, A., Ifo, S. A.,
1579 Jeffery, K. J., Jucker, T., Yakusu, E. K., Kearsley, E., Kenfack, D., Koch, A., Leal, M. E., Levesley, A., Lindsell, J. A.,
1580 Lisingo, J., Lopez-Gonzalez, G., Lovett, J. C., Makana, J.-R., Malhi, Y., Marshall, A. R., Martin, J., Martin, E. H., Mbayu,
1581 F. M., Medjibe, V. P., Mihindou, V., Mitchard, E. T. A., Moore, S., Munishi, P. K. T., Bengone, N. N., Ojo, L., Ondo, F.



- 1582 E., Peh, K. S.-H., Pickavance, G. C., Poulsen, A. D., Poulsen, J. R., Qie, L., Reitsma, J., Rovero, F., Swaine, M. D., Talbot,
1583 J., Taplin, J., Taylor, D. M., Thomas, D. W., Toirambe, B., Mukendi, J. T., Tuagben, D., Umunay, P. M., et al.:
1584 Asynchronous carbon sink saturation in African and Amazonian tropical forests, *Nature*, 579, 80–87,
1585 <https://doi.org/10.1038/s41586-020-2035-0>, 2020.
- 1586 Humbel, F.-X.: Caractérisation, par des mesures physiques, hydriques et d'enracinement, de sols de Guyane française à
1587 dynamique de l'eau superficielle, *Sciences du sol*, 2, 83–94, 1978.
- 1588 Humboldt, A. von: Aspects of nature, in different lands and different climates; with scientific elucidations, Lea and Blanchard,
1589 512 pp., 1849.
- 1590 Huntingford, C., Zelazowski, P., Galbraith, D., Mercado, L. M., Sitch, S., Fisher, R., Lomas, M., Walker, A. P., Jones, C. D.,
1591 Booth, B. B. B., Malhi, Y., Hemming, D., Kay, G., Good, P., Lewis, S. L., Phillips, O. L., Atkin, O. K., Lloyd, J., Gloor,
1592 E., Zaragoza-Castells, J., Meir, P., Betts, R., Harris, P. P., Nobre, C., Marengo, J., and Cox, P. M.: Simulated resilience of
1593 tropical rainforests to CO₂-induced climate change, *Nature Geosci*, 6, 268–273, <https://doi.org/10.1038/ngeo1741>, 2013.
- 1594 Hutchinson, G. E.: Concluding remarks, *Cold Spring Harbor Symposia on Quantitative Biology*, 22, 415–427, 1957.
- 1595 Igarashi, S., Yoshida, S., Kenzo, T., Sakai, S., Nagamasu, H., Hyodo, F., Tayasu, I., Mohamad, M., and Ichie, T.: No evidence
1596 of carbon storage usage for seed production in 18 dipterocarp masting species in a tropical rain forest, *Oecologia*,
1597 <https://doi.org/10.1007/s00442-024-05527-w>, 2024.
- 1598 Iida, Y., Poorter, L., Sterck, F. J., Kassim, A. R., Kubo, T., Potts, M. D., and Kohyama, T. S.: Wood density explains
1599 architectural differentiation across 145 co-occurring tropical tree species, *Funct. Ecol.*, 26, 274–282,
1600 <https://doi.org/10.1111/j.1365-2435.2011.01921.x>, 2012.
- 1601 Ivanov, V. Y., Hutrya, L. R., Wofsy, S. C., Munger, J. W., Saleska, S. R., Oliveira, R. C. de, and Camargo, P. B. de: Root
1602 niche separation can explain avoidance of seasonal drought stress and vulnerability of overstory trees to extended drought
1603 in a mature Amazonian forest, *Water Resources Research*, 48, <https://doi.org/10.1029/2012WR011972>, 2012.
- 1604 Jackson, R. B., Canadell, J., Ehleringer, J. R., Mooney, H. A., Sala, O. E., and Schulze, E. D.: A global analysis of root
1605 distributions for terrestrial biomes, *Oecologia*, 108, 389–411, <https://doi.org/10.1007/BF00333714>, 1996.
- 1606 Jackson, R. B., Moore, L. A., Hoffmann, W. A., Pockman, W. T., and Linder, C. R.: Ecosystem rooting depth determined with
1607 caves and DNA, *PNAS*, 96, 11387–11392, <https://doi.org/10.1073/pnas.96.20.11387>, 1999.
- 1608 Jarvis, P. G. and McNaughton, K. G.: Stomatal Control of Transpiration: Scaling Up from Leaf to Region, *Advances in
1609 Ecological Research*, 15, 1–49, [https://doi.org/10.1016/S0065-2504\(08\)60119-1](https://doi.org/10.1016/S0065-2504(08)60119-1), 1986.
- 1610 Joetzier, E., Delire, C., Douville, H., Ciais, P., Decharme, B., Fisher, R., Christoffersen, B., Calvet, J. C., da Costa, A. C. L.,
1611 Ferreira, L. V., and Meir, P.: Predicting the response of the Amazon rainforest to persistent drought conditions under current
1612 and future climates: a major challenge for global land surface models, *Geosci. Model Dev.*, 7, 2933–2950,
1613 <https://doi.org/10.5194/gmd-7-2933-2014>, 2014.



- 1614 Joetzjer, E., Maignan, F., Chave, J., Goll, D., Poulter, B., Barichivich, J., Maréchaux, I., Luysaert, S., Guimberteau, M.,
1615 Naudts, K., Bonal, D., and Ciais, P.: Effect of tree demography and flexible root water uptake for modeling the carbon and
1616 water cycles of Amazonia, *Ecological Modelling*, 469, 109969, <https://doi.org/10.1016/j.ecolmodel.2022.109969>, 2022.
- 1617 Johnson, D. J., Condit, R., Hubbell, S. P., and Comita, L. S.: Abiotic niche partitioning and negative density dependence drive
1618 tree seedling survival in a tropical forest, *Proc. R. Soc. B*, 284, 20172210, <https://doi.org/10.1098/rspb.2017.2210>, 2017.
- 1619 Johnson, M. O., Galbraith, D., Gloor, M., De Deurwaerder, H., Guimberteau, M., Rammig, A., Thonicke, K., Verbeeck, H.,
1620 von Randow, C., Monteagudo, A., Phillips, O. L., Brienen, R. J. W., Feldpausch, T. R., Lopez Gonzalez, G., Fauset, S.,
1621 Quesada, C. A., Christoffersen, B., Ciais, P., Sampaio, G., Kruijt, B., Meir, P., Moorcroft, P., Zhang, K., Alvarez-Davila,
1622 E., Alves de Oliveira, A., Amaral, I., Andrade, A., Aragao, L. E. O. C., Araujo-Murakami, A., Arets, E. J. M. M., Arroyo,
1623 L., Aymard, G. A., Baraloto, C., Barroso, J., Bonal, D., Boot, R., Camargo, J., Chave, J., Cogollo, A., Cornejo Valverde,
1624 F., Lola da Costa, A. C., Di Fiore, A., Ferreira, L., Higuchi, N., Honorio, E. N., Killeen, T. J., Laurance, S. G., Laurance,
1625 W. F., Licona, J., Lovejoy, T., Malhi, Y., Marimon, B., Marimon, B. H., Matos, D. C. L., Mendoza, C., Neill, D. A., Pardo,
1626 G., Peña-Claros, M., Pitman, N. C. A., Poorter, L., Prieto, A., Ramirez-Angulo, H., Roopsind, A., Rudas, A., Salomao, R.
1627 P., Silveira, M., Stropp, J., ter Steege, H., Terborgh, J., Thomas, R., Toledo, M., Torres-Lezama, A., van der Heijden, G.
1628 M. F., Vasquez, R., Guimarães Vieira, I. C., Vilanova, E., Vos, V. A., and Baker, T. R.: Variation in stem mortality rates
1629 determines patterns of above-ground biomass in Amazonian forests: implications for dynamic global vegetation models,
1630 *Glob Change Biol*, 22, 3996–4013, <https://doi.org/10.1111/gcb.13315>, 2016.
- 1631 Jones, H. G.: *Plants and Microclimate: A Quantitative Approach to Environmental Plant Physiology*, 3rd ed., Cambridge
1632 University Press, Cambridge, <https://doi.org/10.1017/CBO9780511845727>, 2013.
- 1633 Jourdan, M., Kunstler, G., and Morin, X.: How neighbourhood interactions control the temporal stability and resilience to
1634 drought of trees in mountain forests, *Journal of Ecology*, 108, 666–677, <https://doi.org/10.1111/1365-2745.13294>, 2020.
- 1635 Journé, V., Barnagaud, J.-Y., Bernard, C., Crochet, P.-A., and Morin, X.: Correlative climatic niche models predict real and
1636 virtual species distributions equally well, *Ecology*, 101, e02912, <https://doi.org/10.1002/ecy.2912>, 2020.
- 1637 Jucker, T., Caspersen, J., Chave, J., Antin, C., Barbier, N., Bongers, F., Dalponte, M., van Ewijk, K. Y., Forrester, D. I., Haeni,
1638 M., Higgins, S. I., Holdaway, R. J., Iida, Y., Lorimer, C., Marshall, P. L., Momo, S., Moncrieff, G. R., Ploton, P., Poorter,
1639 L., Rahman, K. A., Schlund, M., Sonké, B., Sterck, F. J., Trugman, A. T., Usoltsev, V. A., Vanderwel, M. C., Waldner, P.,
1640 Wedeux, B. M. M., Wirth, C., Wöll, H., Woods, M., Xiang, W., Zimmermann, N. E., and Coomes, D. A.: Allometric
1641 equations for integrating remote sensing imagery into forest monitoring programmes, *Glob Change Biol*, 23, 177–190,
1642 <https://doi.org/10.1111/gcb.13388>, 2017.
- 1643 Jucker, T., Hardwick, S. R., Both, S., Elias, D. M. O., Ewers, R. M., Milodowski, D. T., Swinfield, T., and Coomes, D. A.:
1644 Canopy structure and topography jointly constrain the microclimate of human-modified tropical landscapes, *Global Change
1645 Biology*, 24, 5243–5258, <https://doi.org/10.1111/gcb.14415>, 2018.
- 1646 Jucker, T., Fischer, F. J., Chave, J., Coomes, D. A., Caspersen, J., Ali, A., Loubota Panzou, G. J., Feldpausch, T. R., Falster,
1647 D., Usoltsev, V. A., Adu-Bredu, S., Alves, L. F., Aminpour, M., Angoboy, I. B., Anten, N. P. R., Antin, C., Askari, Y.,



- 1648 Muñoz, R., Ayyappan, N., Balvanera, P., Banin, L., Barbier, N., Battles, J. J., Beeckman, H., Bocko, Y. E., Bond-Lamberty,
1649 B., Bongers, F., Bowers, S., Brade, T., van Breugel, M., Chantrain, A., Chaudhary, R., Dai, J., Dalponte, M., Dimobe, K.,
1650 Domec, J.-C., Doucet, J.-L., Duursma, R. A., Enríquez, M., van Ewijk, K. Y., Farfán-Rios, W., Fayolle, A., Forni, E.,
1651 Forrester, D. I., Gilani, H., Godlee, J. L., Gourlet-Fleury, S., Haeni, M., Hall, J. S., He, J.-K., Hemp, A., Hernández-
1652 Stefanoni, J. L., Higgins, S. I., Holdaway, R. J., Hussain, K., Hutley, L. B., Ichie, T., Iida, Y., Jiang, H., Joshi, P. R., Kaboli,
1653 H., Larsary, M. K., Kenzo, T., Klooppel, B. D., Kohyama, T., Kunwar, S., Kuyah, S., Kvasnica, J., Lin, S., Lines, E. R.,
1654 Liu, H., Lorimer, C., Loumeto, J.-J., Malhi, Y., Marshall, P. L., Mattsson, E., Matula, R., Meave, J. A., Mensah, S., Mi,
1655 X., Momo, S., Moncrieff, G. R., Mora, F., Nissanka, S. P., O'Hara, K. L., Pearce, S., Pelissier, R., Peri, P. L., Ploton, P.,
1656 Poorter, L., Pour, M. J., Pourbabaei, H., Dupuy-Rada, J. M., Ribeiro, S. C., Ryan, C., Sanaei, A., Sanger, J., Schlund, M.,
1657 Sellan, G., et al.: Tallo: A global tree allometry and crown architecture database, *Global Change Biology*, 28, 5254–5268,
1658 <https://doi.org/10.1111/gcb.16302>, 2022.
- 1659 Kattge, J. and Knorr, W.: Temperature acclimation in a biochemical model of photosynthesis: a reanalysis of data from 36
1660 species, *Plant, Cell & Environment*, 30, 1176–1190, <https://doi.org/10.1111/j.1365-3040.2007.01690.x>, 2007.
- 1661 Kattge, J., Díaz, S., Lavorel, S., Prentice, I. C., Leadley, P., Bönisch, G., Garnier, E., Westoby, M., Reich, P. B., Wright, I. J.,
1662 Cornelissen, J. H. C., Violle, C., Harrison, S. P., Van Bodegom, P. M., Reichstein, M., Enquist, B. J., Soudzilovskaia, N.
1663 A., Ackerly, D. D., Anand, M., Atkin, O., Bahn, M., Baker, T. R., Baldocchi, D., Bekker, R., Blanco, C. C., Blonder, B.,
1664 Bond, W. J., Bradstock, R., Bunker, D. E., Casanoves, F., Cavender-bares, J., Chambers, J. Q., Chapin Iii, F. S., Chave, J.,
1665 Coomes, D., Cornwell, W. K., Craine, J. M., Dobrin, B. H., Duarte, L., Durka, W., Elser, J., Esser, G., Estiarte, M., Fagan,
1666 W. F., Fang, J., Fernández-méndez, F., Fidelis, A., Finegan, B., Flores, O., Ford, H., Frank, D., Freschet, G. T., Fyllas, N.
1667 M., Gallagher, R. V., Green, W. A., Gutierrez, A. G., Hickler, T., Higgins, S. I., Hodgson, J. G., Jalili, A., Jansen, S., Joly,
1668 C. A., Kerkhoff, A. J., Kirkup, D., Kitajima, K., Kleyer, M., Klotz, S., Knops, J. M. H., Kramer, K., Kühn, I., Kurokawa,
1669 H., Laughlin, D., Lee, T. D., Leishman, M., Lens, F., Lenz, T., Lewis, S. L., Lloyd, J., Llusià, J., Louault, F., Ma, S.,
1670 Mahecha, M. D., Manning, P., Massad, T., Medlyn, B. E., Messier, J., Moles, A. T., Müller, S. C., Nadrowski, K., Naeem,
1671 S., Niinemets, Ü., Nöllert, S., Nüske, A., Ogaya, R., Oleksyn, J., Onipchenko, V. G., Onoda, Y., Ordoñez, J., Overbeck,
1672 G., et al.: TRY – a global database of plant traits, *Global Change Biology*, 17, 2905–2935, <https://doi.org/10.1111/j.1365-2486.2011.02451.x>, 2011.
- 1674 Kattge, J., Bönisch, G., Díaz, S., Lavorel, S., Prentice, I. C., Leadley, P., Tautenhahn, S., Werner, G. D. A., Aakala, T., Abedi,
1675 M., Acosta, A. T. R., Adamidis, G. C., Adamson, K., Aiba, M., Albert, C. H., Alcántara, J. M., C, C. A., Aleixo, I., Ali,
1676 H., Amiaud, B., Ammer, C., Amoroso, M. M., Anand, M., Anderson, C., Anten, N., Antos, J., Apgaua, D. M. G., Ashman,
1677 T.-L., Asmara, D. H., Asner, G. P., Aspinwall, M., Atkin, O., Aubin, I., Baastrup-Spohr, L., Bahalkeh, K., Bahn, M., Baker,
1678 T., Baker, W. J., Bakker, J. P., Baldocchi, D., Baltzer, J., Banerjee, A., Baranger, A., Barlow, J., Barneche, D. R., Baruch,
1679 Z., Bastianelli, D., Battles, J., Bauerle, W., Bauters, M., Bazzato, E., Beckmann, M., Beeckman, H., Beierkuhnlein, C.,
1680 Bekker, R., Belfry, G., Belluau, M., Beloiu, M., Benavides, R., Benomar, L., Berdugo-Lattke, M. L., Berenguer, E.,
1681 Bergamin, R., Bergmann, J., Carlucci, M. B., Berner, L., Bernhardt-Römermann, M., Bigler, C., Bjorkman, A. D.,



- 1682 Blackman, C., Blanco, C., Blonder, B., Blumenthal, D., Bocanegra-González, K. T., Boeckx, P., Bohlman, S., Böhning-
1683 Gaese, K., Boisvert-Marsh, L., Bond, W., Bond-Lamberty, B., Boom, A., Boonman, C. C. F., Bordin, K., Boughton, E. H.,
1684 Boukili, V., Bowman, D. M. J. S., Bravo, S., Brendel, M. R., Broadley, M. R., Brown, K. A., Bruelheide, H., Brumnich,
1685 F., Bruun, H. H., Bruy, D., Buchanan, S. W., Bucher, S. F., Buchmann, N., Buitenwerf, R., Bunker, D. E., et al.: TRY plant
1686 trait database – enhanced coverage and open access, *Global Change Biology*, 26, 119–188,
1687 <https://doi.org/10.1111/gcb.14904>, 2020.
- 1688 Kazmierczak, M., Wiegand, T., and Huth, A.: A neutral vs. non-neutral parametrizations of a physiological forest gap model,
1689 *Ecological Modelling*, 288, 94–102, <https://doi.org/10.1016/j.ecolmodel.2014.05.002>, 2014.
- 1690 Kearney, M. and Porter, W.: Mechanistic niche modelling: combining physiological and spatial data to predict species' ranges,
1691 *Ecology Letters*, 12, 334–350, <https://doi.org/10.1111/j.1461-0248.2008.01277.x>, 2009.
- 1692 Keenan, T., Sabate, S., and Gracia, C.: Soil water stress and coupled photosynthesis–conductance models: Bridging the gap
1693 between conflicting reports on the relative roles of stomatal, mesophyll conductance and biochemical limitations to
1694 photosynthesis, *Agricultural and Forest Meteorology*, 150, 443–453, <https://doi.org/10.1016/j.agrformet.2010.01.008>,
1695 2010.
- 1696 Kennedy, D., Swenson, S., Oleson, K. W., Lawrence, D. M., Fisher, R., Costa, A. C. L. da, and Gentine, P.: Implementing
1697 Plant Hydraulics in the Community Land Model, Version 5, *Journal of Advances in Modeling Earth Systems*, 11, 485–
1698 513, <https://doi.org/10.1029/2018MS001500>, 2019.
- 1699 Kenzo, T., Ichie, T., Hattori, D., Itioka, T., Handa, C., Ohkubo, T., Kendawang, J. J., Nakamura, M., Sakaguchi, M., Takahashi,
1700 N., Okamoto, M., Tanaka-Oda, A., Sakurai, K., and Ninomiya, I.: Development of allometric relationships for accurate
1701 estimation of above- and below-ground biomass in tropical secondary forests in Sarawak, Malaysia, *Journal of Tropical*
1702 *Ecology*, 25, 371–386, <https://doi.org/10.1017/S0266467409006129>, 2009.
- 1703 Khan, S., Maréchaux, I., Vieilledent, G., Guitet, S., Brunaux, O., Ferry, B., Soulard, F., Stahl, C., Baraloto, C., Fortunel, C.,
1704 and Freycon, V.: Regional Soil Profile Data Reveals the Predominant Role of Geomorphology and Geology in Accurately
1705 Deriving Digital Soil Texture Maps in a Tropical Area, <https://doi.org/10.2139/ssrn.4789279>, 9 April 2024.
- 1706 King, D. A., Davies, S. J., Tan, S., and Noor, N. S. Md.: The role of wood density and stem support costs in the growth and
1707 mortality of tropical trees, *Journal of Ecology*, 94, 670–680, <https://doi.org/10.1111/j.1365-2745.2006.01112.x>, 2006.
- 1708 Kitajima, K., Mulkey, S., and Wright, S.: Decline of photosynthetic capacity with leaf age in relation to leaf longevities for
1709 five tropical canopy tree species., *Am. J. Bot.*, 84, 702–702, 1997a.
- 1710 Kitajima, K., Mulkey, S. S., and Wright, S. J.: Seasonal leaf phenotypes in the canopy of a tropical dry forest: photosynthetic
1711 characteristics and associated traits, *Oecologia*, 109, 490–498, <https://doi.org/10.1007/s004420050109>, 1997b.
- 1712 Kitajima, K., Mulkey, S. S., Samaniego, M., and Wright, S. J.: Decline of photosynthetic capacity with leaf age and position
1713 in two tropical pioneer tree species, *Am. J. Bot.*, 89, 1925–1932, <https://doi.org/10.3732/ajb.89.12.1925>, 2002.
- 1714 Kitajima, K., Mulkey, S. S., and Wright, S. J.: Variation in crown light utilization characteristics among tropical canopy trees,
1715 *Ann Bot*, 95, 535–547, <https://doi.org/10.1093/aob/mci051>, 2005.



- 1716 Koch, A., Hubau, W., and Lewis, S. L.: Earth System Models Are Not Capturing Present-Day Tropical Forest Carbon
1717 Dynamics, *Earth's Future*, 9, e2020EF001874, <https://doi.org/10.1029/2020EF001874>, 2021.
- 1718 Köhler, P. and Huth, A.: The effects of tree species grouping in tropical rainforest modelling: simulations with the individual-
1719 based model Formind, *Ecological Modelling*, 109, 301–321, [https://doi.org/10.1016/S0304-3800\(98\)00066-0](https://doi.org/10.1016/S0304-3800(98)00066-0), 1998.
- 1720 Köhler, P., Ditzer, T., and Huth, A.: Concepts for the aggregation of tropical tree species into functional types and the
1721 application to Sabah's lowland rain forests, *Journal of Tropical Ecology*, 16, 591–602, <https://doi.org/null>, 2000.
- 1722 König, L. A., Mohren, F., Schelhaas, M.-J., Bugmann, H., and Nabuurs, G.-J.: Tree regeneration in models of forest dynamics
1723 – Suitability to assess climate change impacts on European forests, *Forest Ecology and Management*, 520, 120390,
1724 <https://doi.org/10.1016/j.foreco.2022.120390>, 2022.
- 1725 Körner, C.: Paradigm shift in plant growth control, *Current Opinion in Plant Biology*, 25, 107–114,
1726 <https://doi.org/10.1016/j.pbi.2015.05.003>, 2015.
- 1727 Kraft, N. J. B., Metz, M. R., Condit, R. S., and Chave, J.: The relationship between wood density and mortality in a global
1728 tropical forest data set, *New Phytologist*, 188, 1124–1136, <https://doi.org/10.1111/j.1469-8137.2010.03444.x>, 2010.
- 1729 Krinner, G., Viovy, N., de Noblet-Ducoudré, N., Ogée, J., Polcher, J., Friedlingstein, P., Ciais, P., Sitch, S., and Prentice, I.
1730 C.: A dynamic global vegetation model for studies of the coupled atmosphere-biosphere system, *Global Biogeochem.*
1731 *Cycles*, 19, GB1015, <https://doi.org/10.1029/2003GB002199>, 2005.
- 1732 Kume, A., Nasahara, K. N., Nagai, S., and Muraoka, H.: The ratio of transmitted near-infrared radiation to photosynthetically
1733 active radiation (PAR) increases in proportion to the adsorbed PAR in the canopy, *J Plant Res*, 124, 99–106,
1734 <https://doi.org/10.1007/s10265-010-0346-1>, 2011.
- 1735 Kupers, S. J., Engelbrecht, B. M. J., Hernández, A., Wright, S. J., Wirth, C., and Rüger, N.: Growth responses to soil water
1736 potential indirectly shape local species distributions of tropical forest seedlings, *Journal of Ecology*, 107, 860–874,
1737 <https://doi.org/10.1111/1365-2745.13096>, 2019.
- 1738 Kursar, T. A., Engelbrecht, B. M. J., Burke, A., Tyree, M. T., El Omari, B., and Giraldo, J. P.: Tolerance to low leaf water
1739 status of tropical tree seedlings is related to drought performance and distribution, *Functional Ecology*, 23, 93–102,
1740 <https://doi.org/10.1111/j.1365-2435.2008.01483.x>, 2009.
- 1741 Lagarrigues, G., Jabot, F., Lafond, V., and Courbaud, B.: Approximate Bayesian computation to recalibrate individual-based
1742 models with population data: illustration with a forest simulation model, *Ecological Modelling*, 306, 278–286,
1743 <https://doi.org/10.1016/j.ecolmodel.2014.09.023>, 2015.
- 1744 Laio, F., Porporato, A., Ridolfi, L., and Rodriguez-Iturbe, I.: Plants in water-controlled ecosystems: active role in hydrologic
1745 processes and response to water stress: II. Probabilistic soil moisture dynamics, *Advances in Water Resources*, 24, 707–
1746 723, [https://doi.org/10.1016/S0309-1708\(01\)00005-7](https://doi.org/10.1016/S0309-1708(01)00005-7), 2001.
- 1747 Lamour, J., Davidson, K. J., Ely, K. S., Le Moguédec, G., Leakey, A. D. B., Li, Q., Serbin, S. P., and Rogers, A.: An improved
1748 representation of the relationship between photosynthesis and stomatal conductance leads to more stable estimation of



- 1749 conductance parameters and improves the goodness-of-fit across diverse data sets, *Global Change Biology*, 28, 3537–3556,
1750 <https://doi.org/10.1111/gcb.16103>, 2022.
- 1751 Lamour, J., Souza, D. C., Gimenez, B. O., Higuchi, N., Chave, J., Chambers, J., and Rogers, A.: Wood-density has no effect
1752 on stomatal control of leaf-level water use efficiency in an Amazonian forest, *Plant, Cell & Environment*, 46, 3806–3821,
1753 <https://doi.org/10.1111/pce.14704>, 2023.
- 1754 Lapola, D. M., Pinho, P., Barlow, J., Aragão, L. E. O. C., Berenguer, E., Carmenta, R., Liddy, H. M., Seixas, H., Silva, C. V.
1755 J., Silva-Junior, C. H. L., Alencar, A. A. C., Anderson, L. O., Armenteras, D., Brovkin, V., Calders, K., Chambers, J.,
1756 Chini, L., Costa, M. H., Faria, B. L., Fearnside, P. M., Ferreira, J., Gatti, L., Gutierrez-Velez, V. H., Han, Z., Hibbard, K.,
1757 Koven, C., Lawrence, P., Pongratz, J., Portela, B. T. T., Rounsevell, M., Ruane, A. C., Schaldach, R., da Silva, S. S., von
1758 Randow, C., and Walker, W. S.: The drivers and impacts of Amazon forest degradation, *Science*, 379, eabp8622,
1759 <https://doi.org/10.1126/science.abp8622>, 2023.
- 1760 Laurans, M., Munoz, F., Charles-Dominique, T., Heuret, P., Fortunel, C., Isnard, S., Sabatier, S.-A., Caraglio, Y., and Violle,
1761 C.: Why incorporate plant architecture into trait-based ecology?, *Trends in Ecology & Evolution*, 0,
1762 <https://doi.org/10.1016/j.tree.2023.11.011>, 2024.
- 1763 LeBauer, D. S., Wang, D., Richter, K. T., Davidson, C. C., and Dietze, M. C.: Facilitating feedbacks between field
1764 measurements and ecosystem models, *Ecological Monographs*, 83, 133–154, <https://doi.org/10.1890/12-0137.1>, 2013.
- 1765 Ledo, A., Paul, K. I., Burslem, D. F. R. P., Ewel, J. J., Barton, C., Battaglia, M., Brooksbank, K., Carter, J., Eid, T. H., England,
1766 J. R., Fitzgerald, A., Jonson, J., Mencuccini, M., Montagu, K. D., Montero, G., Mugasha, W. A., Pinkard, E., Roxburgh,
1767 S., Ryan, C. M., Ruiz-Peinado, R., Sochacki, S., Specht, A., Wildy, D., Wirth, C., Zerihun, A., and Chave, J.: Tree size
1768 and climatic water deficit control root to shoot ratio in individual trees globally, *New Phytologist*, 217, 8–11,
1769 <https://doi.org/10.1111/nph.14863>, 2018.
- 1770 Leitold, V., Morton, D. C., Longo, M., dos-Santos, M. N., Keller, M., and Scaranello, M.: El Niño drought increased canopy
1771 turnover in Amazon forests, *New Phytologist*, 219, 959–971, <https://doi.org/10.1111/nph.15110>, 2018.
- 1772 Lenz, T. I., Wright, I. J., and Westoby, M.: Interrelations among pressure–volume curve traits across species and water
1773 availability gradients, *Physiologia Plantarum*, 127, 423–433, <https://doi.org/10.1111/j.1399-3054.2006.00680.x>, 2006.
- 1774 Leuning, R., Kelliher, F. M., Pury, D. G. G., and Schulze, E. -d: Leaf nitrogen, photosynthesis, conductance and transpiration:
1775 scaling from leaves to canopies, *Plant, Cell & Environment*, 18, 1183–1200, <https://doi.org/10.1111/j.1365-3040.1995.tb00628.x>, 1995.
- 1777 Li, Q., Serbin, S. P., Lamour, J., Davidson, K. J., Ely, K. S., and Rogers, A.: Implementation and evaluation of the unified
1778 stomatal optimization approach in the Functionally Assembled Terrestrial Ecosystem Simulator (FATES), *Geoscientific
1779 Model Development*, 15, 4313–4329, <https://doi.org/10.5194/gmd-15-4313-2022>, 2022.
- 1780 Liang, J. and Picard, N.: Matrix Model of Forest Dynamics: An Overview and Outlook, *Forest Science*, 59, 359–378,
1781 <https://doi.org/10.5849/forsci.11-123>, 2013.



- 1782 Liang, X., Lettenmaier, D. P., Wood, E. F., and Burges, S. J.: A simple hydrologically based model of land surface water and
1783 energy fluxes for general circulation models, *J. Geophys. Res.*, 99, 14415–14428, <https://doi.org/10.1029/94JD00483>,
1784 1994.
- 1785 Lin, Y.-S., Medlyn, B. E., Duursma, R. A., Prentice, I. C., Wang, H., Baig, S., Eamus, D., de Dios, V. R., Mitchell, P.,
1786 Ellsworth, D. S., de Beeck, M. O., Wallin, G., Uddling, J., Tarvainen, L., Linderson, M.-L., Cernusak, L. A., Nippert, J.
1787 B., Ocheltree, T. W., Tissue, D. T., Martin-StPaul, N. K., Rogers, A., Warren, J. M., De Angelis, P., Hikosaka, K., Han,
1788 Q., Onoda, Y., Gimeno, T. E., Barton, C. V. M., Bennie, J., Bonal, D., Bosc, A., Löw, M., Macinins-Ng, C., Rey, A.,
1789 Rowland, L., Setterfield, S. A., Tausz-Posch, S., Zaragoza-Castells, J., Broadmeadow, M. S. J., Drake, J. E., Freeman, M.,
1790 Ghannoum, O., Hutley, L. B., Kelly, J. W., Kikuzawa, K., Kolari, P., Koyama, K., Limousin, J.-M., Meir, P., Lola da
1791 Costa, A. C., Mikkelsen, T. N., Salinas, N., Sun, W., and Wingate, L.: Optimal stomatal behaviour around the world, *Nature*
1792 *Clim. Change*, 5, 459–464, <https://doi.org/10.1038/nclimate2550>, 2015.
- 1793 Liu, Y., Parolari, A. J., Kumar, M., Huang, C.-W., Katul, G. G., and Porporato, A.: Increasing atmospheric humidity and CO₂
1794 concentration alleviate forest mortality risk, *PNAS*, 114, 9918–9923, <https://doi.org/10.1073/pnas.1704811114>, 2017.
- 1795 Long, S. P., Postl, W. F., and Bolhár-Nordenkampf, H. R.: Quantum yields for uptake of carbon dioxide in C₃ vascular
1796 plants of contrasting habitats and taxonomic groupings, *Planta*, 189, 226–234, <https://doi.org/10.1007/BF00195081>,
1797 1993.
- 1798 Longo, M., Knox, R. G., Medvigy, D. M., Levine, N. M., Dietze, M. C., Kim, Y., Swann, A. L. S., Zhang, K., Rollinson, C.
1799 R., Bras, R. L., Wofsy, S. C., and Moorcroft, P. R.: The biophysics, ecology, and biogeochemistry of functionally diverse,
1800 vertically and horizontally heterogeneous ecosystems: the Ecosystem Demography model, version 2.2 – Part 1: Model
1801 description, *Geoscientific Model Development*, 12, 4309–4346, <https://doi.org/10.5194/gmd-12-4309-2019>, 2019.
- 1802 Loubry, D.: La phénologie des arbres caducifoliés en forêt guyanaise (5° de latitude nord) : illustration d'un déterminisme à
1803 composantes endogène et exogène, *Can. J. Bot.*, 72, 1843–1857, <https://doi.org/10.1139/b94-226>, 1994.
- 1804 Maclean, I. M. D. and Klings, D. H.: Microclimc: A mechanistic model of above, below and within-canopy microclimate,
1805 *Ecological Modelling*, 451, 109567, <https://doi.org/10.1016/j.ecolmodel.2021.109567>, 2021.
- 1806 Mahnken, M., Cailleret, M., Collalti, A., Trotta, C., Biondo, C., D'Andrea, E., Dalmonech, D., Marano, G., Mäkelä, A.,
1807 Minunno, F., Peltoniemi, M., Trotsiuk, V., Nadal-Sala, D., Sabaté, S., Vallet, P., Aussenac, R., Cameron, D. R., Bohn, F.
1808 J., Grote, R., Augustynczyk, A. L. D., Yousefpour, R., Huber, N., Bugmann, H., Merganičová, K., Merganic, J., Valent, P.,
1809 Lasch-Born, P., Hartig, F., Vega del Valle, I. D., Volkholz, J., Gutsch, M., Matteucci, G., Krejza, J., Ibrom, A., Meesenburg,
1810 H., Rötzer, T., van der Maaten-Theunissen, M., van der Maaten, E., and Reyer, C. P. O.: Accuracy, realism and general
1811 applicability of European forest models, *Global Change Biology*, 28, 6921–6943, <https://doi.org/10.1111/gcb.16384>, 2022.
- 1812 Malhi, Y.: The productivity, metabolism and carbon cycle of tropical forest vegetation, *Journal of Ecology*, 100, 65–75,
1813 <https://doi.org/10.1111/j.1365-2745.2011.01916.x>, 2012.



- 1814 Malhi, Y., Dougherty, C., and Galbraith, D.: The allocation of ecosystem net primary productivity in tropical forests,
1815 Philosophical Transactions of the Royal Society of London B: Biological Sciences, 366, 3225–3245,
1816 <https://doi.org/10.1098/rstb.2011.0062>, 2011.
- 1817 Manabe, S.: Climate and the ocean circulation: I. The atmospheric circulation and the hydrology of the earth's surface, *Mon.*
1818 *Wea. Rev.*, 97, 739–774, [https://doi.org/10.1175/1520-0493\(1969\)097<0739:CATOC>2.3.CO;2](https://doi.org/10.1175/1520-0493(1969)097<0739:CATOC>2.3.CO;2), 1969.
- 1819 Manoli, G., Ivanov, V. Y., and Fatichi, S.: Dry-Season Greening and Water Stress in Amazonia: The Role of Modeling Leaf
1820 Phenology, *Journal of Geophysical Research: Biogeosciences*, 123, 1909–1926, <https://doi.org/10.1029/2017JG004282>,
1821 2018.
- 1822 Manzoni, S.: Integrating plant hydraulics and gas exchange along the drought-response trait spectrum, *Tree Physiol*, tpu088,
1823 <https://doi.org/10.1093/treephys/tpu088>, 2014.
- 1824 Maréchaux, I. and Chave, J.: An individual-based forest model to jointly simulate carbon and tree diversity in Amazonia:
1825 description and applications, *Ecol Monogr*, 87, 632–664, <https://doi.org/10.1002/ecm.1271>, 2017.
- 1826 Maréchaux, I., Bartlett, M. K., Sack, L., Baraloto, C., Engel, J., Joetzier, E., and Chave, J.: Drought tolerance as predicted by
1827 leaf water potential at turgor loss point varies strongly across species within an Amazonian forest, *Funct Ecol*, 29, 1268–
1828 1277, <https://doi.org/10.1111/1365-2435.12452>, 2015.
- 1829 Maréchaux, I., Bartlett, M. K., Gaucher, P., Sack, L., and Chave, J.: Causes of variation in leaf-level drought tolerance within
1830 an Amazonian forest, *Journal of Plant Hydraulics*, 3, e004, 2016.
- 1831 Maréchaux, I., Bonal, D., Bartlett, M. K., Burban, B., Coste, S., Courtois, E. A., Dulormne, M., Goret, J.-Y., Mira, E., Mirabel,
1832 A., Sack, L., Stahl, C., and Chave, J.: Dry-season decline in tree sapflux is correlated with leaf turgor loss point in a tropical
1833 rainforest, *Functional Ecology*, 32, 2285–2297, <https://doi.org/10.1111/1365-2435.13188>, 2018.
- 1834 Maréchaux, I., Saint-André, L., Bartlett, M. K., Sack, L., and Chave, J.: Leaf drought tolerance cannot be inferred from classic
1835 leaf traits in a tropical rainforest, *Journal of Ecology*, 108, 1030–1045, <https://doi.org/10.1111/1365-2745.13321>, 2020.
- 1836 Maréchaux, I., Langerwisch, F., Huth, A., Bugmann, H., Morin, X., Reyer, C. P. O., Seidl, R., Collalti, A., Paula, M. D. de,
1837 Fischer, R., Gutsch, M., Lexer, M. J., Lischke, H., Rammig, A., Rödig, E., Sakschewski, B., Taubert, F., Thonicke, K.,
1838 Vacchiano, G., and Bohn, F. J.: Tackling unresolved questions in forest ecology: The past and future role of simulation
1839 models, *Ecology and Evolution*, 11, 3746–3770, <https://doi.org/10.1002/ece3.7391>, 2021.
- 1840 Marthews, T. R., Malhi, Y., and Iwata, H.: Calculating downward longwave radiation under clear and cloudy conditions over
1841 a tropical lowland forest site: an evaluation of model schemes for hourly data, *Theor Appl Climatol*, 107, 461–477,
1842 <https://doi.org/10.1007/s00704-011-0486-9>, 2012.
- 1843 Marthews, T. R., Quesada, C. A., Galbraith, D. R., Malhi, Y., Mullins, C. E., Hodnett, M. G., and Dharssi, I.: High-resolution
1844 hydraulic parameter maps for surface soils in tropical South America, *Geoscientific Model Development*, 7, 711, 2014.
- 1845 Martínez-Vilalta, J., Sala, A., Asensio, D., Galiano, L., Hoch, G., Palacio, S., Piper, F. I., and Lloret, F.: Dynamics of non-
1846 structural carbohydrates in terrestrial plants: a global synthesis, *Ecol Monogr*, 86, 495–516,
1847 <https://doi.org/10.1002/ecm.1231>, 2016.



- 1848 Martin-StPaul, N., Delzon, S., and Cochard, H.: Plant resistance to drought depends on timely stomatal closure, *Ecol Lett*, 20,
1849 1437–1447, <https://doi.org/10.1111/ele.12851>, 2017.
- 1850 McDowell, N. G., Sapes, G., Pivovarov, A., Adams, H. D., Allen, C. D., Anderegg, W. R. L., Arend, M., Breshears, D. D.,
1851 Brodribb, T., Choat, B., Cochard, H., De Cáceres, M., De Kauwe, M. G., Grossiord, C., Hammond, W. M., Hartmann, H.,
1852 Hoch, G., Kahmen, A., Klein, T., Mackay, D. S., Mantova, M., Martínez-Vilalta, J., Medlyn, B. E., Mencuccini, M.,
1853 Nardini, A., Oliveira, R. S., Sala, A., Tissue, D. T., Torres-Ruiz, J. M., Trowbridge, A. M., Trugman, A. T., Wiley, E., and
1854 Xu, C.: Mechanisms of woody-plant mortality under rising drought, CO₂ and vapour pressure deficit, *Nat Rev Earth
1855 Environ*, 1–15, <https://doi.org/10.1038/s43017-022-00272-1>, 2022.
- 1856 McMahon, S. M., Harrison, S. P., Armbruster, W. S., Bartlein, P. J., Beale, C. M., Edwards, M. E., Kattge, J., Midgley, G.,
1857 Morin, X., and Prentice, I. C.: Improving assessment and modelling of climate change impacts on global terrestrial
1858 biodiversity, *Trends in Ecology & Evolution*, 26, 249–259, <https://doi.org/10.1016/j.tree.2011.02.012>, 2011.
- 1859 Medlyn, B. E., Robinson, A. P., Clement, R., and McMurtrie, R. E.: On the validation of models of forest CO₂ exchange using
1860 eddy covariance data: some perils and pitfalls, *Tree Physiol*, 25, 839–857, <https://doi.org/10.1093/treephys/25.7.839>, 2005.
- 1861 Medlyn, B. E., Pepper, D. A., O’Grady, A. P., and Keith, H.: Linking leaf and tree water use with an individual-tree model,
1862 *Tree Physiol*, 27, 1687–1699, <https://doi.org/10.1093/treephys/27.12.1687>, 2007.
- 1863 Medlyn, B. E., Duursma, R. A., Eamus, D., Ellsworth, D. S., Prentice, I. C., Barton, C. V. M., Crous, K. Y., De Angelis, P.,
1864 Freeman, M., and Wingate, L.: Reconciling the optimal and empirical approaches to modelling stomatal conductance,
1865 *Global Change Biology*, 17, 2134–2144, <https://doi.org/10.1111/j.1365-2486.2010.02375.x>, 2011.
- 1866 Medlyn, B. E., Zaehle, S., De Kauwe, M. G., Walker, A. P., Dietze, M. C., Hanson, P. J., Hickler, T., Jain, A. K., Luo, Y.,
1867 Parton, W., Prentice, I. C., Thornton, P. E., Wang, S., Wang, Y.-P., Weng, E., Iversen, C. M., McCarthy, H. R., Warren, J.
1868 M., Oren, R., and Norby, R. J.: Using ecosystem experiments to improve vegetation models, *Nature Clim. Change*, 5, 528–
1869 534, <https://doi.org/10.1038/nclimate2621>, 2015.
- 1870 Medlyn, B. E., De Kauwe, M. G., Zaehle, S., Walker, A. P., Duursma, R. A., Luus, K., Mishurov, M., Pak, B., Smith, B.,
1871 Wang, Y.-P., Yang, X., Crous, K. Y., Drake, J. E., Gimeno, T. E., Macdonald, C. A., Norby, R. J., Power, S. A., Tjoelker,
1872 M. G., and Ellsworth, D. S.: Using models to guide field experiments: a priori predictions for the CO₂ response of a
1873 nutrient- and water-limited native Eucalypt woodland, *Glob Change Biol*, 22, 2834–2851,
1874 <https://doi.org/10.1111/gcb.13268>, 2016.
- 1875 van der Meer, P. J. and Bongers, F.: Patterns of tree-fall and branch-fall in a tropical rain forest in French Guiana, *Journal of
1876 Ecology*, 84, 19–29, <https://doi.org/10.2307/2261696>, 1996.
- 1877 Meinzer, F. C., Andrade, J. L., Goldstein, G., Holbrook, N. M., Cavelier, J., and Jackson, P.: Control of transpiration from the
1878 upper canopy of a tropical forest: the role of stomatal, boundary layer and hydraulic architecture components, *Plant, Cell
1879 & Environment*, 20, 1242–1252, <https://doi.org/10.1046/j.1365-3040.1997.d01-26.x>, 1997.



- 1880 Meinzer, F. C., Woodruff, D. R., Marias, D. E., Smith, D. D., McCulloh, K. A., Howard, A. R., and Magedman, A. L.: Mapping
1881 ‘hydroscares’ along the iso- to anisohydric continuum of stomatal regulation of plant water status, *Ecol Lett*, 19, 1343–
1882 1352, <https://doi.org/10.1111/ele.12670>, 2016.
- 1883 Meir, P. and Grace, J.: Scaling relationships for woody tissue respiration in two tropical rain forests, *Plant, Cell & Environment*,
1884 25, 963–973, <https://doi.org/10.1046/j.1365-3040.2002.00877.x>, 2002.
- 1885 Meir, P., Grace, J., and Miranda, A. C.: Leaf respiration in two tropical rainforests: constraints on physiology by phosphorus,
1886 nitrogen and temperature, *Functional Ecology*, 15, 378–387, <https://doi.org/10.1046/j.1365-2435.2001.00534.x>, 2001.
- 1887 Meir, P., Cox, P., and Grace, J.: The influence of terrestrial ecosystems on climate, *Trends in Ecology & Evolution*, 21, 254–
1888 260, <https://doi.org/10.1016/j.tree.2006.03.005>, 2006.
- 1889 Mencuccini, M., Martínez-Vilalta, J., Vanderklein, D., Hamid, H. A., Korakaki, E., Lee, S., and Michiels, B.: Size-mediated
1890 ageing reduces vigour in trees, *Ecology Letters*, 8, 1183–1190, <https://doi.org/10.1111/j.1461-0248.2005.00819.x>, 2005.
- 1891 Menezes, J., Garcia, S., Grandis, A., Nascimento, H., Domingues, T. F., Guedes, A. V., Aleixo, I., Camargo, P., Campos, J.,
1892 Damasceno, A., Dias-Silva, R., Fleischer, K., Kruijt, B., Cordeiro, A. L., Martins, N. P., Meir, P., Norby, R. J., Pereira, I.,
1893 Portela, B., Rammig, A., Ribeiro, A. G., Lapola, D. M., and Quesada, C. A.: Changes in leaf functional traits with leaf age:
1894 when do leaves decrease their photosynthetic capacity in Amazonian trees?, *Tree Physiology*, tpab042,
1895 <https://doi.org/10.1093/treephys/tpab042>, 2021.
- 1896 Mercado, L. M., Lloyd, J., Dolman, A. J., Sitch, S., and Patiño, S.: Modelling basin-wide variations in Amazon forest
1897 productivity – Part 1: model calibration, evaluation and upscaling functions for canopy photosynthesis, *Biogeosciences*, 6,
1898 1247–1272, <https://doi.org/10.5194/bg-6-1247-2009>, 2009.
- 1899 Mercado, L. M., Patiño, S., Domingues, T. F., Fyllas, N. M., Weedon, G. P., Sitch, S., Quesada, C. A., Phillips, O. L., Aragão,
1900 L. E. O. C., Malhi, Y., Dolman, A. J., Restrepo-Coupe, N., Saleska, S. R., Baker, T. R., Almeida, S., Higuchi, N., and
1901 Lloyd, J.: Variations in Amazon forest productivity correlated with foliar nutrients and modelled rates of photosynthetic
1902 carbon supply, *Phil. Trans. R. Soc. B*, 366, 3316–3329, <https://doi.org/10.1098/rstb.2011.0045>, 2011.
- 1903 Merganičová, K., Merganič, J., Lehtonen, A., Vacchiano, G., Zorana, M., Ostrogović, S., Augustynczyk, A. L. D., Grote, R.,
1904 Kyselová, I., Mäkelä, A., Yousefpour, R., Krejza, J., Collalti, A., and Reyer, C.: Forest carbon allocation modelling under
1905 climate change, *Tree Physiology*, <https://doi.org/10.1093/treephys/tpz105>, 2019.
- 1906 Merlin, O., Stefan, V. G., Amazirh, A., Chanzy, A., Ceschia, E., Er-Raki, S., Gentine, P., Tallec, T., Ezzahar, J., Bircher, S.,
1907 Beringer, J., and Khabba, S.: Modeling soil evaporation efficiency in a range of soil and atmospheric conditions using a
1908 meta-analysis approach, *Water Resources Research*, 52, 3663–3684, <https://doi.org/10.1002/2015WR018233>, 2016.
- 1909 Metcalfe, D. B., Meir, P., Aragão, L. E. O. C., Costa, A. C. L. da, Braga, A. P., Gonçalves, P. H. L., Junior, J. de A. S.,
1910 Almeida, S. S. de, Dawson, L. A., Malhi, Y., and Williams, M.: The effects of water availability on root growth and
1911 morphology in an Amazon rainforest, *Plant and Soil*, 311, 189–199, <https://doi.org/10.1007/s11104-008-9670-9>, 2008.



- 1912 Mokany, K., Ferrier, S., Connolly, S. R., Dunstan, P. K., Fulton, E. A., Harfoot, M. B., Harwood, T. D., Richardson, A. J.,
1913 Roxburgh, S. H., Scharlemann, J. P. W., Tittensor, D. P., Westcott, D. A., and Wintle, B. A.: Integrating modelling of
1914 biodiversity composition and ecosystem function, *Oikos*, 125, 10–19, <https://doi.org/10.1111/oik.02792>, 2016.
- 1915 Moles, A. T. and Westoby, M.: Seed size and plant strategy across the whole life cycle, *Oikos*, 113, 91–105,
1916 <https://doi.org/10.1111/j.0030-1299.2006.14194.x>, 2006.
- 1917 Moles, A. T., Falster, D. S., Leishman, M. R., and Westoby, M.: Small-seeded species produce more seeds per square metre
1918 of canopy per year, but not per individual per lifetime, *Journal of Ecology*, 92, 384–396, <https://doi.org/10.1111/j.0022-0477.2004.00880.x>, 2004.
- 1920 Moorcroft, P. R.: Recent advances in ecosystem-atmosphere interactions: an ecological perspective, *Proceedings of the Royal*
1921 *Society of London B: Biological Sciences*, 270, 1215–1227, <https://doi.org/10.1098/rspb.2002.2251>, 2003.
- 1922 Moorcroft, P. R.: How close are we to a predictive science of the biosphere?, *Trends in Ecology & Evolution*, 21, 400–407,
1923 <https://doi.org/10.1016/j.tree.2006.04.009>, 2006.
- 1924 Moorcroft, P. R., Hurtt, G. C., and Pacala, S. W.: A method for scaling vegetation dynamics: the ecosystem demography model
1925 (ed), *Ecological Monographs*, 71, 557–586, [https://doi.org/10.1890/0012-9615\(2001\)071\[0557:AMFSVD\]2.0.CO;2](https://doi.org/10.1890/0012-9615(2001)071[0557:AMFSVD]2.0.CO;2),
1926 2001.
- 1927 Morin, X. and Lechowicz, M. J.: Contemporary perspectives on the niche that can improve models of species range shifts
1928 under climate change, *Biology Letters*, 4, 573–576, <https://doi.org/10.1098/rsbl.2008.0181>, 2008.
- 1929 Morin, X. and Thuiller, W.: Comparing niche-and process-based models to reduce prediction uncertainty in species range
1930 shifts under climate change, *Ecology*, 90, 1301–1313, 2009.
- 1931 Mualem, Y.: A new model for predicting the hydraulic conductivity of unsaturated porous media, *Water Resources Research*,
1932 12, 513–522, <https://doi.org/10.1029/WR012i003p00513>, 1976.
- 1933 Muir, C. D.: Making pore choices: repeated regime shifts in stomatal ratio, *Proceedings of the Royal Society B: Biological*
1934 *Sciences*, 282, 20151498, <https://doi.org/10.1098/rspb.2015.1498>, 2015.
- 1935 Muller, B., Pantin, F., Génard, M., Turc, O., Freixes, S., Piques, M., and Gibon, Y.: Water deficits uncouple growth from
1936 photosynthesis, increase C content, and modify the relationships between C and growth in sink organs, *J. Exp. Bot.*, erq438,
1937 <https://doi.org/10.1093/jxb/erq438>, 2011.
- 1938 Muller-Landau, H. C., Wright, S. J., Calderón, O., Condit, R., and Hubbell, S. P.: Interspecific variation in primary seed
1939 dispersal in a tropical forest, *Journal of Ecology*, 96, 653–667, <https://doi.org/10.1111/j.1365-2745.2008.01399.x>, 2008.
- 1940 Muñoz-Sabater, J., Dutra, E., Agustí-Panareda, A., Albergel, C., Arduini, G., Balsamo, G., Boussetta, S., Choulga, M.,
1941 Harrigan, S., Hersbach, H., Martens, B., Miralles, D. G., Piles, M., Rodríguez-Fernández, N. J., Zsoter, E., Buontempo, C.,
1942 and Thépaut, J.-N.: ERA5-Land: a state-of-the-art global reanalysis dataset for land applications, *Earth System Science*
1943 *Data*, 13, 4349–4383, <https://doi.org/10.5194/essd-13-4349-2021>, 2021.
- 1944 Naudts, K., Ryder, J., McGrath, M. J., Otto, J., Chen, Y., Valade, A., Bellasen, V., Berhongaray, G., Bönisch, G., Campioli,
1945 M., Ghattas, J., De Groote, T., Haverd, V., Kattge, J., MacBean, N., Maignan, F., Merilä, P., Penuelas, J., Peylin, P., Pinty,



- 1946 B., Pretzsch, H., Schulze, E. D., Solyga, D., Vuichard, N., Yan, Y., and Luyssaert, S.: A vertically discretised canopy
1947 description for ORCHIDEE (SVN r2290) and the modifications to the energy, water and carbon fluxes, *Geosci. Model*
1948 *Dev.*, 8, 2035–2065, <https://doi.org/10.5194/gmd-8-2035-2015>, 2015.
- 1949 Nemetschek, D., Derroire, G., Marcon, E., Aubry-Kientz, M., Auer, J., Badouard, V., Baraloto, C., Bauman, D., Le Blaye, Q.,
1950 Boisseaux, M., Bonal, D., Coste, S., Dardevet, E., Heuret, P., Hietz, P., Levionnois, S., Maréchaux, I., McMahon, S. M.,
1951 Stahl, C., Vleminckx, J., Wanek, W., Ziegler, C., and Fortunel, C.: Climate anomalies and neighbourhood crowding interact
1952 in shaping tree growth in old-growth and selectively logged tropical forests, *Journal of Ecology*, 112, 590–612,
1953 <https://doi.org/10.1111/1365-2745.14256>, 2024.
- 1954 Nemetschek, D., Fortunel, C., Marcon, E., Auer, J., Badouard, V., Baraloto, C., Boisseaux, M., Bonal, D., Coste, S.,
1955 Dardevette, E., Heuret, P., Hietz, P., Levionnois, S., Maréchaux, I., Stahl, C., Vleminckx, J., Wanek, W., Ziegler, C., and
1956 Derroire, G.: Love thy neighbour? Tropical tree growth and its response to climate anomalies is mediated by neighbourhood
1957 hierarchy and dissimilarity in carbon and water related traits., <https://doi.org/10.22541/au.171366417.71658960/v1>, 21
1958 April 2024.
- 1959 Nepstad, D. C., de Carvalho, C. R., Davidson, E. A., Jipp, P. H., Lefebvre, P. A., Negreiros, G. H., da Silva, E. D., Stone, T.
1960 A., Trumbore, S. E., and Vieira, S.: The role of deep roots in the hydrological and carbon cycles of Amazonian forests and
1961 pastures, *Nature*, 372, 666–669, <https://doi.org/10.1038/372666a0>, 1994.
- 1962 Newman, E. I.: Resistance to Water Flow in Soil and Plant. I. Soil Resistance in Relation to Amounts of Root: Theoretical
1963 Estimates, *Journal of Applied Ecology*, 6, 1–12, <https://doi.org/10.2307/2401297>, 1969.
- 1964 Nicolini, E., Beauchêne, J., de la Vallée, B. L., Ruelle, J., Mangenet, T., and Heuret, P.: Dating branch growth units in a
1965 tropical tree using morphological and anatomical markers: the case of *Parkia velutina* Benoist (Mimosoïdeae), *Annals of*
1966 *Forest Science*, 69, 543–555, <https://doi.org/10.1007/s13595-011-0172-1>, 2012.
- 1967 Norby, R. J., De Kauwe, M. G., Domingues, T. F., Duursma, R. A., Ellsworth, D. S., Goll, D. S., Lapola, D. M., Luus, K. A.,
1968 MacKenzie, A. R., Medlyn, B. E., Pavlick, R., Rammig, A., Smith, B., Thomas, R., Thonicke, K., Walker, A. P., Yang,
1969 X., and Zaehle, S.: Model–data synthesis for the next generation of forest free-air CO₂ enrichment (FACE) experiments,
1970 *New Phytol*, 209, 17–28, <https://doi.org/10.1111/nph.13593>, 2016.
- 1971 Norden, N., Chave, J., Belbenoit, P., Caubère, A., Châtelet, P., Forget, P.-M., and Thébaud, C.: Mast fruiting is a frequent
1972 strategy in woody species of eastern South America, *PLOS ONE*, 2, e1079, <https://doi.org/10.1371/journal.pone.0001079>,
1973 2007.
- 1974 Novick, K. A., Ficklin, D. L., Stoy, P. C., Williams, C. A., Bohrer, G., Oishi, A. C., Papuga, S. A., Blanken, P. D., Noormets,
1975 A., Sulman, B. N., Scott, R. L., Wang, L., and Phillips, R. P.: The increasing importance of atmospheric demand for
1976 ecosystem water and carbon fluxes, *Nature Climate Change*, 6, 1023–1027, <https://doi.org/10.1038/nclimate3114>, 2016.
- 1977 Novick, K. A., Ficklin, D. L., Baldocchi, D., Davis, K. J., Ghezzehei, T. A., Konings, A. G., MacBean, N., Raoult, N., Scott,
1978 R. L., Shi, Y., Sulman, B. N., and Wood, J. D.: Confronting the water potential information gap, *Nat. Geosci.*, 15, 158–
1979 164, <https://doi.org/10.1038/s41561-022-00909-2>, 2022.



- 1980 Nunes, M. H., Camargo, J. L. C., Vincent, G., Calders, K., Oliveira, R. S., Huete, A., Mendes de Moura, Y., Nelson, B., Smith,
1981 M. N., Stark, S. C., and Maeda, E. E.: Forest fragmentation impacts the seasonality of Amazonian evergreen canopies, *Nat*
1982 *Commun*, 13, 917, <https://doi.org/10.1038/s41467-022-28490-7>, 2022.
- 1983 Ogée, J., Brunet, Y., Loustau, D., Berbigier, P., and Delzon, S.: MuSICA, a CO₂, water and energy multilayer, multileaf pine
1984 forest model: evaluation from hourly to yearly time scales and sensitivity analysis, *Global Change Biology*, 9, 697–717,
1985 <https://doi.org/10.1046/j.1365-2486.2003.00628.x>, 2003.
- 1986 Oleson, K. W., Niu, G.-Y., Yang, Z.-L., Lawrence, D. M., Thornton, P. E., Lawrence, P. J., Stöckli, R., Dickinson, R. E.,
1987 Bonan, G. B., Levis, S., Dai, A., and Qian, T.: Improvements to the Community Land Model and their impact on the
1988 hydrological cycle, *J. Geophys. Res.*, 113, G01021, <https://doi.org/10.1029/2007JG000563>, 2008.
- 1989 Oliveira, R. S., Dawson, T. E., Burgess, S. S. O., and Nepstad, D. C.: Hydraulic redistribution in three Amazonian trees,
1990 *Oecologia*, 145, 354–363, <https://doi.org/10.1007/s00442-005-0108-2>, 2005.
- 1991 d’Orgeval, T., Polcher, J., and de Rosnay, P.: Sensitivity of the West African hydrological cycle in ORCHIDEE to infiltration
1992 processes, *Hydrol. Earth Syst. Sci.*, 12, 1387–1401, <https://doi.org/10.5194/hess-12-1387-2008>, 2008.
- 1993 Pacala, S. W. and Rees, M.: Models Suggesting Field Experiments to Test Two Hypotheses Explaining Successional Diversity,
1994 *The American Naturalist*, 152, 729–737, <https://doi.org/10.1086/286203>, 1998.
- 1995 Paine, C. E. T., Deasey, A., and Duthie, A. B.: Towards the general mechanistic prediction of community dynamics, *Functional*
1996 *Ecology*, 32, 1681–1692, <https://doi.org/10.1111/1365-2435.13096>, 2018.
- 1997 Pan, Y., Birdsey, R. A., Fang, J., Houghton, R., Kauppi, P. E., Kurz, W. A., Phillips, O. L., Shvidenko, A., Lewis, S. L.,
1998 Canadell, J. G., Ciais, P., Jackson, R. B., Pacala, S. W., McGuire, A. D., Piao, S., Rautiainen, A., Sitch, S., and Hayes, D.:
1999 A Large and Persistent Carbon Sink in the World’s Forests, *Science*, 333, 988–993,
2000 <https://doi.org/10.1126/science.1201609>, 2011.
- 2001 Pantin, F., Simonneau, T., and Muller, B.: Coming of leaf age: control of growth by hydraulics and metabolics during leaf
2002 ontogeny, *New Phytologist*, 196, 349–366, <https://doi.org/10.1111/j.1469-8137.2012.04273.x>, 2012.
- 2003 Paschalis, A., Fatichi, S., Zscheischler, J., Ciais, P., Bahn, M., Boysen, L., Chang, J., De Kauwe, M., Estiarte, M., Goll, D.,
2004 Hanson, P. J., Harper, A. B., Hou, E., Kigel, J., Knapp, A. K., Larsen, K. S., Li, W., Lienert, S., Luo, Y., Meir, P., Nabel,
2005 J. E. M. S., Ogaya, R., Parolari, A. J., Peng, C., Peñuelas, J., Pongratz, J., Rambal, S., Schmidt, I. K., Shi, H., Sternberg,
2006 M., Tian, H., Tschumi, E., Ukkola, A., Vicca, S., Viovy, N., Wang, Y.-P., Wang, Z., Williams, K., Wu, D., and Zhu, Q.:
2007 Rainfall manipulation experiments as simulated by terrestrial biosphere models: Where do we stand?, *Global Change*
2008 *Biology*, 26, 3336–3355, <https://doi.org/10.1111/gcb.15024>, 2020.
- 2009 Paschalis, A., De Kauwe, M. G., Sabot, M., and Fatichi, S.: When do plant hydraulics matter in terrestrial biosphere
2010 modelling?, *Global Change Biology*, 30, e17022, <https://doi.org/10.1111/gcb.17022>, 2024.
- 2011 Pavlick, R., Drewry, D. T., Bohn, K., Reu, B., and Kleidon, A.: The Jena Diversity-Dynamic Global Vegetation Model (JeDi-
2012 DGVM): a diverse approach to representing terrestrial biogeography and biogeochemistry based on plant functional
2013 trade-offs, *Biogeosciences*, 10, 4137–4177, <https://doi.org/10.5194/bg-10-4137-2013>, 2013.



- 2014 Peters, R. L., Kaewmano, A., Fu, P.-L., Fan, Z.-X., Sterck, F., Steppe, K., and Zuidema, P. A.: High vapour pressure deficit
2015 enhances turgor limitation of stem growth in an Asian tropical rainforest tree, *Plant, Cell & Environment*, 46, 2747–2762,
2016 <https://doi.org/10.1111/pce.14661>, 2023.
- 2017 Picard, N. and Franc, A.: Are ecological groups of species optimal for forest dynamics modelling?, *Ecological Modelling*, 163,
2018 175–186, [https://doi.org/10.1016/S0304-3800\(03\)00010-3](https://doi.org/10.1016/S0304-3800(03)00010-3), 2003.
- 2019 Picard, N., Köhler, P., Mortier, F., and Gourlet-Fleury, S.: A comparison of five classifications of species into functional
2020 groups in tropical forests of French Guiana, *Ecological Complexity*, 11, 75–83,
2021 <https://doi.org/10.1016/j.ecocom.2012.03.003>, 2012.
- 2022 Pitman, A. J.: The evolution of, and revolution in, land surface schemes designed for climate models, *Int. J. Climatol.*, 23,
2023 479–510, <https://doi.org/10.1002/joc.893>, 2003.
- 2024 Poggio, L., de Sousa, L. M., Batjes, N. H., Heuvelink, G. B. M., Kempen, B., Ribeiro, E., and Rossiter, D.: SoilGrids 2.0:
2025 producing soil information for the globe with quantified spatial uncertainty, *SOIL*, 7, 217–240, [https://doi.org/10.5194/soil-](https://doi.org/10.5194/soil-7-217-2021)
2026 [7-217-2021](https://doi.org/10.5194/soil-7-217-2021), 2021.
- 2027 Poorter, L., Bongers, L., and Bongers, F.: Architecture of 54 moist-forest tree species: traits, trade-offs, and functional groups,
2028 *Ecology*, 87, 1289–1301, [https://doi.org/10.1890/0012-9658\(2006\)87\[1289:AOMTST\]2.0.CO;2](https://doi.org/10.1890/0012-9658(2006)87[1289:AOMTST]2.0.CO;2), 2006.
- 2029 Poorter, L., Wright, S. J., Paz, H., Ackerly, D. D., Condit, R., Ibarra-Manríquez, G., Harms, K. E., Licona, J. C., Martínez-
2030 Ramos, M., Mazer, S. J., Muller-Landau, H. C., Peña-Claros, M., Webb, C. O., and Wright, I. J.: Are functional traits good
2031 predictors of demographic rates? Evidence from five Neotropical forests, *Ecology*, 89, 1908–1920,
2032 <https://doi.org/10.1890/07-0207.1>, 2008.
- 2033 Poorter, L., Oberbauer, S. F., and Clark, D. B.: Leaf optical properties along a vertical gradient in a tropical rain forest
2034 canopy in Costa Rica, *American Journal of Botany*, 82, 1257–1263, <https://doi.org/10.2307/2446248>, 1995.
- 2035 Poorter, L., van der Sande, M. T., Thompson, J., Arets, E. J. M. M., Alarcón, A., Álvarez-Sánchez, J., Ascarrunz, N., Balvanera,
2036 P., Barajas-Guzmán, G., Boit, A., Bongers, F., Carvalho, F. A., Casanoves, F., Cornejo-Tenorio, G., Costa, F. R. C., de
2037 Castilho, C. V., Duivenvoorden, J. F., Dutrieux, L. P., Enquist, B. J., Fernández-Méndez, F., Finegan, B., Gormley, L. H.
2038 L., Healey, J. R., Hoosbeek, M. R., Ibarra-Manríquez, G., Junqueira, A. B., Levis, C., Licona, J. C., Lisboa, L. S.,
2039 Magnusson, W. E., Martínez-Ramos, M., Martínez-Yrizar, A., Martorano, L. G., Maskell, L. C., Mazzei, L., Meave, J. A.,
2040 Mora, F., Muñoz, R., Nytch, C., Pansonato, M. P., Parr, T. W., Paz, H., Pérez-García, E. A., Rentería, L. Y., Rodríguez-
2041 Velazquez, J., Rozendaal, D. M. A., Ruschel, A. R., Sakschewski, B., Salgado-Negret, B., Schiatti, J., Simões, M., Sinclair,
2042 F. L., Souza, P. F., Souza, F. C., Stropp, J., ter Steege, H., Swenson, N. G., Thonicke, K., Toledo, M., Uriarte, M., van der
2043 Hout, P., Walker, P., Zamora, N., and Peña-Claros, M.: Diversity enhances carbon storage in tropical forests, *Global
2044 Ecology and Biogeography*, 24, 1314–1328, <https://doi.org/10.1111/geb.12364>, 2015.
- 2045 Poorter, L., Amissah, L., Bongers, F., Hordijk, I., Kok, J., Laurance, S. G. W., Lohbeck, M., Martínez-Ramos, M., Matsuo,
2046 T., Meave, J. A., Muñoz, R., Peña-Claros, M., and van der Sande, M. T.: Successional theories, *Biological Reviews*, 98,
2047 2049–2077, <https://doi.org/10.1111/brv.12995>, 2023.



- 2048 Porté, A. and Bartelink, H. H.: Modelling mixed forest growth: a review of models for forest management, *Ecological*
2049 *Modelling*, 150, 141–188, [https://doi.org/10.1016/S0304-3800\(01\)00476-8](https://doi.org/10.1016/S0304-3800(01)00476-8), 2002.
- 2050 Poulter, B., Ciais, P., Hodson, E., Lischke, H., Maignan, F., Plummer, S., and Zimmermann, N. E.: Plant functional type
2051 mapping for earth system models, *Geosci. Model Dev.*, 4, 993–1010, <https://doi.org/10.5194/gmd-4-993-2011>, 2011.
- 2052 Powell, T. L., Galbraith, D. R., Christoffersen, B. O., Harper, A., Imbuzeiro, H. M. A., Rowland, L., Almeida, S., Brando, P.
2053 M., da Costa, A. C. L., Costa, M. H., Levine, N. M., Malhi, Y., Saleska, S. R., Sotta, E., Williams, M., Meir, P., and
2054 Moorcroft, P. R.: Confronting model predictions of carbon fluxes with measurements of Amazon forests subjected to
2055 experimental drought, *New Phytologist*, 200, 350–365, <https://doi.org/10.1111/nph.12390>, 2013.
- 2056 Powell, T. L., Wheeler, J. K., Oliveira, A. A. R. de, Costa, A. C. L. da, Saleska, S. R., Meir, P., and Moorcroft, P. R.:
2057 Differences in xylem and leaf hydraulic traits explain differences in drought tolerance among mature Amazon rainforest
2058 trees, *Global Change Biology*, 23, 4280–4293, <https://doi.org/10.1111/gcb.13731>, 2017.
- 2059 Prentice, I. C., Bondeau, A., Cramer, W., Harrison, S. P., Hickler, T., Lucht, W., Sitch, S., Smith, B., and Sykes, M. T.:
2060 Dynamic Global Vegetation Modeling: Quantifying Terrestrial Ecosystem Responses to Large-Scale Environmental
2061 Change, in: *Terrestrial ecosystems in a changing world*, edited by: Canadell, J. G., Pataki, D. E., and Pitelka, L. F., Springer
2062 Berlin Heidelberg, 175–192, 2007.
- 2063 Prentice, I. C., Liang, X., Medlyn, B. E., and Wang, Y.-P.: Reliable, robust and realistic: the three R’s of next-generation land-
2064 surface modelling, *Atmos. Chem. Phys.*, 15, 5987–6005, <https://doi.org/10.5194/acp-15-5987-2015>, 2015.
- 2065 Purves, D. and Pacala, S.: Predictive models of forest dynamics, *Science*, 320, 1452–1453,
2066 <https://doi.org/10.1126/science.1155359>, 2008.
- 2067 Qie, L., Lewis, S. L., Sullivan, M. J. P., Lopez-Gonzalez, G., Pickavance, G. C., Sunderland, T., Ashton, P., Hubau, W., Salim,
2068 K. A., Aiba, S.-I., Banin, L. F., Berry, N., Brearley, F. Q., Burslem, D. F. R. P., Dančák, M., Davies, S. J., Fredriksson, G.,
2069 Hamer, K. C., Hédli, R., Kho, L. K., Kitayama, K., Krisnawati, H., Lhota, S., Malhi, Y., Maycock, C., Metali, F., Mirmanto,
2070 E., Nagy, L., Nilus, R., Ong, R., Pendry, C. A., Poulsen, A. D., Primack, R. B., Rutishauser, E., Samsedin, I., Saragih, B.,
2071 Sist, P., Slik, J. W. F., Sukri, R. S., Svátek, M., Tan, S., Tjoa, A., Nieuwstadt, M. van, Vernimmen, R. R. E., Yassir, I.,
2072 Kidd, P. S., Fitriadi, M., Ideris, N. K. H., Serudin, R. M., Lim, L. S. A., Saparudin, M. S., and Phillips, O. L.: Long-term
2073 carbon sink in Borneo’s forests halted by drought and vulnerable to edge effects, *Nature Communications*, 8, 1966,
2074 <https://doi.org/10.1038/s41467-017-01997-0>, 2017.
- 2075 Rau, E.-P., Fischer, F., Joetjzer, É., Maréchaux, I., Sun, I. F., and Chave, J.: Transferability of an individual- and trait-based
2076 forest dynamics model: A test case across the tropics, *Ecological Modelling*, 463, 109801,
2077 <https://doi.org/10.1016/j.ecolmodel.2021.109801>, 2022a.
- 2078 Rau, E.-P., Gardiner, B. A., Fischer, F. J., Maréchaux, I., Joetjzer, E., Sun, I.-F., and Chave, J.: Wind Speed Controls Forest
2079 Structure in a Subtropical Forest Exposed to Cyclones: A Case Study Using an Individual-Based Model, *Frontiers in*
2080 *Forests and Global Change*, 5, 2022b.



- 2081 Restrepo-Coupe, N., da Rocha, H. R., Hutyra, L. R., da Araujo, A. C., Borma, L. S., Christoffersen, B., Cabral, O. M. R., de
2082 Camargo, P. B., Cardoso, F. L., da Costa, A. C. L., Fitzjarrald, D. R., Goulden, M. L., Kruijt, B., Maia, J. M. F., Malhi, Y.
2083 S., Manzi, A. O., Miller, S. D., Nobre, A. D., von Randow, C., Sá, L. D. A., Sakai, R. K., Tota, J., Wofsy, S. C., Zanchi,
2084 F. B., and Saleska, S. R.: What drives the seasonality of photosynthesis across the Amazon basin? A cross-site analysis of
2085 eddy flux tower measurements from the Brasil flux network, *Agricultural and Forest Meteorology*, 182–183, 128–144,
2086 <https://doi.org/10.1016/j.agrformet.2013.04.031>, 2013.
- 2087 Restrepo-Coupe, N., Levine, N. M., Christoffersen, B. O., Albert, L. P., Wu, J., Costa, M. H., Galbraith, D., Imbuzeiro, H.,
2088 Martins, G., da Araujo, A. C., Malhi, Y. S., Zeng, X., Moorcroft, P., and Saleska, S. R.: Do dynamic global vegetation
2089 models capture the seasonality of carbon fluxes in the Amazon basin? A data-model intercomparison, *Glob Change Biol*,
2090 23, 191–208, <https://doi.org/10.1111/gcb.13442>, 2017.
- 2091 Richards, L. A.: Capillary conduction of liquids through porous mediums, *Physics*, 1, 318–333,
2092 <https://doi.org/10.1063/1.1745010>, 1931.
- 2093 Riva, F. and Fahrig, L.: Landscape-scale habitat fragmentation is positively related to biodiversity, despite patch-scale
2094 ecosystem decay, *Ecology Letters*, 26, 268–277, <https://doi.org/10.1111/ele.14145>, 2023.
- 2095 Rödig, E., Cuntz, M., Heinke, J., Rammig, A., and Huth, A.: Spatial heterogeneity of biomass and forest structure of the
2096 Amazon rain forest: Linking remote sensing, forest modelling and field inventory, *Global Ecology and Biogeography*, 26,
2097 1292–1302, <https://doi.org/10.1111/geb.12639>, 2017.
- 2098 Rodriguez-Dominguez, C. M., Buckley, T. N., Egea, G., de Cires, A., Hernandez-Santana, V., Martorell, S., and Diaz-Espejo,
2099 A.: Most stomatal closure in woody species under moderate drought can be explained by stomatal responses to leaf turgor,
2100 *Plant, Cell & Environment*, 39, 2014–2026, <https://doi.org/10.1111/pce.12774>, 2016.
- 2101 Rodriguez-Iturbe, I., Porporato, A., Ridolfi, L., Isham, V., and Coxi, D. R.: Probabilistic modelling of water balance at a point:
2102 the role of climate, soil and vegetation, *Proceedings of the Royal Society of London A: Mathematical, Physical and*
2103 *Engineering Sciences*, 455, 3789–3805, <https://doi.org/10.1098/rspa.1999.0477>, 1999.
- 2104 Rogers, A., Medlyn, B. E., Dukes, J. S., Bonan, G., von Caemmerer, S., Dietze, M. C., Kattge, J., Leakey, A. D. B., Mercado,
2105 L. M., Niinemets, Ü., Prentice, I. C., Serbin, S. P., Sitch, S., Way, D. A., and Zachle, S.: A roadmap for improving the
2106 representation of photosynthesis in Earth system models, *New Phytol*, 213, 22–42, <https://doi.org/10.1111/nph.14283>,
2107 2017.
- 2108 Rosas, T., Mencuccini, M., Barba, J., Cochard, H., Saura-Mas, S., and Martínez-Vilalta, J.: Adjustments and coordination of
2109 hydraulic, leaf and stem traits along a water availability gradient, *New Phytologist*, 223, 632–646,
2110 <https://doi.org/10.1111/nph.15684>, 2019.
- 2111 Ross, J.: *The radiation regime and architecture of plant stands*, The Hague, The Netherlands, 1981.
- 2112 Rowland, L., Lobo-do-Vale, R. L., Christoffersen, B. O., Melém, E. A., Kruijt, B., Vasconcelos, S. S., Domingues, T., Binks,
2113 O. J., Oliveira, A. A. R., Metcalfe, D., da Costa, A. C. L., Mencuccini, M., and Meir, P.: After more than a decade of soil



- 2114 moisture deficit, tropical rainforest trees maintain photosynthetic capacity, despite increased leaf respiration, *Glob Change*
2115 *Biol*, 21, 4662–4672, <https://doi.org/10.1111/gcb.13035>, 2015.
- 2116 Rowland, L., Costa, A. C. L. da, Oliveira, A. A. R., Oliveira, R. S., Bittencourt, P. L., Costa, P. B., Giles, A. L., Sosa, A. I.,
2117 Coughlin, I., Godlee, J. L., Vasconcelos, S. S., Junior, J. A. S., Ferreira, L. V., Mencuccini, M., and Meir, P.: Drought
2118 stress and tree size determine stem CO₂ efflux in a tropical forest, *New Phytologist*, 218, 1393–1405,
2119 <https://doi.org/10.1111/nph.15024>, 2018.
- 2120 Rowland, L., Ramírez-Valiente, J.-A., Hartley, I. P., and Mencuccini, M.: How woody plants adjust above- and below-ground
2121 traits in response to sustained drought, *New Phytologist*, 239, 1173–1189, <https://doi.org/10.1111/nph.19000>, 2023.
- 2122 Rutter, A. J. and Morton, A. J.: A Predictive Model of Rainfall Interception in Forests. III. Sensitivity of The Model to Stand
2123 Parameters and Meteorological Variables, *Journal of Applied Ecology*, 14, 567–588, <https://doi.org/10.2307/2402568>,
2124 1977.
- 2125 Ryan, M. G., Hubbard, R. M., Clark, D. A., and Jr, R. L. S.: Woody-tissue respiration for *Simarouba amara* and *Minuartia*
2126 *guianensis*, two tropical wet forest trees with different growth habits, *Oecologia*, 100, 213–220,
2127 <https://doi.org/10.1007/BF00316947>, 1994.
- 2128 Ryan, M. G., Binkley, D., and Fownes, J. H.: Age-related decline in forest productivity., *Adv. Ecol. Res.*, 27, 213–262, 1997.
- 2129 Sabot, M. E. B., Kauwe, M. G. D., Pitman, A. J., Medlyn, B. E., Verhoef, A., Ukkola, A. M., and Abramowitz, G.: Plant profit
2130 maximization improves predictions of European forest responses to drought, *New Phytologist*, 226, 1638–1655,
2131 <https://doi.org/10.1111/nph.16376>, 2020.
- 2132 Sabot, M. E. B., De Kauwe, M. G., Pitman, A. J., Medlyn, B. E., Ellsworth, D. S., Martin-StPaul, N. K., Wu, J., Choat, B.,
2133 Limousin, J.-M., Mitchell, P. J., Rogers, A., and Serbin, S. P.: One Stomatal Model to Rule Them All? Toward Improved
2134 Representation of Carbon and Water Exchange in Global Models, *Journal of Advances in Modeling Earth Systems*, 14,
2135 e2021MS002761, <https://doi.org/10.1029/2021MS002761>, 2022.
- 2136 Sakschewski, B., von Bloh, W., Boit, A., Rammig, A., Kattge, J., Poorter, L., Peñuelas, J., and Thonicke, K.: Leaf and stem
2137 economics spectra drive diversity of functional plant traits in a dynamic global vegetation model, *Glob Change Biol*, 21,
2138 2711–2725, <https://doi.org/10.1111/gcb.12870>, 2015.
- 2139 Sakschewski, B., von Bloh, W., Drüke, M., Sörensson, A. A., Ruscica, R., Langerwisch, F., Billing, M., Bereswill, S., Hirota,
2140 M., Oliveira, R. S., Heinke, J., and Thonicke, K.: Variable tree rooting strategies are key for modelling the distribution,
2141 productivity and evapotranspiration of tropical evergreen forests, *Biogeosciences*, 18, 4091–4116,
2142 <https://doi.org/10.5194/bg-18-4091-2021>, 2021.
- 2143 Sander, H.: The porosity of tropical soils and implications for geomorphological and pedogenetic processes and the
2144 movement of solutions within the weathering cover, *CATENA*, 49, 129–137, <https://doi.org/10.1016/S0341->
2145 8162(02)00021-8, 2002.



- 2146 Santos, V. A. H. F. dos, Ferreira, M. J., Rodrigues, J. V. F. C., Garcia, M. N., Ceron, J. V. B., Nelson, B. W., and Saleska, S.
2147 R.: Causes of reduced leaf-level photosynthesis during strong El Niño drought in a Central Amazon forest, *Global Change*
2148 *Biology*, 24, 4266–4279, <https://doi.org/10.1111/gcb.14293>, 2018.
- 2149 Sato, H., Itoh, A., and Kohyama, T.: SEIB-DGVM: a new dynamic global vegetation model using a spatially explicit
2150 individual-based approach, *Ecol. Model.*, 200, 279–307, <https://doi.org/10.1016/j.ecolmodel.2006.09.006>, 2007.
- 2151 Schaphoff, S., von Bloh, W., Rammig, A., Thonicke, K., Biemans, H., Forkel, M., Gerten, D., Heinke, J., Jägermeyr, J.,
2152 Knauer, J., Langerwisch, F., Lucht, W., Müller, C., Rolinski, S., and Waha, K.: LPJmL4 – a dynamic global vegetation
2153 model with managed land – Part 1: Model description, *Geoscientific Model Development*, 11, 1343–1375,
2154 [https://doi.org/Schaphoff,Sibyll,vonBloh,Werner,Rammig,Anja,Thonicke,Kirsten,Biemans,Hester,Forkel,Matthias,Gerten,Dieter,Heinke,Jens,Jägermeyr,Jonas,Knauer,Jürgen,Langerwisch,Fanny,Lucht,Wolfgang,Müller,Christoph,Rolinski,SusanneandWaha,Katharina\(2018\)LPJmL4-a-dynamic-global-vegetation-model-with-managed-land-Part-1:Model-description.OpenAccessGeoscientificModelDevelopment,11\(4\).pp.1343-1375.DOI10.5194/gmd-11-1343-2018](https://doi.org/Schaphoff,Sibyll,vonBloh,Werner,Rammig,Anja,Thonicke,Kirsten,Biemans,Hester,Forkel,Matthias,Gerten,Dieter,Heinke,Jens,Jägermeyr,Jonas,Knauer,Jürgen,Langerwisch,Fanny,Lucht,Wolfgang,Müller,Christoph,Rolinski,SusanneandWaha,Katharina(2018)LPJmL4-a-dynamic-global-vegetation-model-with-managed-land-Part-1:Model-description.OpenAccessGeoscientificModelDevelopment,11(4).pp.1343-1375.DOI10.5194/gmd-11-1343-2018)
2155 <<http://dx.doi.org/10.5194/gmd-11-1343-2018>>., 2018.
- 2156 Scheiter, S., Langan, L., and Higgins, S. I.: Next-generation dynamic global vegetation models: learning from community
2157 ecology, *New Phytol.*, 198, 957–969, <https://doi.org/10.1111/nph.12210>, 2013.
- 2161 Schimel, D., Pavlick, R., Fisher, J. B., Asner, G. P., Saatchi, S., Townsend, P., Miller, C., Frankenberg, C., Hibbard, K., and
2162 Cox, P.: Observing terrestrial ecosystems and the carbon cycle from space, *Global Change Biology*, 21, 1762–1776,
2163 <https://doi.org/10.1111/gcb.12822>, 2015.
- 2164 Schippers, P., Vlam, M., Zuidema, P. A., and Sterck, F.: Sapwood allocation in tropical trees: a test of hypotheses, *Functional*
2165 *Plant Biol.*, 42, 697–709, <https://doi.org/10.1071/FP14127>, 2015.
- 2166 Schmidhalter, U.: The gradient between pre-dawn rhizoplane and bulk soil matric potentials, and its relation to the pre-dawn
2167 root and leaf water potentials of four species, *Plant, Cell & Environment*, 20, 953–960, <https://doi.org/10.1046/j.1365-3040.1997.d01-136.x>, 1997.
- 2169 Schmitt, S., Maréchaux, I., Chave, J., Fischer, F. J., Piponiot, C., Traissac, S., and Hérault, B.: Functional diversity improves
2170 tropical forest resilience: Insights from a long-term virtual experiment, *Journal of Ecology*, 108, 831–843,
2171 <https://doi.org/10.1111/1365-2745.13320>, 2020.
- 2172 Schmitt, S.: Rôle de la biodiversité dans la résilience des écosystèmes forestiers tropicaux après perturbations, AgroParisTech,
2173 Université de Montpellier, Kourou, 2017.
- 2174 Schmitt, S., Salzert, G., Fischer, F. J., Maréchaux, I., and Chave, J.: rcontroll: An R interface for the individual-based forest
2175 dynamics simulator TROLL, *Methods in Ecology and Evolution*, 14, 2749–2757, <https://doi.org/10.1111/2041-210X.14215>, 2023.
- 2177 Schnabel, F., Schwarz, J. A., Dănescu, A., Fichtner, A., Nock, C. A., Bauhus, J., and Potvin, C.: Drivers of productivity and
2178 its temporal stability in a tropical tree diversity experiment, *Global Change Biology*, 25, 4257–4272,
2179 <https://doi.org/10.1111/gcb.14792>, 2019.



- 2180 Schnitzer, S. A. and Carson, W. P.: Would Ecology Fail the Repeatability Test?, *BioScience*, 66, 98–99,
2181 <https://doi.org/10.1093/biosci/biv176>, 2016.
- 2182 Seidl, R., Rammer, W., and Blennow, K.: Simulating wind disturbance impacts on forest landscapes: Tree-level heterogeneity
2183 matters, *Environmental Modelling & Software*, 51, 1–11, <https://doi.org/10.1016/j.envsoft.2013.09.018>, 2014.
- 2184 Seidler, T. G. and Plotkin, J. B.: Seed Dispersal and Spatial Pattern in Tropical Trees, *PLOS Biology*, 4, e344,
2185 <https://doi.org/10.1371/journal.pbio.0040344>, 2006.
- 2186 Sellers, P. J., Mintz, Y., Sud, Y. C., and Dalcher, A.: A Simple Biosphere Model (SIB) for Use within General Circulation
2187 Models, *J. Atmos. Sci.*, 43, 505–531, [https://doi.org/10.1175/1520-0469\(1986\)043<0505:ASBMFU>2.0.CO;2](https://doi.org/10.1175/1520-0469(1986)043<0505:ASBMFU>2.0.CO;2), 1986.
- 2188 Sellers, P. J., Heiser, M. D., and Hall, F. G.: Relations between surface conductance and spectral vegetation indices at
2189 intermediate (100 m² to 15 km²) length scales, *Journal of Geophysical Research: Atmospheres*, 97, 19033–19059,
2190 <https://doi.org/10.1029/92JD01096>, 1992.
- 2191 Sellers, P. J., Dickinson, R. E., Randall, D. A., Betts, A. K., Hall, F. G., Berry, J. A., Collatz, G. J., Denning, A. S., Mooney,
2192 H. A., Nobre, C. A., Sato, N., Field, C. B., and Henderson-Sellers, A.: Modeling the Exchanges of Energy, Water, and
2193 Carbon Between Continents and the Atmosphere, *Science*, 275, 502–509, <https://doi.org/10.1126/science.275.5299.502>,
2194 1997.
- 2195 Sergeant, A. S., Varela, S. A., Barigah, T. S., Badel, E., Cochard, H., Dalla-Salda, G., Delzon, S., Fernández, M. E., Guillemot,
2196 J., Gyenge, J., Lamarque, L. J., Martinez-Meier, A., Rozenberg, P., Torres-Ruiz, J. M., and Martin-StPaul, N. K.: A
2197 comparison of five methods to assess embolism resistance in trees, *Forest Ecology and Management*, 468, 118175,
2198 <https://doi.org/10.1016/j.foreco.2020.118175>, 2020.
- 2199 Sevanto, S., McDowell, N. G., Dickman, L. T., Pangle, R., and Pockman, W. T.: How do trees die? A test of the hydraulic
2200 failure and carbon starvation hypotheses, *Plant Cell Environ*, 37, 153–161, <https://doi.org/10.1111/pce.12141>, 2014.
- 2201 Sheil, D., Burslem, D. F. R. P., and Alder, D.: The interpretation and misinterpretation of mortality rate measures, *Journal of*
2202 *Ecology*, 83, 331–333, <https://doi.org/10.2307/2261571>, 1995.
- 2203 Shugart, H. H., Asner, G. P., Fischer, R., Huth, A., Knapp, N., Le Toan, T., and Shuman, J. K.: Computer and remote-sensing
2204 infrastructure to enhance large-scale testing of individual-based forest models, *Frontiers in Ecology and the Environment*,
2205 13, 503–511, 2015.
- 2206 Shuttleworth, W. J.: Daily variations of temperature and humidity within and above Amazonian forest, *Weather*, 40, 102–108,
2207 <https://doi.org/10.1002/j.1477-8696.1985.tb07489.x>, 1985.
- 2208 Shuttleworth, W. J., Leuning, R., Black, T. A., Grace, J., Jarvis, P. G., Roberts, J., and Jones, H. G.: Micrometeorology of
2209 temperate and tropical forest, *Philosophical Transactions of the Royal Society of London B: Biological Sciences*, 324, 299–
2210 334, <https://doi.org/10.1098/rstb.1989.0050>, 1989.
- 2211 Slik, J. W. F.: El Niño droughts and their effects on tree species composition and diversity in tropical rain forests, *Oecologia*,
2212 141, 114–120, <https://doi.org/10.1007/s00442-004-1635-y>, 2004.



- 2213 Slot, M., Wright, S. J., and Kitajima, K.: Foliar respiration and its temperature sensitivity in trees and lianas: in situ
2214 measurements in the upper canopy of a tropical forest, *Tree Physiol*, 33, 505–515, <https://doi.org/10.1093/treephys/tpt026>,
2215 2013.
- 2216 Slot, M., Nardwattanawong, T., Hernández, G. G., Bueno, A., Riederer, M., and Winter, K.: Large differences in leaf cuticle
2217 conductance and its temperature response among 24 tropical tree species from across a rainfall gradient, *New Phytologist*,
2218 232, 1618–1631, <https://doi.org/10.1111/nph.17626>, 2021.
- 2219 Smith, B., Prentice, I. C., and Sykes, M. T.: Representation of vegetation dynamics in the modelling of terrestrial ecosystems:
2220 comparing two contrasting approaches within European climate space, *Global Ecology and Biogeography*, 10, 621–637,
2221 <https://doi.org/10.1046/j.1466-822X.2001.t01-1-00256.x>, 2001.
- 2222 Smith, N. G. and Dukes, J. S.: Plant respiration and photosynthesis in global-scale models: incorporating acclimation to
2223 temperature and CO₂, *Glob Change Biol*, 19, 45–63, <https://doi.org/10.1111/j.1365-2486.2012.02797.x>, 2013.
- 2224 Smith-Martin, C. M., Xu, X., Medvigy, D., Schnitzer, S. A., and Powers, J. S.: Allometric scaling laws linking biomass and
2225 rooting depth vary across ontogeny and functional groups in tropical dry forest lianas and trees, *New Phytologist*, 226,
2226 714–726, <https://doi.org/10.1111/nph.16275>, 2020.
- 2227 Soberón, J.: Grinnellian and Eltonian niches and geographic distributions of species, *Ecology Letters*, 10, 1115–1123,
2228 <https://doi.org/10.1111/j.1461-0248.2007.01107.x>, 2007.
- 2229 Sobrado, M. A.: Aspects of tissue water relations and seasonal changes of leaf water potential components of evergreen and
2230 deciduous species coexisting in tropical dry forests, *Oecologia*, 68, 413–416, <https://doi.org/10.1007/BF01036748>, 1986.
- 2231 Song, X., Wang, D.-Y., Li, F., and Zeng, X.-D.: Evaluating the performance of CMIP6 Earth system models in simulating
2232 global vegetation structure and distribution, *Advances in Climate Change Research*, 12, 584–595,
2233 <https://doi.org/10.1016/j.accre.2021.06.008>, 2021.
- 2234 Sousa, T. R., Schiatti, J., Ribeiro, I. O., Emílio, T., Fernández, R. H., ter Steege, H., Castilho, C. V., Esquivel-Muelbert, A.,
2235 Baker, T., Pontes-Lopes, A., Silva, C. V. J., Silveira, J. M., Derroire, G., Castro, W., Mendoza, A. M., Ruschel, A., Prieto,
2236 A., Lima, A. J. N., Rudas, A., Araujo-Murakami, A., Gutierrez, A. P., Andrade, A., Roopsind, A., Manzatto, A. G., Di
2237 Fiore, A., Torres-Lezama, A., Dourdain, A., Marimon, B., Marimon, B. H., Burban, B., van Ulf, B., Herault, B., Quesada,
2238 C., Mendoza, C., Stahl, C., Bonal, D., Galbraith, D., Neill, D., de Oliveira, E. A., Hase, E., Jimenez-Rojas, E., Vilanova,
2239 E., Arets, E., Berenguer, E., Alvarez-Davila, E., Honorio Coronado, E. N., Almeida, E., Coelho, F., Valverde, F. C., Elias,
2240 F., Brown, F., Bongers, F., Arevalo, F. R., Lopez-Gonzalez, G., van der Heijden, G., Aymard C., G. A., Llampazo, G. F.,
2241 Pardo, G., Ramirez-Angulo, H., do Amaral, I. L., Vieira, I. C. G., Huamantupa-Chuquimaco, I., Comiskey, J. A., Singh,
2242 J., Espejo, J. S., del Aguila-Pasquel, J., Zwerts, J. A., Talbot, J., Terborgh, J., Ferreira, J., Barroso, J. G., Barlow, J.,
2243 Camargo, J. L., Stropp, J., Peacock, J., Serrano, J., Melgaço, K., Ferreira, L. V., Blanc, L., Poorter, L., Gamarra, L. V.,
2244 Aragão, L., Arroyo, L., Silveira, M., Peñuela-Mora, M. C., Vargas, M. P. N., Toledo, M., Disney, M., Réjou-Méchain, M.,
2245 Baisie, M., Kalamandeen, M., Camacho, N. P., Cardozo, N. D., Silva, N., Pitman, N., Higuchi, N., Banki, O., Loayza, P.



- 2246 A., Graça, P. M. L. A., et al.: Water table depth modulates productivity and biomass across Amazonian forests, *Global*
2247 *Ecology and Biogeography*, 31, 1571–1588, <https://doi.org/10.1111/geb.13531>, 2022.
- 2248 Sperry, J. S., Hacke, U. G., Oren, R., and Comstock, J. P.: Water deficits and hydraulic limits to leaf water supply, *Plant Cell*
2249 *Environ.*, 25, 251–263, 2002.
- 2250 Sperry, J. S., Venturas, M. D., Anderegg, W. R. L., Mencuccini, M., Mackay, D. S., Wang, Y., and Love, D. M.: Predicting
2251 stomatal responses to the environment from the optimization of photosynthetic gain and hydraulic cost, *Plant, Cell &*
2252 *Environment*, 40, 816–830, <https://doi.org/10.1111/pce.12852>, 2017.
- 2253 Stahl, C., Herault, B., Rossi, V., Burban, B., Brechet, C., and Bonal, D.: Depth of soil water uptake by tropical rainforest trees
2254 during dry periods: does tree dimension matter?, *Oecologia*, 173, 1191–1201, <https://doi.org/10.1007/s00442-013-2724-6>,
2255 2013a.
- 2256 Stahl, C., Burban, B., Wagner, F., Goret, J.-Y., Bompy, F., and Bonal, D.: Influence of seasonal variations in soil water
2257 availability on gas exchange of tropical canopy trees, *Biotropica*, 45, 155–164, [https://doi.org/10.1111/j.1744-
2258 7429.2012.00902.x](https://doi.org/10.1111/j.1744-), 2013b.
- 2259 Stephenson, N. L., Das, A. J., Condit, R., Russo, S. E., Baker, P. J., Beckman, N. G., Coomes, D. A., Lines, E. R., Morris, W.
2260 K., Rüger, N., Álvarez, E., Blundo, C., Bunyavejchewin, S., Chuyong, G., Davies, S. J., Duque, Á., Ewango, C. N., Flores,
2261 O., Franklin, J. F., Grau, H. R., Hao, Z., Harmon, M. E., Hubbell, S. P., Kenfack, D., Lin, Y., Makana, J.-R., Malizia, A.,
2262 Malizia, L. R., Pabst, R. J., Pongpattananurak, N., Su, S.-H., Sun, I.-F., Tan, S., Thomas, D., van Mantgem, P. J., Wang,
2263 X., Wisser, S. K., and Zavala, M. A.: Rate of tree carbon accumulation increases continuously with tree size, *Nature*, 507,
2264 90–93, <https://doi.org/10.1038/nature12914>, 2014.
- 2265 Strigul, N., Pristinski, D., Purves, D., Dushoff, J., and Pacala, S.: Scaling from trees to forests: tractable macroscopic equations
2266 for forest dynamics, *Ecological Monographs*, 78, 523–545, <https://doi.org/10.1890/08-0082.1>, 2008.
- 2267 Sun, S., Jung, E.-Y., Gaviria, J., and Engelbrecht, B. M. J.: Drought survival is positively associated with high turgor loss
2268 points in temperate perennial grassland species, *Functional Ecology*, 34, 788–798, [https://doi.org/10.1111/1365-
2269 2435.13522](https://doi.org/10.1111/1365-), 2020.
- 2270 Swaine, M. D. and Whitmore, T. C.: On the definition of ecological species groups in tropical rain forests, *Vegetatio*, 75, 81–
2271 86, <https://doi.org/10.1007/BF00044629>, 1988.
- 2272 Tamme, R., Götzenberger, L., Zobel, M., Bullock, J. M., Hooftman, D. A. P., Kaasik, A., and Pärtel, M.: Predicting species’
2273 maximum dispersal distances from simple plant traits, *Ecology*, 95, 505–513, <https://doi.org/10.1890/13-1000.1>, 2014.
- 2274 Thornley, J. H. M. and Cannell, M. G. R.: Modelling the components of plant respiration: representation and realism, *Ann*
2275 *Bot.*, 85, 55–67, <https://doi.org/10.1006/anbo.1999.0997>, 2000.
- 2276 Thuiller, W., Albert, C., Araújo, M. B., Berry, P. M., Cabeza, M., Guisan, A., Hickler, T., Midgley, G. F., Paterson, J., Schurr,
2277 F. M., Sykes, M. T., and Zimmermann, N. E.: Predicting global change impacts on plant species’ distributions: Future
2278 challenges, *Perspectives in Plant Ecology, Evolution and Systematics*, 9, 137–152,
2279 <https://doi.org/10.1016/j.ppees.2007.09.004>, 2008.



- 2280 Tomasella, J. and Hodnett, M. G.: Estimating soil water retention characteristics from limited data in Brazilian Amazonia.,
2281 Soil science, 163, 190–202, 1998.
- 2282 Trueba, S., Pan, R., Scoffoni, C., John, G. P., Davis, S. D., and Sack, L.: Thresholds for leaf damage due to dehydration:
2283 declines of hydraulic function, stomatal conductance and cellular integrity precede those for photochemistry, New
2284 Phytologist, 223, 134–149, <https://doi.org/10.1111/nph.15779>, 2019.
- 2285 Trugman, A. T., Medvigy, D., Mankin, J. S., and Anderegg, W. R. L.: Soil Moisture Stress as a Major Driver of Carbon Cycle
2286 Uncertainty, Geophysical Research Letters, 45, 6495–6503, <https://doi.org/10.1029/2018GL078131>, 2018.
- 2287 Turner, B. L., Brenes-Arguedas, T., and Condit, R.: Pervasive phosphorus limitation of tree species but not communities in
2288 tropical forests, Nature, 555, 367–370, <https://doi.org/10.1038/nature25789>, 2018.
- 2289 Tuzet, A., Perrier, A., and Leuning, R.: A coupled model of stomatal conductance, photosynthesis and transpiration, Plant,
2290 Cell & Environment, 26, 1097–1116, <https://doi.org/10.1046/j.1365-3040.2003.01035.x>, 2003.
- 2291 Tymen, B., Vincent, G., Courtois, E. A., Heurtebize, J., Dazat, J., Marechaux, I., and Chave, J.: Quantifying micro-
2292 environmental variation in tropical rainforest understory at landscape scale by combining airborne LiDAR scanning and a
2293 sensor network, Annals of Forest Science, 74, 32, <https://doi.org/10.1007/s13595-017-0628-z>, 2017.
- 2294 Urbina, I., Grau, O., Sardans, J., Margalef, O., Peguero, G., Asensio, D., LLusià, J., Ogaya, R., Gargallo-Garriga, A., Van
2295 Langenhove, L., Verryckt, L. T., Courtois, E. A., Stahl, C., Soong, J. L., Chave, J., Hérault, B., Janssens, I. A., Sayer, E.,
2296 and Peñuelas, J.: High foliar K and P resorption efficiencies in old-growth tropical forests growing on nutrient-poor soils,
2297 Ecology and Evolution, 11, 8969–8982, <https://doi.org/10.1002/ece3.7734>, 2021.
- 2298 Vacchiano, G., Ascoli, D., Berzaghi, F., Lucas-Borja, M. E., Caignard, T., Collalti, A., Mairota, P., Palaghianu, C., Reyser, C.
2299 P. O., Sanders, T. G. M., Schermer, E., Wohlgemuth, T., and Hacket-Pain, A.: Reproducing reproduction: How to simulate
2300 mast seeding in forest models, Ecological Modelling, 376, 40–53, <https://doi.org/10.1016/j.ecolmodel.2018.03.004>, 2018.
- 2301 Van Bodegom, P. M., Douma, J. C., and Verheijen, L. M.: A fully traits-based approach to modeling global vegetation
2302 distribution, PNAS, 111, 13733–13738, <https://doi.org/10.1073/pnas.1304551110>, 2014.
- 2303 Van Nes, E. H. and Scheffer, M.: A strategy to improve the contribution of complex simulation models to ecological theory,
2304 Ecological Modelling, 185, 153–164, <https://doi.org/10.1016/j.ecolmodel.2004.12.001>, 2005.
- 2305 Vanclay, J. K.: Aggregating tree species to develop diameter increment equations for tropical rainforests, Forest Ecology and
2306 Management, 42, 143–168, [https://doi.org/10.1016/0378-1127\(91\)90022-N](https://doi.org/10.1016/0378-1127(91)90022-N), 1991.
- 2307 Vanclay, J. K.: Modelling forest growth and yield: applications to mixed tropical forests., CAB International, Wallingford,
2308 312 pp., 1994.
- 2309 Vargas Godoy, M. R., Markonis, Y., Hanel, M., Kyselý, J., and Papalexiou, S. M.: The Global Water Cycle Budget: A
2310 Chronological Review, Surv Geophys, 42, 1075–1107, <https://doi.org/10.1007/s10712-021-09652-6>, 2021
- 2311 Verbeeck, H., Peylin, P., Bacour, C., Bonal, D., Steppe, K., and Ciais, P.: Seasonal patterns of CO₂ fluxes in Amazon forests:
2312 Fusion of eddy covariance data and the ORCHIDEE model, J. Geophys. Res.-Biogeosci., 116,
2313 <https://doi.org/10.1029/2010JG001544>, 2011.



- 2314 Verheijen, L. M., Aerts, R., Brovkin, V., Cavender-Bares, J., Cornelissen, J. H. C., Kattge, J., and van Bodegom, P. M.:
2315 Inclusion of ecologically based trait variation in plant functional types reduces the projected land carbon sink in an earth
2316 system model, *Glob Change Biol*, 21, 3074–3086, <https://doi.org/10.1111/gcb.12871>, 2015.
- 2317 Verhoef, A. and Egea, G.: Modeling plant transpiration under limited soil water: Comparison of different plant and soil
2318 hydraulic parameterizations and preliminary implications for their use in land surface models, *Agricultural and Forest
2319 Meteorology*, 191, 22–32, <https://doi.org/10.1016/j.agrformet.2014.02.009>, 2014.
- 2320 Vezy, R., Christina, M., Roupsard, O., Nouvellon, Y., Duursma, R., Medlyn, B., Soma, M., Charbonnier, F., Blitz-Frayret, C.,
2321 Stape, J.-L., Laclau, J.-P., de Melo Virginio Filho, E., Bonnefond, J.-M., Rapidel, B., Do, F. C., Rocheteau, A., Picart, D.,
2322 Borgonovo, C., Loustau, D., and le Maire, G.: Measuring and modelling energy partitioning in canopies of varying
2323 complexity using MAESPA model, *Agricultural and Forest Meteorology*, 253–254, 203–217,
2324 <https://doi.org/10.1016/j.agrformet.2018.02.005>, 2018.
- 2325 Villar, R., Held, A. A., and Merino, J.: Dark Leaf Respiration in Light and Darkness of an Evergreen and a Deciduous Plant
2326 Species, *Plant Physiology*, 107, 421–427, <https://doi.org/10.1104/pp.107.2.421>, 1995.
- 2327 Visser, M. D., Bruijning, M., Wright, S. J., Muller-Landau, H. C., Jongejans, E., Comita, L. S., and de Kroon, H.: Functional
2328 traits as predictors of vital rates across the life cycle of tropical trees, *Funct Ecol*, 30, 168–180,
2329 <https://doi.org/10.1111/1365-2435.12621>, 2016.
- 2330 Vleminckx, J., Fortunel, C., Valverde-Barrantes, O., Timothy Paine, C. E., Engel, J., Petronelli, P., Dourdain, A. K., Guevara,
2331 J., Bérroujon, S., and Baraloto, C.: Resolving whole-plant economics from leaf, stem and root traits of 1467 Amazonian
2332 tree species, *Oikos*, 130, 1193–1208, <https://doi.org/10.1111/oik.08284>, 2021.
- 2333 Wagner, F. H., Anderson, L. O., Baker, T. R., Bowman, D. M., Cardoso, F. C., Chidumayo, E. N., Clark, D. A., Drew, D. M.,
2334 Griffiths, A. D., Maria, V. R., and others: Climate seasonality limits leaf carbon assimilation and wood productivity in
2335 tropical forests, *Biogeosciences*, 13, 2537, 2016.
- 2336 Walker, A. P., Beckerman, A. P., Gu, L., Kattge, J., Cernusak, L. A., Domingues, T. F., Scales, J. C., Wohlfahrt, G.,
2337 Wullschleger, S. D., and Woodward, F. I.: The relationship of leaf photosynthetic traits – V_{cmax} and J_{max} – to leaf
2338 nitrogen, leaf phosphorus, and specific leaf area: a meta-analysis and modeling study, *Ecol Evol*, 4, 3218–3235,
2339 <https://doi.org/10.1002/ece3.1173>, 2014.
- 2340 Wang, Y. P. and Jarvis, P. G.: Description and validation of an array model — MAESTRO, *Agricultural and Forest
2341 Meteorology*, 51, 257–280, [https://doi.org/10.1016/0168-1923\(90\)90112-J](https://doi.org/10.1016/0168-1923(90)90112-J), 1990.
- 2342 Wang, Y.-P. and Leuning, R.: A two-leaf model for canopy conductance, photosynthesis and partitioning of available energy
2343 I., *Agricultural and Forest Meteorology*, 91, 89–111, [https://doi.org/10.1016/S0168-1923\(98\)00061-6](https://doi.org/10.1016/S0168-1923(98)00061-6), 1998.
- 2344 Warneke, C. R., Caughlin, T. T., Damschen, E. I., Haddad, N. M., Levey, D. J., and Brudvig, L. A.: Habitat fragmentation
2345 alters the distance of abiotic seed dispersal through edge effects and direction of dispersal, *Ecology*, 103, e03586,
2346 <https://doi.org/10.1002/ecy.3586>, 2022.
- 2347 Watt, A. S.: Pattern and Process in the Plant Community, *Journal of Ecology*, 35, 1–22, <https://doi.org/10.2307/2256497>, 1947.



- 2348 Weemstra, M., Mommer, L., Visser, E. J. W., van Ruijven, J., Kuiper, T. W., Mohren, G. M. J., and Sterck, F. J.: Towards a
2349 multidimensional root trait framework: a tree root review, *New Phytol*, 211, 1159–1169,
2350 <https://doi.org/10.1111/nph.14003>, 2016.
- 2351 Weerasinghe, L. K., Creek, D., Crous, K. Y., Xiang, S., Liddell, M. J., Turnbull, M. H., and Atkin, O. K.: Canopy position
2352 affects the relationships between leaf respiration and associated traits in a tropical rainforest in Far North Queensland, *Tree*
2353 *Physiol*, tpu016, <https://doi.org/10.1093/treephys/tpu016>, 2014.
- 2354 Williams, M., Rastetter, E. B., Fernandes, D. N., Goulden, M. L., Wofsy, S. C., Shaver, G. R., Melillo, J. M., Munger, J. W.,
2355 Fan, S.-M., and Nadelhoffer, K. J.: Modelling the soil-plant-atmosphere continuum in a *Quercus*–*Acer* stand at Harvard
2356 Forest: the regulation of stomatal conductance by light, nitrogen and soil/plant hydraulic properties, *Plant, Cell &*
2357 *Environment*, 19, 911–927, <https://doi.org/10.1111/j.1365-3040.1996.tb00456.x>, 1996.
- 2358 Williams, M., Law, B. E., Anthoni, P. M., and Unsworth, M. H.: Use of a simulation model and ecosystem flux data to examine
2359 carbon–water interactions in ponderosa pine, *Tree Physiol*, 21, 287–298, <https://doi.org/10.1093/treephys/21.5.287>, 2001.
- 2360 Wilson, J. B., Peet, R. K., Dengler, J., and Pärtel, M.: Plant species richness: the world records, *Journal of Vegetation Science*,
2361 23, 796–802, <https://doi.org/10.1111/j.1654-1103.2012.01400.x>, 2012.
- 2362 Wolf, A., Anderegg, W. R. L., and Pacala, S. W.: Optimal stomatal behavior with competition for water and risk of hydraulic
2363 impairment, *PNAS*, 113, E7222–E7230, <https://doi.org/10.1073/pnas.1615144113>, 2016.
- 2364 Wolz, K. J., Wertin, T. M., Abordo, M., Wang, D., and Leakey, A. D. B.: Diversity in stomatal function is integral to modelling
2365 plant carbon and water fluxes, *Nat Ecol Evol*, 1, 1292–1298, <https://doi.org/10.1038/s41559-017-0238-z>, 2017.
- 2366 Woodruff, D. R. and Meinzer, F. C.: Water stress, shoot growth and storage of non-structural carbohydrates along a tree height
2367 gradient in a tall conifer, *Plant, Cell & Environment*, 34, 1920–1930, <https://doi.org/10.1111/j.1365-3040.2011.02388.x>,
2368 2011.
- 2369 Wright, S. J., Kitajima, K., Kraft, N. J. B., Reich, P. B., Wright, I. J., Bunker, D. E., Condit, R., Dalling, J. W., Davies, S. J.,
2370 Díaz, S., Engelbrecht, B. M. J., Harms, K. E., Hubbell, S. P., Marks, C. O., Ruiz-Jaen, M. C., Salvador, C. M., and Zanne,
2371 A. E.: Functional traits and the growth–mortality trade-off in tropical trees, *Ecology*, 91, 3664–3674,
2372 <https://doi.org/10.1890/09-2335.1>, 2010.
- 2373 Wu, J., Albert, L. P., Lopes, A. P., Restrepo-Coupe, N., Hayek, M., Wiedemann, K. T., Guan, K., Stark, S. C., Christoffersen,
2374 B., Prohaska, N., Tavares, J. V., Marostica, S., Kobayashi, H., Ferreira, M. L., Campos, K. S., Silva, R. da, Brando, P. M.,
2375 Dye, D. G., Huxman, T. E., Huete, A. R., Nelson, B. W., and Saleska, S. R.: Leaf development and demography explain
2376 photosynthetic seasonality in Amazon evergreen forests, *Science*, 351, 972–976, <https://doi.org/10.1126/science.aad5068>,
2377 2016.
- 2378 Wu, J., Serbin, S. P., Xu, X., Albert, L. P., Chen, M., Meng, R., Saleska, S. R., and Rogers, A.: The phenology of leaf quality
2379 and its within-canopy variation is essential for accurate modeling of photosynthesis in tropical evergreen forests, *Global*
2380 *Change Biology*, 23, 4814–4827, <https://doi.org/10.1111/gcb.13725>, 2017.



- 2381 Wu, J., Serbin, S. P., Ely, K. S., Wolfe, B. T., Dickman, L. T., Grossiord, C., Michaletz, S. T., Collins, A. D., Detto, M.,
2382 McDowell, N. G., Wright, S. J., and Rogers, A.: The response of stomatal conductance to seasonal drought in tropical
2383 forests, *Global Change Biology*, 26, 823–839, <https://doi.org/10.1111/gcb.14820>, 2020.
- 2384 Xu, X., Medvigy, D., Powers, J. S., Becknell, J. M., and Guan, K.: Diversity in plant hydraulic traits explains seasonal and
2385 inter-annual variations of vegetation dynamics in seasonally dry tropical forests, *New Phytol*, 212, 80–95,
2386 <https://doi.org/10.1111/nph.14009>, 2016.
- 2387 Yang, X., Wu, J., Chen, X., Ciais, P., Maignan, F., Yuan, W., Piao, S., Yang, S., Gong, F., Su, Y., Dai, Y., Liu, L., Zhang, H.,
2388 Bonal, D., Liu, H., Chen, G., Lu, H., Wu, S., Fan, L., Gentine, P., and Wright, S. J.: A comprehensive framework for
2389 seasonal controls of leaf abscission and productivity in evergreen broadleaved tropical and subtropical forests, *The*
2390 *Innovation*, 2, 100154, <https://doi.org/10.1016/j.xinn.2021.100154>, 2021.
- 2391 Yao, Y., Joetzjer, E., Ciais, P., Viovy, N., Cresto Aleina, F., Chave, J., Sack, L., Bartlett, M., Meir, P., Fisher, R., and Luyssaert,
2392 S.: Forest fluxes and mortality response to drought: model description (ORCHIDEE-CAN-NHA r7236) and evaluation at
2393 the Caxiuanã drought experiment, *Geoscientific Model Development*, 15, 7809–7833, [https://doi.org/10.5194/gmd-15-](https://doi.org/10.5194/gmd-15-7809-2022)
2394 [7809-2022](https://doi.org/10.5194/gmd-15-7809-2022), 2022.
- 2395 Yao, Y., Ciais, P., Viovy, N., Joetzjer, E., and Chave, J.: How drought events during the last century have impacted biomass
2396 carbon in Amazonian rainforests, *Global Change Biology*, 29, 747–762, <https://doi.org/10.1111/gcb.16504>, 2023.
- 2397 Yao, Y., Ciais, P., Joetzjer, E., Li, W., Zhu, L., Wang, Y., Frankenberg, C., and Viovy, N.: The impacts of elevated CO₂ on
2398 forest growth, mortality and recovery in the Amazon rainforest, *Earth System Dynamics Discussions*, 1–23,
2399 <https://doi.org/10.5194/esd-2024-5>, 2024.
- 2400 Yoda, K., Shinozaki, K., Ogawa, H., Hozumi, K., and Kira, T.: Estimation of the total amount of respiration in woody organs
2401 of trees and forest communities., *J. Biol. Osaka City Univ*, 16, 15–26, 1965.
- 2402 Yu, W., Albert, G., Rosenbaum, B., Schnabel, F., Bruelheide, H., Connolly, J., Härdtle, W., von Oheimb, G., Trogisch, S.,
2403 Rürger, N., and Brose, U.: Systematic distributions of interaction strengths across tree interaction networks yield positive
2404 diversity–productivity relationships, *Ecology Letters*, 27, e14338, <https://doi.org/10.1111/ele.14338>, 2024.
- 2405 Zaehle, S., Sitch, S., Smith, B., and Hatterman, F.: Effects of parameter uncertainties on the modeling of terrestrial biosphere
2406 dynamics, *Global Biogeochem. Cycles*, 19, GB3020, <https://doi.org/10.1029/2004GB002395>, 2005.
- 2407 Zellweger, F., Frenne, P. D., Lenoir, J., Rocchini, D., and Coomes, D.: Advances in Microclimate Ecology Arising from
2408 Remote Sensing, *Trends in Ecology & Evolution*, 34, 327–341, <https://doi.org/10.1016/j.tree.2018.12.012>, 2019.
- 2409 Zhou, S., Duursma, R. A., Medlyn, B. E., Kelly, J. W. G., and Prentice, I. C.: How should we model plant responses to drought?
2410 An analysis of stomatal and non-stomatal responses to water stress, *Agric. For. Meteorol.*, 182, 204–214,
2411 <https://doi.org/10.1016/j.agrformet.2013.05.009>, 2013.
- 2412 Zhou, S., Medlyn, B., Sabaté, S., Sperlich, D., Prentice, I. C., and others: Short-term water stress impacts on stomatal,
2413 mesophyll and biochemical limitations to photosynthesis differ consistently among tree species from contrasting climates,
2414 *Tree Physiology*, 34, 1035–46, 2014.



2415 Ziegler, C., Coste, S., Stahl, C., Delzon, S., Levionnois, S., Cazal, J., Cochard, H., Esquivel-Muelbert, A., Goret, J.-Y., Heuret,
2416 P., Jaouen, G., Santiago, L. S., and Bonal, D.: Large hydraulic safety margins protect Neotropical canopy rainforest tree
2417 species against hydraulic failure during drought, *Annals of Forest Science*, 76, 115, <https://doi.org/10.1007/s13595-019->
2418 0905-0, 2019.



2419 **Appendix A**

2420 **Table A1. List of symbols and variables.**

Symbols	Definition	Units	Nature	Equations
Physical constants				
M_w	Molar mass of water vapor	kg mol ⁻¹	Constant	12
R	ideal gas constant	J mol ⁻¹ K ⁻¹	Constant	12-13, 28-31, 46-47
V_w	Partial molal volume of water	m ³ mol ⁻¹	Constant	13
κ	von Karman constant	unitless	Constant	8, 15
g	Gravity constant	m s ⁻²	Constant	37
ρ	Density of water	kg m ⁻³	Constant	37
M_a	Molecular mass of air	kg mol ⁻¹	Constant	41, 48
C_p	Heat capacity of air	J kg ⁻¹ K ⁻¹	Constant	41, 48
γ	Psychrometric constant	Pa K ⁻¹	Constant	41
D_H	Molecular diffusivity to heat	m ² s ⁻¹	Constant	46
σ	Stefan-Boltzmann constant	W m ⁻² K ⁻⁴	Constant	44, 48
Aboveground environment				
PPFD _{top}	Photosynthetic photon flux density at canopy top	$\mu\text{mol photons m}^{-2} \text{s}^{-1}$	Updated at half hourly step, given as input	1
T_{top}	Temperature at canopy top	°C	Updated at half hourly step, given as input	4, 6, 44
VPD _{top}	Vapour pressure deficit at canopy top	kPa	Updated at half hourly step, given as input	5, 7
u_{top}	Wind speed at a reference height above the canopy	m s ⁻¹	Updated at half hourly step, given as input	Sections 2.1 and 2.2
T_{night}	Nighttime temperature	°C	Updated daily, given as input	Section 2.2
PPFD	Incident photosynthetic photon flux density	$\mu\text{mol photons m}^{-2} \text{s}^{-1}$	Computed every half hour	1, 25
T	Temperature	°C	Computed every half hour	4, 42, 46-48
VPD	Vapour pressure deficit	kPa	Computed every half hour	5
u	Wind speed	m s ⁻¹	Computed every half hour	8, 9, 15, 47
c_a	CO ₂ concentration	$\mu\text{mol mol}^{-1}$ (ppm)	Constant	Section 2.5
P_{ress}	Atmospheric pressure	Pa	Constant	46-47
PPFD _{abs}	Absorbed photosynthetic photon flux density	$\mu\text{mol photons m}^{-2} \text{s}^{-1}$	Computed every half hour	2
T_{mean}	Temperature, averaged per crown layer	°C	Computed every half hour	6
VPD _{mean}	Vapour pressure deficit, averaged per crown layer	kPa	Computed every half hour	7
LAI	Cumulated leaf area per ground area	m ² m ⁻²	Computed daily for each voxel	1-3, 11, 43
dens	Averaged leaf area density per unit ground area	m ² m ⁻²	Computed daily, averaged per layer	3, 6-7



k	Effective light extinction coefficient	unitless	Fixed, computed from k_{geom} and $absorptance_{leaves}$	1
k_{geom}	Light extinction coefficient reflecting the geometric arrangement of leaves	unitless	Constant, given as input	1
$absorptan_{ce_{leaves}}$	Fraction of absorbed light within a single leaf	unitless	Constant, given as input	1
LAI_{sat}	LAI threshold for computing microenvironmental variation within the canopy	$m^2 m^{-2}$	Constant	4-7
ΔT	Parameter of the within-canopy variation in temperature	$^{\circ}C$	Constant	4, 6
C_{VPD0}	Parameter of the within-canopy variation in vapour pressure deficit	unitless	Constant	5, 7
u^*	friction velocity	$m s^{-1}$	Constant	
d	zero-plane displacement height	m	Computed from the locally averaged canopy height (H)	8
z_0	aerodynamic roughness	m	Computed from the locally averaged canopy height (H)	8
H	Top canopy height	m	Computed daily	8-9
α	Parameter of wind speed decrease within the canopy	unitless	Constant	9
<hr/>				
Water balance				
P	Precipitation	mm	Updated daily, given as input	10
I	Interception	mm	Computed daily	10, 11
Q	Run-off	m^3	Computed daily	10
E	Evaporation from the soil	$kg m^{-2} s^{-1}$	Computed daily	10, 12
T	Tree transpiration	m^3	Computed daily	10
L	Leakage	m^3	Computed daily	10
K	Parameter for rainfall interception	mm	Constant	11
T_s	Temperature at soil surface	K	Computed daily	12, 13
e_s	Vapor pressure of the soil surface	Pa	Computed daily	12
e_a	Vapor pressure of air above the soil surface	Pa	Computed daily	12
e_{sat}	saturated vapor pressure	Pa	Computed daily	13
r_{soil}	Soil surface resistance	$s m^{-1}$	Computed daily	12, 14
r_{aero}	Aerodynamic resistance to heat transfer	$s m^{-1}$	Computed daily	12, 15
Z	Reference height for r_{aero} computation	m	Constant	15
Z_m	Momentum soil roughness	m	Constant	15
ψ_l	Soil water potential of layer l	MPa	Computed daily	21
K_l	Soil hydraulic conductivity of layer l	$kg m^{-2} s^{-1}$	Computed daily	22



$\psi_{soil,top}$	Water potential of the top soil belowground voxel	MPa	Computed daily	13
θ_{top}	Water content of the top soil belowground voxel	m^3	Computed daily	14
$\theta_{fc,top}$	water content at field capacity of the top soil belowground voxel	m^3	Computed daily	14
Species and tree characteristics				
LMA	Leaf mass per area	$g\ m^{-2}$	Species-specific means: constant, provided as input; tree-specific values: randomly attributed at tree birth	26, 27, 32, 56
LA	Leaf area	cm^2	Species-specific means: constant, provided as input; tree-specific values: randomly attributed at tree birth	46-47
N	Leaf nitrogen content per dry mass	$mg\ g^{-1}$	Species-specific means: constant, provided as input; tree-specific values: randomly attributed at tree birth	26, 27, 32
P	Leaf phosphorous content per dry mass	$mg\ g^{-1}$	Species-specific means: constant, provided as input; tree-specific values: randomly attributed at tree birth	26, 27, 32
wsg	Wood specific gravity	$g\ cm^{-3}$	Species-specific means: constant, provided as input; tree-specific values: randomly attributed at tree birth	36, 55, 60-61, 66
π_{tlp}	Leaf water potential at turgor loss point	MPa	Species-specific means: constant, provided as input; tree-specific values: randomly attributed at tree birth	39-40, 58, 68, section 2.7.1
dbh_{thres}	Threshold diameter at breast height, beyond which growth senescence starts	m	Species-specific means: constant, provided as input; tree-specific values: randomly attributed at tree birth	62, 63



dbh_{max}	Maximal tree diameter at breast height	m	Computed once per tree	Section 2.6.4
h_{lim}	Asymptotic height (parameter of Michaelis-Menten function)	m	Species-specific means: constant, provided as input	16
h_{max}	Maximal tree height	m	Species-specific means: constant, provided as input	67
a_h	Parameter of Michaelis-Menten function	m	Species-specific means: constant, provided as input	16
$f_{reg,s}$	Relative abundance of species s in the external seed rain	unitless	Species-specific, provide as input	64
w_l	Leaf width	m	Computed for each tree	46-47
LL	Leaf lifespan	yr	Computed for each tree	57
$\varepsilon_{i,j}$	Individual effects for trait or variable i and tree j	See traits	Randomly attributed at tree birth	Sections 2.4.1 and 2.4.2
σ_i	standard deviation for intraspecific variability in trait or variable i	See traits	Constant, provided as input	Sections 2.4.1 and 2.4.2
dbh	Tree diameter at breast height	m	Tree variable, updated at each timestep	16, 17, 19, 60-62
h	Tree height	m	Tree variable, updated at each timestep	16, 37, 54-55, 58, 60
cr	Tree crown radius	m	Tree variable, updated at each timestep	17
cd	Tree crown depth	m	Tree variable, updated at each timestep	18, 54
a_{cr}	Coefficients of crown radius allometry	unitless	Species-independent constant, provided as input	17
b_{cr}	Coefficients of crown radius allometry	unitless	Species-independent constant, provided as input	17
a_{cd}	Coefficients of crown depth allometry	m	Species-independent constant, provided as input	18
b_{cd}	Coefficients of crown depth allometry	unitless	Species-independent constant, provided as input	18
$shape_{crown}$	Ratio between the radius of the crown at the top of the tree to the radius at the bottom of the crown being a global parameter	unitless	Global parameter, provided as input	Section 2.4.2
f_{gap}	Fraction of gaps (openings) in tree crowns	unitless	Constant, provided as input	Section 2.4.2
RD	Tree root depth	m	Tree variable, updated at each timestep	19
RB _{<i>t</i>}	Total tree fine root biomass	g	Tree variable, updated at each timestep	20



RB_l	Tree fine root biomass in layer l	g	Tree variable, updated at each timestep	20
ψ_{root}	Soil water potential in the tree root zone	MPa	Tree variable, updated at each timestep	21, 37
$\psi_{R,min}$	Root water potential below which there is no soil water uptake	MPa	Constant	21
G_l	soil-to-root water conductance in layer l	$\text{mmol H}_2\text{O m}^{-2} \text{s}^{-1} \text{MPa}^{-1}$	Variable, computed for each tree and layer at each timestep	21, 22
$L_{a,l}$	Tree total root length per unit area in layer l	m m^{-2}	Variable, computed for each tree and layer at each timestep	22
$L_{v,l}$	Tree total root length per unit soil volume in layer l	m m^{-3}	Variable, computed for each tree and layer at each timestep	23
SRL	Specific root length	m g^{-1}	Constant	22
r_s	Mean fine root radius	m	Constant	22
r_s	half of the mean distance between roots	m	Variable, computed for each tree and layer at each timestep	22, 23
Leaf physiology				
T_l	Leaf temperature	°C	Computed half-hourly for each crown layer	24, 25, 28-31, 33, 46
VPD_s	Vapor pressure deficit at the leaf surface	kPa	Computed half-hourly for each crown layer	35
c_s	CO ₂ concentration at the leaf surface	$\mu\text{mol mol}^{-1}$ (ppm or μbar)	Computed half-hourly for each crown layer	34
c_i	CO ₂ concentration at carboxylation sites	$\mu\text{mol mol}^{-1}$ (ppm or μbar)	Computed half-hourly for each crown layer	24, 34
A_n	Leaf-level net carbon assimilation rate	$\mu\text{mol CO}_2 \text{m}^{-2} \text{s}^{-1}$	Computed half-hourly for each crown layer	24, 52
A_v	Leaf-level net carbon assimilation rate limited by Rubisco activity	$\mu\text{mol CO}_2 \text{m}^{-2} \text{s}^{-1}$	Computed half-hourly for each crown layer	24
A_j	Leaf-level net carbon assimilation rate limited by RuBP regeneration	$\mu\text{mol CO}_2 \text{m}^{-2} \text{s}^{-1}$	Computed half-hourly for each crown layer	24
R_p	Photorespiration rate	$\mu\text{mol C m}^{-2} \text{s}^{-1}$	Computed half-hourly for each crown layer	24
R_d	Leaf dark respiration rate	$\mu\text{mol C m}^{-2} \text{s}^{-1}$	Computed half-hourly for each crown layer	33
R_{d-M}	Leaf dark respiration rate on a leaf dry mass basis	$\text{nmol CO}_2 \text{g}^{-1} \text{s}^{-1}$	Computed half-hourly for each crown layer	32
V_{cmax}	Maximum rate of carboxylation	$\mu\text{mol CO}_2 \text{m}^{-2} \text{s}^{-1}$	Computed half-hourly for each crown layer	24, 26, 28
V_{cmax-M}	Maximum rate of carboxylation on a leaf dry mass basis	$\mu\text{mol CO}_2 \text{g}^{-1} \text{s}^{-1}$	Computed half-hourly for each crown layer	26
J	Electron transport rate	$\mu\text{mol } e^- \text{m}^{-2} \text{s}^{-1}$	Computed half-hourly for each crown layer	24, 25
J_{max}	maximal electron transport capacity	$\mu\text{mol } e^- \text{m}^{-2} \text{s}^{-1}$	Computed half-hourly for each crown layer	25, 29



J_{max-M}	maximal electron transport capacity on a leaf dry mass basis	$\mu\text{mol } e^- \text{ g}^{-1} \text{ s}^{-1}$	Computed half-hourly for each crown layer	27
Γ^*	CO ₂ compensation point in the absence of dark respiration	μbar	Computed half-hourly for each crown layer	24, 30
K_m	Apparent kinetic constant of the Rubisco	μbar	Computed half-hourly for each crown layer	24, 31
θ	Curvature factor	unitless	Constant	25
α	Apparent quantum yield to electron transport	$\text{mol } e^- \text{ mol photons}^{-1}$	Constant	25
LSQ	Effective spectral quality of light	unitless	Constant	25
g_s	stomatal conductance to CO ₂	$\text{mol CO}_2 \text{ m}^{-2} \text{ s}^{-1}$	Computed half-hourly for each crown layer	34
g_{sw}	stomatal conductance to water vapor	$\text{mol H}_2\text{O m}^{-2} \text{ s}^{-1}$	Computed half-hourly for each crown layer	35
g_0	minimum leaf conductance for water vapor	$\text{mol H}_2\text{O m}^{-2} \text{ s}^{-1}$	Constant, provided by the user	35
g_1	Parameter of the stomatal conductance model	$\text{kPa}^{0.5}$	Computed daily for each tree	35, 36
ψ_{pd}	Leaf predawn water potential	MPa	Tree variable, computed daily	24, 25, 28, 29, 36-40
WSF_{ns}	Water stress factor for non-stomatal limitation	unitless	Tree variable, computed daily	28, 29, 40
WSF_s	Water stress factor for stomatal limitation	unitless	Tree variable, computed daily	36, 38-39
a	Parameter of WSF_{ns}	unitless	Constant	40
b	Parameter of WSF_s	unitless	Computed from tree-specific ψ_{ttp}	39, 39
E_l	Leaf-level transpiration rate	$\text{mol H}_2\text{O m}^{-2} \text{ s}^{-1}$	Computed half-hourly for each crown layer	41
λ	Latent heat of water vapor	J mol^{-1}	Computed half-hourly for each crown layer	41, 42
s	slope of the (locally linearized) relationship between saturated vapor pressure and temperature	Pa K^{-1}	Computed half-hourly for each crown layer	41
R_{ni}	isothermal net radiation	$\text{J m}^{-2} \text{ s}^{-1}$	Computed half-hourly for each crown layer	41, 43
g_H	total leaf conductance to heat	$\text{mol m}^{-2} \text{ s}^{-1}$	Computed half-hourly for each crown layer	41, 45
g_{bHf}	boundary layer conductance for free convection	$\text{mol m}^{-2} \text{ s}^{-1}$	Computed half-hourly for each crown layer	45, 46, 50
g_{bHu}	boundary layer for forced convection	$\text{mol m}^{-2} \text{ s}^{-1}$	Computed half-hourly for each crown layer	45, 47, 50
g_r	radiation conductance	$\text{mol m}^{-2} \text{ s}^{-1}$	Computed half-hourly for each crown layer	45, 48
g_w	total leaf conductance to water vapor	$\text{mol H}_2\text{O m}^{-2} \text{ s}^{-1}$	Computed half-hourly for each crown layer	41, 49
g_{bw}	boundary layer conductance to water vapor	$\text{mol H}_2\text{O m}^{-2} \text{ s}^{-1}$	Computed half-hourly for each crown layer	49, 50
S_{abs}	Absorbed solar radiation (PAR and NIR)	$\text{J m}^{-2} \text{ s}^{-1}$	Computed half-hourly for each crown layer	43



$B_{n,0}$	Net longwave radiation at the top of the canopy	$\text{J m}^{-2} \text{s}^{-1}$	Computed every half hour	43, 44
k_d	Coefficient of extinction of longwave radiation	Unitless	Constant	43
ε_l	Emissivity of the canopy leaves	Unitless	Constant	44, 48
ε_a	Emissivity of the atmosphere	Unitless	Computed every half hour	44
Tree carbon allocation and demography				
GPP_{ind}	Tree-level gross primary productivity	gC	Computed daily	51
NPP_{ind}	Tree-level net primary productivity	gC	Computed daily	51
NPP_{leaves}	Tree-level net primary productivity allocated to leaf production	gC	Computed daily	56
NPP_{wood}	Tree-level net primary productivity allocated to woody growth	gC	Computed daily	61
AGB	Tree aboveground biomass	kg	Computed daily	59-60
$R_{maintenan}$	Tree-level maintenance respiration	gC	Computed daily	51
R_{stem}	Stem maintenance respiration	$\mu\text{mol C s}^{-1}$	Computed daily	54
R_{growth}	Tree-level growth respiration	gC	Computed daily	51
LA_t	Tree-level total leaf area	m^2	Updated daily	55
LA_{opt}	Optimal tree leaf area	m^2	Updated daily	Section 2.6.2
LA_l	Leaf area in tree crown layer 1	m^2	Updated daily	51, 52-53
LA_{young}	Tree-level young leaf area	m^2	Updated daily	52-53, 56
LA_{mature}	Tree-level mature leaf area	m^2	Updated daily	52-53, 56
LA_{old}	Tree-level old leaf area	m^2	Updated daily	52-53, 56
q	Ratio of young or old leaf assimilation rate over mature leaf assimilation rate	unitless	Constant	52
q'	Ratio of young or old leaf respiration rate over mature leaf respiration rate	unitless	Constant	53
τ_{young}	Leaf residence time in the young age pool	yr	Computed for each tree	56
τ_{mature}	Leaf residence time in the young age pool	yr	Computed for each tree	56
τ_{old}	Leaf residence time in the young age pool	yr	Computed for each tree	56
SA	Tree sapwood area	m^2	Updated daily	54, 55
λ_1	Parameter for sapwood area computation	$\text{m}^2 \text{cm}^{-2}$	Constant	55
λ_2	Parameter for sapwood area computation	m cm^{-2}	Constant	55
δ_1	Parameter for sapwood area computation	$\text{m}^2 \text{cm}^{-2}$	Constant	55
δ_2	Parameter for sapwood area computation	$\text{cm}^3 \text{g}^{-1}$	Constant	55



f_{canopy}	Fraction of NPP_{ind} allocated to tree canopy (including leaves, fruits and twigs)	unitless	Constant, given as input	Sections 2.6.1 and 2.6.2
f_{leaves}	Fraction of NPP_{ind} allocated to leaves	unitless	Constant	Section 2.6.2, 56
f_{fruit}	Fraction of NPP_{ind} allocated to fruits	unitless	Constant	Section 2.6.1
f_{twigs}	Fraction of NPP_{ind} allocated to twigs	unitless	Constant	Section 2.6.1
f_{wood}	Fraction of NPP_{ind} allocated to wood	unitless	Constant, given as input	Section 2.6.2
$\psi_{T,o}$	Water potential threshold for accelerating old leaf shedding	MPa	Computed daily for each tree	58
$a_{T,o}$	Parameter to compute $\psi_{T,o}$ (modulates old leaf drought tolerance)	unitless	Constant, given as input	58
$b_{T,o}$	Parameter to compute $\psi_{T,o}$ (modulates the height dependence of leaf susceptibility to drought)	MPa	Constant, given as input	58
f_o	Factor of the acceleration of old leaf shedding	unitless	Updated daily for each tree	Section 2.6.2
δ_o	Parameter controlling the pace of old leaf shedding acceleration (Δf_o)	unitless	Constant, given as input	
NSC_r	Maximal amount of stored non-structural carbohydrates	gC	Updated daily for each tree	59
ΔV	Increment of stem volume	m ³	Computed daily for each tree	61
$Senesc$	Growth senescence factor	unitless	Computed daily for each tree	61-62
Δdbh	Trunk diameter growth	m	Computed daily for each tree	Section 2.6.4
dbh_{mature}	Diameter threshold beyond which the tree is fertile	m	Computed once for each tree	63
σ_{disp}	Scale parameter of the Rayleigh distribution for seed dispersal	m	Constant	Section 2.7.1
n_s	Number of reproduction opportunities per mature tree	number of seeds	Constant	Section 2.7.1
N_{tot}	Intensity of the external seed rain	number of seeds per hectare	Constant, given as input	64
$n_{\text{ext},s}$	Species-specific number of dispersal events due to the external seed rain	number of seeds	Computed once for each species	64
n_{ha}	Area of the simulated plot	ha	Constant, computed from dimensions given as input	64
LAI_{max}	LAI threshold beyond which the seedling leaf carbon balance is negative	m ² m ⁻²	Computed once for each tree	Section 2.7.1



d	Tree death rate	events yr ⁻¹	Updated daily at tree level	65-66
d_b	Background death rate	events yr ⁻¹	Computed once per tree	65
m	reference background mortality rate	events yr ⁻¹	Constant, provided as input	66
$ws_{g_{lim}}$	Parameter of d_b	g cm ⁻³	Constant	66
d_{starv}	Death rate due to carbon starvation	events yr ⁻¹	Updated daily at tree level	65
$d_{treefall}$	Death rate due to treefall	events yr ⁻¹	Updated daily at tree level	65
θ	Parameter of treefall probability	m	Computed once per tree	67
$d_{drought}$	Death rate due to drought	events yr ⁻¹	Updated daily at tree level	65
v_T	Variance for treefall probability	unitless	Computed once per tree	67
hurt	Parameter of secondary treefall probability	m	Updated daily for each tree	Section 2.7.2
ψ_{lethal}	Water potential threshold for drought-induced mortality	MPa	Computed once per tree	68

2421

Appendix B

Table B1. Representation of stomatal conductance, water stress effect on leaf gas exchange and tree transpiration in several vegetation

models. g_0 , cuticular or minimal stomatal conductance, i.e. g_s when $A \rightarrow 0$; A , CO_2 assimilation rate; c_s , CO_2 concentration at the leaf surface; D_s , vapour pressure deficit at the leaf surface; h_s , fractional relative humidity at the leaf surface; Γ , CO_2 compensation point; V_{cmax} and J_{max} are the maximum carboxylation rate and electron transport rate. All 0 subscript denotes the values without water stress (except for g_0 by convention). Note stomatal conductance to H_2O is 1.6 times higher than stomatal conductance to CO_2 , we here only represent stomatal conductance to H_2O .

Name	Vegetation model		Stomatal conductance		Water stress effect on leaf gas exchange		Tree transpiration
	Reference	Type	Model	Reference/type	Stomatal limitations	Non-stomatal limitations	
ED2	(Longo et al., 2018; Medvigy et al., 2009)	Cohort-based vegetation model	$g_s = g_0 + \frac{a_1 \times A}{(c_s - \Gamma)(1 + \frac{D_s}{D_0})}$	(Leuning, 1995)/ empirical model	<p>The plant net CO_2 assimilation and evapotranspiration rates (x_{net}) are computed as a linear combination of their rates under open (x_o) and close (x_c) stomata:</p> $x_{net} = f x_o + (1 - f) x_c$ <p>with $f = \frac{1}{1 + \frac{Demand}{Supply}} = \frac{1}{1 + \frac{E_0 \times LA}{K \times W_{avail,tot} \times B_{root}}}$</p> <p>where E_0 is the evapotranspiration rate under conditions of open stomata times and LA the total plant leaf surface area, and $W_{avail,tot}$ is the amount of water accessible by the vegetation layer, B_{root} the plant root biomass, and K an optimized constant.</p>	<p>Computed with: $E_0 = \varphi_0 \times SLA \times B_{leaf}$ with B_{leaf} the tree leaf biomass and φ_0 its evapotranspiration rate, obtained by solving a set of 6 equations of 6 unknowns (after determining the leaf temperature using a surface energy balance submodel), among which: $\varphi_0 = g_{bw} \times (e_s - e_a)$ $\varphi_0 = g_s \times (e_l - e_s)$</p>	
ED2-hydro	(Powell et al., 2018; Xu et al., 2016)	ED2 with a new module of plant hydraulics	<p>Solution of:</p> $\frac{\partial}{\partial g_w} (A_{net} - \lambda g_w D_a) = 0$ <p>with $g_w = \frac{g_s g_b}{g_s + g_b}$</p> <p>and λ is the Lagrangian multiplier of the optimization problem, representing the marginal water use efficiency (marginal increase in A_{net} per unit change of water loss)</p>	(Vico et al., 2013)/ optimization model, under CO_2 (Rubisco) and light (RuBP regeneration/electr on transport) co-limitations	$\lambda = \lambda_0 \times \exp(\beta \times \psi_{pot})$ with λ_0 the value of λ when there is no water stress and β an empirical factor taken from Manzoni et al. (2011)	$V_{cmax} = V_{cmax,0} \times \left[1 + \left(\frac{\psi_{leaf}}{\pi_{tip}} \right)^a \right]^{-1}$ $J_{max} = J_{max,0} \times \left[1 + \left(\frac{\psi_{leaf}}{\pi_{tip}} \right)^a \right]^{-1}$ where $V_{cmax,0}$ and $J_{max,0}$ denotes the photosynthetic capacities without water stress, and a is a shape factor estimated from Brodribb et al. (2003).	Similarly to Medvigy et al. 2009, $E_0 = \frac{g_s g_b}{g_s + g_b} \times D_a \times LA$
TFS	(Fyllas et al., 2014)		$g_s = g_0 + 1.6 \times \left(1 + \frac{g_1}{\sqrt{D_s}} \right) \times \frac{A}{c_s}$ <p>g_1 is an empirical coefficient*, associated to the water use efficiency (to the Lagrangian).</p>	(Medlyn et al., 2011)/ optimization, for ele tron-transport limited photosynthesis (light limitation)	$g_s = g_{s,0} \times \frac{\theta_l - \theta_{wp}}{\theta_{fc} - \theta_{wp}}$ where θ_{wp} , θ_{fc} , θ_{wp} are the actual soil water available for tree i, and the soil water content at field capacity and wilting point respectively.	-	Following MAESTRA (Medlyn et al., 2007), an iterative procedure is used to solve the energy balance of the canopy of each tree, under which the Penman-Monteith equation is used to estimate canopy transpiration.



TFS-Hydro	(Christoffersen et al., 2016)	TFS with a new module of plant hydraulics	$g_s = g_{s,0} \times \left[\frac{\psi_{leaf}}{1 + \psi_{g_s,50}} \right]^{a_{g_s}-1}$ <p>where $\psi_{g_s,50}$ is the leaf water potential at 50% stomatal closure (assumed a 1:1 relationship between $\psi_{g_s,50}$ and the water potential at 20% loss of xylem hydraulic conductivity ($P_{20,x}$), following results from (Brodrribb et al., 2003)), and a_{g_s} is the slope of the curve at $\psi_{leaf} = \psi_{g_s,50}$, computed from $\psi_{g_s,50}$ using the same relationship that relates α_x and $P_{50,x}$.</p>	$g_0 = g_{0,0} \times \sum_j \tau_j \frac{\psi_j - \psi_c}{\psi_o - \psi_c}$ <p>where ψ_j is the soil water potential of soil layer j, and ψ_o and ψ_c are the soil water potential at which the stomata are fully open and fully closed respectively, and τ_j is the relative root fraction of soil layer j.</p>	$V_{c,max} = V_{c,max,0} \times \sum_j \tau_j \frac{\psi_j - \psi_c}{\psi_o - \psi_c}$	<p>Iterative procedure</p> <p>An iterative procedure is used to solve the energy balance (determine the leaf temperature and internal CO₂)</p>
Multi-layer CLM4.5	(Bonan et al., 2014)	DGM	$g_s = g_0 + g_1 \times A \times \frac{h_s}{C_s}$ <p>g_s is iteratively computed such that (1) further opening does not yield a sufficient carbon gain per unit water loss (defined by a stomatal efficiency parameter) or (2) further opening causes leaf water potential to decrease below the minimum sustainable leaf water potential that prevents xylem cavitation</p>	<p>Inspired from the SPA model (Williams et al., 1996)/ optimization within limitations imposed by water use efficiency, plant water storage, and soil-to-leaf water transport</p> <p>(Medlyn et al., 2011)/ optimization, under light</p>	<p>The optimization includes a dependence to ψ_{leaf}, where ψ_{leaf} is computed at each timestep (30-60 min) with Darcy's law (soil-to-leaf pathway, including capacitance).</p>	<p>CML4.5 default: $V_{c,max} = V_{c,max,0} \times \sum_j \tau_j \frac{\psi_j - \psi_c}{\psi_o - \psi_c}$</p>
CLM5	(Kennedy et al., 2019)	Stand-based	$g_s = g_0 + 1.6 \times \left(1 + \frac{g_1}{\sqrt{D_s}} \right) \times \frac{A}{C_s}$			



MAESPA	(Duursma et al., 2012)	Individual- and stand-based model	<p>g_s is an empirical coefficient*, associated to the water use efficiency (to the Lagrangian).</p> $g_s = g_0 + 1.6 \times \frac{A}{C_s} \times \frac{1 + e^{s_f \psi_f}}{1 + e^{s_f(\psi_f - \psi_{leaf})}}$ <p>where ψ_{leaf} is computed at each time step using Darcy's law ($E_L = k_L \times (\psi_{soil} - \psi_{leaf})$)</p>	limitation (RuBP regeneration)	(Tuzet et al., 2003)/ empirical	<p>Already implemented in g_s computation.</p>	$V_{c,max}$ $= V_{c,max,0} \times 2^{-\frac{(\psi_{leaf})^{a_{g_s}}}{(\psi_{g_s,50})^{a_{g_s}}}}$ <p>where $\psi_{g_s,50}$ is the leaf water potential at 50% loss of stomatal conductance and a_{g_s} is a shape-fitting parameter. The solution for vegetation water potential is the set of values that matches supply with demand, maintaining water balance across each of the vegetation water potential nodes (ψ_{root}, ψ_{stem}, $\psi_{shoot-leaf}$, $\psi_{shade-leaf}$) based on Darcy's law (without capacitance).</p>	concentration), under which transpiration is computed as $E_0 = \frac{g_s g_b}{g_s + g_b} \times D_a \times LA$
CABLE	(De Kauwe et al., 2015a, b)	DGVM (vegetation is represented using a single layer, two-leaf canopy model separated into sunlit and shaded)	<p>Standard version of CABLE (De Kauwe et al., 2015a) :</p> $g_1 = g_{1,0} \times \sum_j \frac{\theta_i - \theta_{wp}}{\theta_{fc} - \theta_{wp}}$ <p>with θ_i the volumetric soil water content and θ_{fc} the fraction of root mass in soil layer j, and θ_{wp} the soil wilting point and θ_{fc} its field capacity.</p> <p>New expression for drought sensitivity of gas exchange: $V_{c,max} = V_{c,max,0} \times \frac{1 + e^{s_f \psi_f}}{1 + e^{s_f(\psi_f - \psi_{pd})}}$ where b is a fitted (species-specific) parameter representing the sensitivity of g_1 to leaf predawn water potential ψ_{pd} and taken from (Zhou et al., 2013, 2014), while $g_{1,0}$ values are drawn from (Lin et al., 2015).</p>	<p>(Medlyn et al., 2011)/ optimization, under light limitation (RuBP regeneration)</p> <p>(was the model of (Leuning, 1995) in previous versions of CABLE (Wang et al., 2011)</p>	<p>Standard version of CABLE (De Kauwe et al., 2015a) :</p> $g_1 = g_{1,0} \times \sum_j \frac{\theta_i - \theta_{wp}}{\theta_{fc} - \theta_{wp}}$ <p>with θ_i the volumetric soil water content and θ_{fc} the fraction of root mass in soil layer j, and θ_{wp} the soil wilting point and θ_{fc} its field capacity.</p> <p>New expression for drought sensitivity of gas exchange: $V_{c,max} = V_{c,max,0} \times \frac{1 + e^{s_f \psi_f}}{1 + e^{s_f(\psi_f - \psi_{pd})}}$ where b is a fitted (species-specific) parameter representing the sensitivity of g_1 to leaf predawn water potential ψ_{pd} and taken from (Zhou et al., 2013, 2014), while $g_{1,0}$ values are drawn from (Lin et al., 2015).</p>	<p>Following MAESTRA (Medlyn et al., 2007), an iterative procedure is used to solve the energy balance of the canopy of each tree, under which the Penman-Monteith equation is used to estimate canopy transpiration.</p> <p>transpiration from the vegetation to the atmosphere is controlled by several resistances operating in series, both above (aerodynamic) and within the canopy (stomatal and leaf boundary layer), and longwave radiative balance through radiative conductance on net available energy. These resistances in serial, result in a relatively weak coupling between the canopy surface and the atmosphere.</p>	<p>Following MAESTRA (Medlyn et al., 2007), an iterative procedure is used to solve the energy balance of the canopy of each tree, under which the Penman-Monteith equation is used to estimate canopy transpiration.</p> <p>transpiration from the vegetation to the atmosphere is controlled by several resistances operating in series, both above (aerodynamic) and within the canopy (stomatal and leaf boundary layer), and longwave radiative balance through radiative conductance on net available energy. These resistances in serial, result in a relatively weak coupling between the canopy surface and the atmosphere.</p>	
ORCHID EE	(Krinner et al., 2005; Naudts et al., 2015)	DGVM	$g_s = mA \frac{h_r}{c_a} + b$	(Ball et al., 1987)	<p>In the version of (Krinner et al., 2005): The photosynthetic capacities, $V_{c,max}$ and J_{max}, are multiplied by a water stress factor that is:</p>	<p>In the version of (Krinner et al., 2005): The photosynthetic capacities, $V_{c,max}$ and J_{max}, are multiplied by a water stress factor that is:</p>		



<p>with m and b derived from laboratory measurements.</p>		<p>1 if $f_w > f_o$</p> $1 - \frac{f_w - f_c}{f_o - f_c} \text{ if } f_c < f_w < f_o$ <p>0 if $f_w < f_c$</p> <p>with f_w the water fraction available for the plant in the root zone, and f_c and f_o the soil water fractions inducing, respectively, closure and maximum opening of stomata.</p>	
	<p>In the CAN version of (Naudts et al., 2015):</p> <p>The model calculates plant water supply according to the implementation of hydraulic architecture by (Hickler et al., 2006), i.e. using Darcy's law and accounting for the hydraulic resistances of fine roots, sapwood and leaves. If the transpiration calculated by the energy budget exceeds the amount of water a plant can transport from the soil to its stomata, transpiration is limited to the plant water supply, and stomatal conductance is then recalculated such that the transpiration equals the amount of water a plant can transport. The energy budget and photosynthesis are then recalculated. This may require up to 10 iterations to converge.</p>		



LPI	(Sitch et al., 2003)	<p>The model uses the Farquhar model of photosynthesis as generalized for global modelling purposes by (Collatz et al., 1991). In absence of water stress, canopy conductance is derived from the daytime carbon assimilation rate:</p> $g_c = g_{min} + \frac{1.6 A}{c_a(1 - \lambda)}$	(Collatz et al., 1991)	<p>Under water stress i.e. when $\min [1, \frac{E_{supply}}{E_{demand}}] < 1$,</p> <p>The equations of evapotranspiration rate, assimilation rate and the one related assimilation rate and canopy conductance are solved simultaneously to yield values of canopy conductance consistent with the transpiration rate.</p>	<p>< 1 Daily evapotranspiration is calculated for each PFT as the minimum of a plant- and soil-limited supply function (E_{supply}) and the atmospheric demand (E_{demand}). E_{supply} is the product of a plant root-weighted soil moisture availability and a maximum transpiration rate; E_{demand} is calculated following Monteith's empirical relation between evaporation efficiency and surface conductance, that uses g_{pot}, the nonwater-stressed potential canopy conductance calculated by the photosynthesis routine</p>
-----	----------------------	--	------------------------	--	--

30 *although fitted empirically to leaf exchange experimental data (Lin et al., 2015), attempts have been made to relate g_l to functional traits and/or
 31 climatological variables (wood density, Lin et al., 2015; leaf $\delta^{13}C$, Franks et al., 2018), based on the premise that water use efficiency should be
 32 associated to functional strategies. See also values reported in Domingues et al. (2014).



2434 **Table B2. Examples of observational or experimental studies that explored the relative roles of stomatal and non-**
 2435 **stomatal limitations of photosynthesis under drought conditions.**

Key message for vegetation models	Reference	Studied system	Main results
Stomatal-limitation only	Santos et al., 2018	57 canopy and understory trees within a central Amazonian forest	Photosynthesis decreased during the extreme dry season, and this was only related to stomatal closure (decline in stomatal conductance) and not to leaf biochemical changes (sustained chlorophyll concentration and fluorescence, and nutrient concentration).
	Rowland et al., 2015	Trees in the Throughfall Exclusion and control plots in Caixuana, Amazonia.	No differences in V_{cmax} and J_{max} between the throughfall exclusion plot and the control plot.
	Trueba et al., 2019	Mature individuals of 10 angiosperms species located on the campus of UCLA and a park in LA	The stomatal and leaf hydraulic systems (50% loss of g_s , K_{leaf}) show early functional declines before cell integrity is lost. Substantial damage to the photochemical apparatus (maximum quantum yield of the photosystem) occurs at extreme dehydration, after turgor loss and complete stomatal closure, and seems to be irreversible.
Both stomatal and non-stomatal limitations	Zhou et al., 2013	Meta-analysis of 22 experimental datasets where photosynthesis, stomatal conductance and predawn leaf water potential were measured at increasing water stress, spanning a range of plant functional types	Photosynthesis was found almost universally to decrease more than could be explained by the reduction in g_1 (parameter of the Medlyn model), implying a decline in apparent carboxylation capacity (V_{cmax}).
	Zhou et al., 2014	Two experiments, one in Australia on Eucalyptus, one in Spain on Quercus, on plants grown in glasshouses under control conditions. The non-stomatal response was partitioned into effects on mesophyll conductance (g_m), the maximum Rubisco activity (V_{cmax}) and the maximum electron transport rate (J_{max}).	They found consistency among the drought responses of g_1 , g_m , V_{cmax} and J_{max} , suggesting that drought imposes limitations on Rubisco activity and RuBP regeneration capacity concurrently with declines in stomatal and mesophyll conductance. Within each experiment, the more xeric species showed relatively high g_1 under moist conditions, low drought sensitivity of g_1 , g_m , V_{cmax} and J_{max} , and more negative values of the critical pre-dawn water potential at which V_{cmax} declines most steeply, compared with the more mesic species. Results showed that the decline in V_{cmax} is not explained just by the decline in g_m , but by the decline in both g_m and V_{cmax} .
	Egea et al., 2011	Outputs from a coupled A-gs model that uses a soil water content-dependent water stress factor were compared to leaf-level values obtained from the literature.	The sensitivity analyses emphasized the necessity to combine both stomatal and non-stomatal limitations of A in coupled A-gs models to accurately capture the observed functional relationships A vs. g_s and A/ g_s vs. g_s in response to drought. Accounting for water stress in coupled A-gs models by imposing either stomatal or biochemical limitations of A, as commonly practiced in most ecosystem models, failed to reproduce the observed functional relationship between key leaf gas exchange attributes.
	Drake et al., 2017	Plants in pots of four tree species originating from contrasting	as soil water content (θ) was reduced under increasing drought, all species responded by reducing g_s , resulting in reduced C_i and A_{sat} . However, A_{sat} was reduced to



		hydrological environment, placed in the field under rainout shelters. Comparison with coupled stomatal conductance-photosynthesis model.	a larger degree than would be predicted only by stomatal reduction of C_i , indicating a coincident reduction in photosynthetic capacity with declining θ . The best model include both stomatal and non-stomatal limitations.
--	--	--	---

2436

2437

2438

2439 **References of Appendix B**

2440

2441 Ball, J. T., Woodrow, I. E., and Berry, J. A.: A model predicting stomatal conductance and its contribution to the control of
2442 photosynthesis under different environmental conditions, in: Progress in photosynthesis research, edited by: Biggins, J.,
2443 Springer Netherlands, 221–224, https://doi.org/10.1007/978-94-017-0519-6_48, 1987.

2444 Bonan, G. B., Williams, M., Fisher, R. A., and Oleson, K. W.: Modeling stomatal conductance in the earth system: linking
2445 leaf water-use efficiency and water transport along the soil–plant–atmosphere continuum, *Geosci. Model Dev.*, 7, 2193–
2446 2222, <https://doi.org/10.5194/gmd-7-2193-2014>, 2014.

2447 Bondeau, A., Smith, P. C., Zaehle, S., Schaphoff, S., Lucht, W., Cramer, W., Gerten, D., Lotze-Campen, H., Müller, C.,
2448 Reichstein, M., and Smith, B.: Modelling the role of agriculture for the 20th century global terrestrial carbon balance,
2449 *Global Change Biology*, 13, 679–706, <https://doi.org/10.1111/j.1365-2486.2006.01305.x>, 2007.

2450 Brodribb, T. J., Holbrook, N. M., Edwards, E. J., and Gutiérrez, M. V.: Relations between stomatal closure, leaf turgor and
2451 xylem vulnerability in eight tropical dry forest trees, *Plant, Cell & Environment*, 26, 443–450,
2452 <https://doi.org/10.1046/j.1365-3040.2003.00975.x>, 2003.

2453 Christoffersen, B. O., Gloor, M., Fauset, S., Fyllas, N. M., Galbraith, D. R., Baker, T. R., Kruijt, B., Rowland, L., Fisher, R.
2454 A., Binks, O. J., Sevanto, S., Xu, C., Jansen, S., Choat, B., Mencuccini, M., McDowell, N. G., and Meir, P.: Linking
2455 hydraulic traits to tropical forest function in a size-structured and trait-driven model (TFS v.1-Hydro), *Geosci. Model Dev.*,
2456 9, 4227–4255, <https://doi.org/10.5194/gmd-9-4227-2016>, 2016.

2457 Collatz, G. J., Ball, J. T., Grivet, C., and Berry, J. A.: Physiological and environmental regulation of stomatal conductance,
2458 photosynthesis and transpiration: a model that includes a laminar boundary layer, *Agricultural and Forest Meteorology*, 54,
2459 107–136, [https://doi.org/10.1016/0168-1923\(91\)90002-8](https://doi.org/10.1016/0168-1923(91)90002-8), 1991.

2460 De Kauwe, M. G., Kala, J., Lin, Y.-S., Pitman, A. J., Medlyn, B. E., Duursma, R. A., Abramowitz, G., Wang, Y.-P., and
2461 Miralles, D. G.: A test of an optimal stomatal conductance scheme within the CABLE land surface model, *Geoscientific
2462 Model Development*, 8, 431–452, <https://doi.org/10.5194/gmd-8-431-2015>, 2015a.

2463 De Kauwe, M. G., Zhou, S.-X., Medlyn, B. E., Pitman, A. J., Wang, Y.-P., Duursma, R. A., and Prentice, I. C.: Do land surface
2464 models need to include differential plant species responses to drought? Examining model predictions across a mesic-xeric
2465 gradient in Europe, *Biogeosciences*, 12, 7503–7518, <https://doi.org/10.5194/bg-12-7503-2015>, 2015b.



- 2466 Domingues, T. F., Martinelli, L. A., and Ehleringer, J. R.: Seasonal patterns of leaf-level photosynthetic gas exchange in an
2467 eastern Amazonian rain forest, *Plant Ecology & Diversity*, 7, 189–203, <https://doi.org/10.1080/17550874.2012.748849>,
2468 2014.
- 2469 Drake, J. E., Power, S. A., Duursma, R. A., Medlyn, B. E., Aspinwall, M. J., Choat, B., Creek, D., Eamus, D., Maier, C.,
2470 Pfautsch, S., Smith, R. A., Tjoelker, M. G., and Tissue, D. T.: Stomatal and non-stomatal limitations of photosynthesis for
2471 four tree species under drought: A comparison of model formulations, *Agricultural and Forest Meteorology*, 247, 454–466,
2472 <https://doi.org/10.1016/j.agrformet.2017.08.026>, 2017.
- 2473 Duursma, R. A., Medlyn, B. E., and others: MAESPA: a model to study interactions between water limitation, environmental
2474 drivers and vegetation function at tree and stand levels, with an example application to $[\text{CO}_2]$ drought interactions,
2475 2012.
- 2476 Egea, G., Verhoef, A., and Vidale, P. L.: Towards an improved and more flexible representation of water stress in coupled
2477 photosynthesis–stomatal conductance models, *Agricultural and Forest Meteorology*, 151, 1370–1384,
2478 <https://doi.org/10.1016/j.agrformet.2011.05.019>, 2011.
- 2479 Franks, P. J., Bonan, G. B., Berry, J. A., Lombardozzi, D. L., Holbrook, N. M., Herold, N., and Oleson, K. W.: Comparing
2480 optimal and empirical stomatal conductance models for application in Earth system models, *Global Change Biology*, 24,
2481 5708–5723, <https://doi.org/10.1111/gcb.14445>, 2018.
- 2482 Fyllas, N. M., Gloor, E., Mercado, L. M., Sitch, S., Quesada, C. A., Domingues, T. F., Galbraith, D. R., Torre-Lezama, A.,
2483 Vilanova, E., Ramírez-Angulo, H., Higuchi, N., Neill, D. A., Silveira, M., Ferreira, L., Aymard C., G. A., Malhi, Y.,
2484 Phillips, O. L., and Lloyd, J.: Analysing Amazonian forest productivity using a new individual and trait-based model (TFS
2485 v.1), *Geosci. Model Dev.*, 7, 1251–1269, <https://doi.org/10.5194/gmd-7-1251-2014>, 2014.
- 2486 Hickler, T., Prentice, I. C., Smith, B., Sykes, M. T., and Zaehle, S.: Implementing plant hydraulic architecture within the LPJ
2487 Dynamic Global Vegetation Model, *Global Ecology and Biogeography*, 15, 567–577, <https://doi.org/10.1111/j.1466-8238.2006.00254.x>, 2006.
- 2489 Kennedy, D., Swenson, S., Oleson, K. W., Lawrence, D. M., Fisher, R., Costa, A. C. L. da, and Gentine, P.: Implementing
2490 Plant Hydraulics in the Community Land Model, Version 5, *Journal of Advances in Modeling Earth Systems*, 11, 485–
2491 513, <https://doi.org/10.1029/2018MS001500>, 2019.
- 2492 Krinner, G., Viovy, N., de Noblet-Ducoudré, N., Ogée, J., Polcher, J., Friedlingstein, P., Ciais, P., Sitch, S., and Prentice, I.
2493 C.: A dynamic global vegetation model for studies of the coupled atmosphere-biosphere system, *Global Biogeochem.*
2494 *Cycles*, 19, GB1015, <https://doi.org/10.1029/2003GB002199>, 2005.
- 2495 Leuning, R.: A critical appraisal of a combined stomatal-photosynthesis model for C3 plants, *Plant, Cell & Environment*, 18,
2496 339–355, <https://doi.org/10.1111/j.1365-3040.1995.tb00370.x>, 1995.
- 2497 Lin, Y.-S., Medlyn, B. E., Duursma, R. A., Prentice, I. C., Wang, H., Baig, S., Eamus, D., de Dios, V. R., Mitchell, P.,
2498 Ellsworth, D. S., de Beeck, M. O., Wallin, G., Uddling, J., Tarvainen, L., Linderson, M.-L., Cernusak, L. A., Nippert, J.
2499 B., Ocheltree, T. W., Tissue, D. T., Martin-StPaul, N. K., Rogers, A., Warren, J. M., De Angelis, P., Hikosaka, K., Han,



- 2500 Q., Onoda, Y., Gimeno, T. E., Barton, C. V. M., Bennie, J., Bonal, D., Bosc, A., Löw, M., Macinins-Ng, C., Rey, A.,
2501 Rowland, L., Setterfield, S. A., Tausz-Posch, S., Zaragoza-Castells, J., Broadmeadow, M. S. J., Drake, J. E., Freeman, M.,
2502 Ghannoum, O., Hutley, L. B., Kelly, J. W., Kikuzawa, K., Kolari, P., Koyama, K., Limousin, J.-M., Meir, P., Lola da
2503 Costa, A. C., Mikkelsen, T. N., Salinas, N., Sun, W., and Wingate, L.: Optimal stomatal behaviour around the world, *Nature*
2504 *Clim. Change*, 5, 459–464, <https://doi.org/10.1038/nclimate2550>, 2015.
- 2505 Longo, M., Knox, R. G., Levine, N. M., Alves, L. F., Bonal, D., Camargo, P. B., Fitzjarrald, D. R., Hayek, M. N., Restrepo-
2506 Coupe, N., Saleska, S. R., Silva, R. da, Stark, S. C., Tapajós, R. P., Wiedemann, K. T., Zhang, K., Wofsy, S. C., and
2507 Moorcroft, P. R.: Ecosystem heterogeneity and diversity mitigate Amazon forest resilience to frequent extreme droughts,
2508 *New Phytologist*, 914–931, <https://doi.org/10.1111/nph.15185>@10.1111/(ISSN)1469-
2509 8137.DroughtImpactsonTropicalForests, 2018.
- 2510 Manzoni, S., Vico, G., Katul, G., Fay, P. A., Polley, W., Palmroth, S., and Porporato, A.: Optimizing stomatal conductance
2511 for maximum carbon gain under water stress: a meta-analysis across plant functional types and climates, *Functional*
2512 *Ecology*, 25, 456–467, <https://doi.org/10.1111/j.1365-2435.2010.01822.x>, 2011.
- 2513 Medlyn, B. E., Pepper, D. A., O’Grady, A. P., and Keith, H.: Linking leaf and tree water use with an individual-tree model,
2514 *Tree Physiol*, 27, 1687–1699, <https://doi.org/10.1093/treephys/27.12.1687>, 2007.
- 2515 Medlyn, B. E., Duursma, R. A., Eamus, D., Ellsworth, D. S., Prentice, I. C., Barton, C. V. M., Crous, K. Y., De Angelis, P.,
2516 Freeman, M., and Wingate, L.: Reconciling the optimal and empirical approaches to modelling stomatal conductance,
2517 *Global Change Biology*, 17, 2134–2144, <https://doi.org/10.1111/j.1365-2486.2010.02375.x>, 2011.
- 2518 Medvigy, D., Wofsy, S. C., Munger, J. W., Hollinger, D. Y., and Moorcroft, P. R.: Mechanistic scaling of ecosystem function
2519 and dynamics in space and time: Ecosystem Demography model version 2, *J. Geophys. Res.*, 114, G01002,
2520 <https://doi.org/10.1029/2008JG000812>, 2009.
- 2521 Naudts, K., Ryder, J., McGrath, M. J., Otto, J., Chen, Y., Valade, A., Bellasen, V., Berhongaray, G., Bönisch, G., Campioli,
2522 M., Ghattas, J., De Groote, T., Haverd, V., Kattge, J., MacBean, N., Maignan, F., Merilä, P., Penuelas, J., Peylin, P., Pinty,
2523 B., Pretzsch, H., Schulze, E. D., Solyga, D., Vuichard, N., Yan, Y., and Luysaert, S.: A vertically discretised canopy
2524 description for ORCHIDEE (SVN r2290) and the modifications to the energy, water and carbon fluxes, *Geosci. Model*
2525 *Dev.*, 8, 2035–2065, <https://doi.org/10.5194/gmd-8-2035-2015>, 2015.
- 2526 Powell, T. L., Koven, C. D., Johnson, D. J., Faybishenko, B., Fisher, R. A., Knox, R. G., McDowell, N. G., Condit, R., Hubbell,
2527 S. P., Wright, S. J., Chambers, J. Q., and Kueppers, L. M.: Variation in hydroclimate sustains tropical forest biomass and
2528 promotes functional diversity, *New Phytologist*, 219, 932–946, <https://doi.org/10.1111/nph.15271>, 2018.
- 2529 Rowland, L., Lobo-do-Vale, R. L., Christoffersen, B. O., Melém, E. A., Kruijt, B., Vasconcelos, S. S., Domingues, T., Binks,
2530 O. J., Oliveira, A. A. R., Metcalfe, D., da Costa, A. C. L., Mencuccini, M., and Meir, P.: After more than a decade of soil
2531 moisture deficit, tropical rainforest trees maintain photosynthetic capacity, despite increased leaf respiration, *Glob Change*
2532 *Biol*, 21, 4662–4672, <https://doi.org/10.1111/gcb.13035>, 2015.



- 2533 Sakschewski, B., von Bloh, W., Boit, A., Rammig, A., Kattge, J., Poorter, L., Peñuelas, J., and Thonicke, K.: Leaf and stem
2534 economics spectra drive diversity of functional plant traits in a dynamic global vegetation model, *Glob Change Biol*, n/a/
2535 n/a, <https://doi.org/10.1111/gcb.12870>, 2015.
- 2536 Sakschewski, B., von Bloh, W., Boit, A., Poorter, L., Peña-Claros, M., Heinke, J., Joshi, J., and Thonicke, K.: Resilience of
2537 Amazon forests emerges from plant trait diversity, *Nature Climate Change*, 6, 1032–1036,
2538 <https://doi.org/10.1038/nclimate3109>, 2016.
- 2539 Santos, V. A. H. F. dos, Ferreira, M. J., Rodrigues, J. V. F. C., Garcia, M. N., Ceron, J. V. B., Nelson, B. W., and Saleska, S.
2540 R.: Causes of reduced leaf-level photosynthesis during strong El Niño drought in a Central Amazon forest, *Global Change*
2541 *Biology*, 24, 4266–4279, <https://doi.org/10.1111/gcb.14293>, 2018.
- 2542 Sitch, S., Smith, B., Prentice, I. C., Arneth, A., Bondeau, A., Cramer, W., Kaplan, J. O., Levis, S., Lucht, W., Sykes, M. T.,
2543 Thonicke, K., and Venevsky, S.: Evaluation of ecosystem dynamics, plant geography and terrestrial carbon cycling in the
2544 LPJ dynamic global vegetation model, *Glob. Change Biol.*, 9, 161–185, <https://doi.org/10.1046/j.1365-2486.2003.00569.x>,
2545 2003.
- 2546 Smith, B., Prentice, I. C., and Sykes, M. T.: Representation of vegetation dynamics in the modelling of terrestrial ecosystems:
2547 comparing two contrasting approaches within European climate space, *Global Ecology and Biogeography*, 10, 621–637,
2548 <https://doi.org/10.1046/j.1466-822X.2001.t01-1-00256.x>, 2001.
- 2549 Trueba, S., Pan, R., Scoffoni, C., John, G. P., Davis, S. D., and Sack, L.: Thresholds for leaf damage due to dehydration:
2550 declines of hydraulic function, stomatal conductance and cellular integrity precede those for photochemistry, *New*
2551 *Phytologist*, 223, 134–149, <https://doi.org/10.1111/nph.15779>, 2019.
- 2552 Tuzet, A., Perrier, A., and Leuning, R.: A coupled model of stomatal conductance, photosynthesis and transpiration, *Plant*,
2553 *Cell & Environment*, 26, 1097–1116, <https://doi.org/10.1046/j.1365-3040.2003.01035.x>, 2003.
- 2554 Vico, G., Manzoni, S., Palmroth, S., Weih, M., and Katul, G.: A perspective on optimal leaf stomatal conductance under CO₂
2555 and light co-limitations, *Agricultural and Forest Meteorology*, 182–183, 191–199,
2556 <https://doi.org/10.1016/j.agrformet.2013.07.005>, 2013.
- 2557 Wang, Y. P., Kowalczyk, E., Leuning, R., Abramowitz, G., Raupach, M. R., Pak, B., Gorsel, E. van, and Luhar, A.: Diagnosing
2558 errors in a land surface model (CABLE) in the time and frequency domains, *Journal of Geophysical Research:*
2559 *Biogeosciences*, 116, <https://doi.org/10.1029/2010JG001385>, 2011.
- 2560 Williams, M., Rastetter, E. B., Fernandes, D. N., Goulden, M. L., Wofsy, S. C., Shaver, G. R., Melillo, J. M., Munger, J. W.,
2561 Fan, S.-M., and Nadelhoffer, K. J.: Modelling the soil-plant-atmosphere continuum in a Quercus–Acer stand at Harvard
2562 Forest: the regulation of stomatal conductance by light, nitrogen and soil/plant hydraulic properties, *Plant, Cell &*
2563 *Environment*, 19, 911–927, <https://doi.org/10.1111/j.1365-3040.1996.tb00456.x>, 1996.
- 2564 Xu, X., Medvigy, D., Powers, J. S., Becknell, J. M., and Guan, K.: Diversity in plant hydraulic traits explains seasonal and
2565 inter-annual variations of vegetation dynamics in seasonally dry tropical forests, *New Phytol*, 212, 80–95,
2566 <https://doi.org/10.1111/nph.14009>, 2016.



- 2567 Zhou, S., Duursma, R. A., Medlyn, B. E., Kelly, J. W. G., and Prentice, I. C.: How should we model plant responses to drought?
2568 An analysis of stomatal and non-stomatal responses to water stress, *Agric. For. Meteorol.*, 182, 204–214,
2569 <https://doi.org/10.1016/j.agrformet.2013.05.009>, 2013.
- 2570 Zhou, S., Medlyn, B., Sabaté, S., Sperlich, D., Prentice, I. C., and others: Short-term water stress impacts on stomatal,
2571 mesophyll and biochemical limitations to photosynthesis differ consistently among tree species from contrasting climates,
2572 *Tree Physiology*, 34, 1035–46, 2014.
- 2573